A diffusion hydrodynamic model (DHM)

T. V. Hromadka II and C. C. Yen

Hydrologists, Williamson and Schmid, 17782 Sky Park Boulevard, Irvine, CA 92714, USA

A diffusion hydrodynamic model of coupled two-dimensional overland flow and one-dimensional open channel flow (DHM) is developed. Because of the diffusion form of the governing flow equations is used in this model, several important hydraulic effects are accommodated which are incapable of being handled by the often-used kinematic routing techniques which are used in most watershed models; namely, backwater effects, channel overflow, combined overland flow and storage effects, and ponding. Because these often ignored hydraulic effects are important in drainage studies involving flood control channel deficiencies and subtle grade differences between watershed boundaries (e.g. alluvial fan hydrology), the DHM approach affords the practicing hydrologist a new tool for drainage system evaluations.

INTRODUCTION

A diffusion hydrodynamic model of coupled two-dimensional overland flow and one-dimensional open channel flow (DHM) is developed. Because the diffusion form of the governing flow equations is used in this model, several important hydraulic effects are accommodated which are incapable of being handled by the often-used kinematic routing techniques which are used in most watershed models; namely, backwater effects, channel overflow, combined overland flow and storage effects, and ponding. Because these often ignored hydraulic effects are important in drainage studies involving flood control channel deficiencies and subtle grade differences between watershed boundaries (e.g. alluvial fan hydrology), the DHM approach affords the practicing hydrologist a new tool for drainage system evaluations.

This paper is organized into six working sections as follows:

Section Number	*Description*
I	DHM model theoretical development
II	verification of the DHM model
III	program description for DHM
IV	applications of DHM
V	comparison between DHM model and kinematic routing technique
VI	appendix – program listings and an example input file

In this paper, the pertinent literature is cited as needed in the text. However, for a general overview, the reader is referred to the Two-Dimensional Flow Modeling Conference Proceedings of the U.S. Army Corps of Engineers (1981).

Because the DHM computer code is surprisingly small, and can be easily handled by most current FORTRAN home computers, FORTRAN listings (and documentation) are included for the reader's convenience.

In typical applications involving large scale problems, pre- and post-processors should be developed to ease the data entry demands, and graphically display the tremendous amount of modelling results generated by the computer models.

Ample applications are included in this paper which hopefully demonstrate the utility of this modelling approach in many civil engineering drainage problems. Problems considered in this paper include: (1) large scale flood plain dam-break analysis; (2) small scale dam-break analysis within a municipality; (3) temporary flood-control debri-basin failure onto a broad plain; (4) dam-break flood flows around a landfill site; (5) rainfall-runoff modelling; (6) development of synthetic S-graphs for unit hydrograph studies; and (7) flooding of a watershed due to open channel deficiencies. Finally, kinematic routing technique is applied to one-dimensional problems. This study indicates that the DHM model is more stable than the kinematic routing technique.

I. MODEL DEVELOPMENT

INTRODUCTION

Many flow phenomena of great importance to the engineer are unsteady in character, and cannot be reduced to steady flow by changing the view-point of the observer. A complete theory of unsteady flow is therefore required, and will be reviewed in this section. The equations of motion are not soluble in the most general case, but approximations and numerical methods can be developed which yield solutions of satisfactory accuracy.

I.1 EQUATION OF CONTINUITY

The law of continuity for unsteady flow may be established by considering the conservation of mass in an infinitesimal space between two channel sections (Fig. 1). In unsteady flow, the discharge changes with distance at a rate $\partial Q/\partial x$, and the depth changes with time at a rate $\partial y/\partial t$. The change in discharge through space in the time dt is $(\partial Q/\partial x)\,dx\,dt$. The corresponding change in channel

Accepted February 1986. Discussion closes November 1986.

0309-1708/86/030118-53$2.00

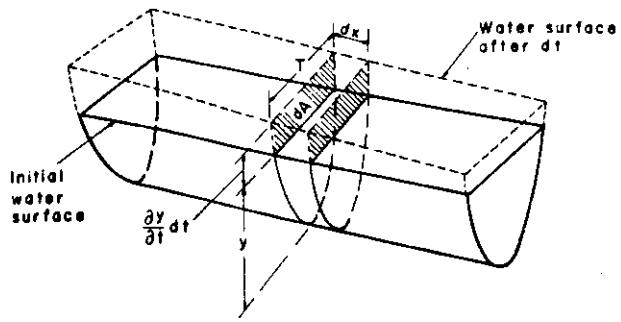

Fig. 1. Continuity of unsteady flow

storage in space is $T\,dx\,(\partial y/\partial t)\,dt = dx\,(\partial A/\partial t)\,dt$. Since water is incompressible, the net change in discharge plus the change in storage should be zero; that is

$$\frac{\partial Q}{\partial x}\,dx\,dt + T\,dx\left(\frac{\partial y}{\partial t}\right)dt = \left(\frac{\partial Q}{\partial x}\right)dx\,dt + dx\left(\frac{\partial A}{\partial t}\right)dt = 0$$

Simplifying,

$$\frac{\partial Q}{\partial x} + T\frac{\partial y}{\partial t} = 0 \tag{1}$$

or

$$\frac{\partial Q}{\partial x} + \frac{\partial A}{\partial t} = 0 \tag{2}$$

At a given section, $Q = VA$; thus equation (1) becomes

$$\frac{\partial (VA)}{\partial x} + T\frac{\partial y}{\partial t} = 0 \tag{3}$$

or

$$A\frac{\partial V}{\partial x} + V\frac{\partial A}{\partial x} + T\frac{\partial y}{\partial t} = 0 \tag{4}$$

Since the hydraulic depth $D = A/T$ and $\partial A = T\,\partial y$, the above equation may be written

$$D\frac{\partial V}{\partial x} + V\frac{\partial y}{\partial x} + \frac{\partial y}{\partial t} = 0 \tag{5}$$

The above equations are all forms of the continuity equation for unsteady flow in open channels. For a rectangular channel of infinite width, equation (1) may be written

$$\frac{\partial q}{\partial x} + \frac{\partial y}{\partial t} = 0 \tag{6}$$

where q is the discharge per unit width.

I.2 EQUATION OF MOTION

In a steady, uniform flow problem, the gradient, dH/dx, of the total energy line is equal in magnitude and opposite in sign to the 'friction slope' $S_f = v^2/(C^2R)$. Indeed this statement was in a sense taken as the definition of S_f; however in the present context we have to consider the more general case in which the flow is nonuniform and the velocity may therefore be changing in the downstream direction. The net force, shear force and pressure force, is no longer zero, since the flow is accelerating. Therefore, the equation of motion becomes

$$-\gamma A\Delta h - \tau_0 P\Delta x = \rho A\Delta x\left(v\frac{\partial v}{\partial x} + \frac{\partial v}{\partial t}\right)$$

i.e.

$$\tau_0 = -\gamma R\left(\frac{\partial h}{\partial x} + \frac{v}{g}\frac{\partial v}{\partial x} + \frac{1}{g}\frac{\partial v}{\partial t}\right)$$

$$= -\gamma R\left(\frac{\partial H}{\partial x} + \frac{1}{g}\frac{\partial v}{\partial t}\right) \tag{7}$$

where τ_0 is the shear stress, γ is the specific weight of fluid, R is the mean hydraulic radius, and ρ is the fluid density. Substituting $\tau_0 = \gamma v^2/C^2$ into equation (7), we obtain

$$\frac{\partial H}{\partial x} + \frac{1}{g}\frac{\partial v}{\partial t} + \frac{v^2}{C^2R} = 0 \tag{8}$$

and this equation may be written as

$$S_e + S_a + S_f = 0 \tag{9}$$

where the three terms of equation (9) are called the energy slope, the acceleration slope, and the friction slope respectively. Fig. 2 depicts the simplified representation of energy in unsteady flow.

By substituting $H = v^2/2g + y + z$ and the bed slope $S_0(-\partial z/\partial x)$ into equation (8), we obtain

$$\frac{\partial H}{\partial x} = \frac{\partial z}{\partial x} + \frac{\partial y}{\partial x} + \frac{v}{g}\frac{\partial v}{\partial x}$$

$$= -S_0 + \frac{\partial y}{\partial x} + \frac{v}{g}\frac{\partial v}{\partial x}$$

$$= -\frac{1}{g}\frac{\partial v}{\partial t} - S_f \tag{10}$$

Hence equation (8) can be written as

$$S_f = S_0 - \frac{\partial y}{\partial x} - \frac{v}{g}\frac{\partial v}{\partial x} - \frac{1}{g}\frac{\partial v}{\partial t} = \frac{v^2}{C^2R}$$

steady uniform flow →
steady nonuniform flow →
unsteady nonuniform flow ⟶ (11)

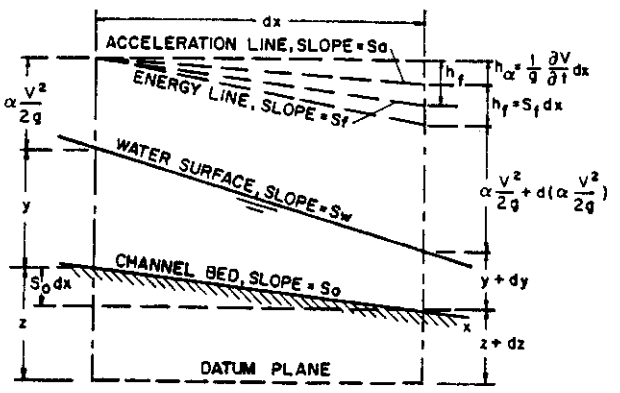

Fig. 2. Simplified representation of energy in unsteady flow

This equation may be applicable as indicated. This arrangement shows how the nonuniformity and unsteadiness of flows introduce extra terms into the governing dynamic equation. For example, it is noted that the steady-flow equation is valid only when the pressure distribution is hydrostatic; that is, when the vertical components of acceleration are negligible.

I.3 DIFFUSION HYDRODYNAMIC MODEL (DHM)

I.3.0 One-dimensional diffusion hydrodynamic model

The mathematical relationships in a one-dimensional diffusion hydrodynamic (DHM) model are based upon the flow equations of continuity (2) and momentum (11) which can be rewritten (Akan and Yen, 1981) as

$$\frac{\partial Q_x}{\partial x}+\frac{\partial A_x}{\partial t}=0 \tag{12}$$

$$\frac{\partial Q_x}{\partial t}+\frac{\partial (Q_x^2/A_x)}{\partial x}+gA_x\left(\frac{\partial H}{\partial x}+S_{fx}\right)=0 \tag{13}$$

where Q_x is the flowrate; x,t are spatial and temporal coordinates; A_x is the flow area; g is gravity; H is the water surface elevation; and S_{fx} is a friction slope. It is assumed that S_{fx} is approximated from Manning's equation for steady flow by (e.g. Akan and Yen, 1981)

$$Q_x=\frac{1.486}{n}A_xR^{2/3}S_{fx}^{1/2} \tag{14}$$

where R is the hydraulic radius; and n is a friction factor which may be increased to account for other energy losses such as expansions and bend losses. Letting m_x be a momentum quantity defined by

$$m_x=\left(\frac{\partial Q_x}{\partial t}+\frac{\partial (Q_x^2/A_x)}{\partial x}\right)\Big/ gA_x \tag{15}$$

then equation (13) can be rewritten as

$$S_{fx}=-\left(\frac{\partial H}{\partial x}+m_x\right) \tag{16}$$

In equation (15), the subscript x included in m_x indicates the directional term. The expansion of equation (13) to the two-dimensional case leads directly to the terms (m_x, m_y) except that now a cross-product of flow velocities are included, increasing the computational effort considerably.

Rewriting equation (14) and including equations (15) and (16), the directional flow rate is computed by

$$Q_x=-K_x\left(\frac{\partial H}{\partial x}+m_x\right) \tag{17}$$

where Q_x indicates a directional term, and K_x is a type of conduction parameter defined by

$$K_x=\frac{1.486}{n}A_xR^{2/3}\Big/\left|\frac{\partial H}{\partial x}+m_x\right|^{1/2} \tag{18}$$

In equation (18), K_x is limited in value by the denominator term being checked for a smallest allowable magnitude.

Substituting the flow rate formulation of equation (17) into equation (12) gives a diffusion type of relationship

$$\frac{\partial}{\partial x}K_x\left(\frac{\partial H}{\partial x}+m_x\right)=\frac{\partial A_x}{\partial t} \tag{19}$$

The one-dimensional diffusion model of Akan and Yen (1981) assumes $m_x=0$ in equation (18). Thus, the one-dimensional DHM is given by

$$\frac{\partial}{\partial x}K_x\frac{\partial H}{\partial x}=\frac{\partial A_x}{\partial t} \tag{20}$$

where K_x is now simplified as

$$K_x=\frac{1.486}{n}A_xR^{2/3}\Big/\left|\frac{\partial H}{\partial x}\right|^{1/2} \tag{21}$$

For a constant channel width, W, equation (20) reduces to

$$\frac{\partial}{\partial x}K_x\frac{\partial H}{\partial x}=W\frac{\partial H}{\partial t} \tag{22}$$

However, it is noted that a family of models is given by equation (19) where m_x is defined by selecting from the possibilities

$$m_x=\begin{cases}\dfrac{\partial (Q_x^2/A_x)}{\partial x}\Big/ gA_x, \text{ (convective acceleration model)}\\[2ex] \dfrac{\partial Q_x}{\partial t}\Big/ gA_x, \text{ (local acceleration model)}\\[2ex] \left(\dfrac{\partial Q_x}{\partial t}+\dfrac{\partial (Q_x^2/A_x)}{\partial x}\right)\Big/ gA_x, \text{ (coupled model)}\\[2ex] 0, \text{ (DHM)}\end{cases} \tag{23}$$

I.3.1 Two-dimensional diffusion hydrodynamic model

The set of (fully dynamic) 2-D unsteady flow equations consists of one equation of continuity

$$\frac{\partial q_x}{\partial x}+\frac{\partial q_y}{\partial y}+\frac{\partial H}{\partial t}=0 \tag{24}$$

and two equations of motion

$$\frac{\partial q_x}{\partial t}+\frac{\partial}{\partial x}\left(\frac{q_x^2}{h}\right)+\frac{\partial}{\partial y}\left(\frac{q_xq_y}{h}\right)+gh\left(S_{fx}+\frac{\partial H}{\partial x}\right)=0 \tag{25}$$

$$\frac{\partial q_y}{\partial t}+\frac{\partial}{\partial y}\left(\frac{q_y^2}{h}\right)+\frac{\partial}{\partial y}\left(\frac{q_xq_y}{h}\right)+gh\left(S_{fy}+\frac{\partial H}{\partial y}\right)=0 \tag{26}$$

in which q_x, q_y are flow rates per unit width in the x,y-directions; S_{fx}, S_{fy} represent friction slopes in x,y-directions; H, h, g stand for, respectively, water-surface elevation, flow depth, and gravitational acceleration; and x, y, t are for spatial and temporal coordinates.

The above equation set is based on the assumptions of constant fluid density with zero sources or sinks in the flow field, of hydrostatic pressure distributions, and of relatively uniform bottom slopes.

The local and convective acceleration terms can be grouped together such that equations (24), (25), and (26) are rewritten as

$$m_z+\left(S_{fz}+\frac{\partial H}{\partial z}\right)=0, \qquad z=x,y \tag{27}$$

where m_z represents the sum of the first three terms in equations (25) and (26) divided by gh. Assuming the friction slope to be approximated by steady flow conditions, the Manning's formula in the U.S. customary units can be used to estimate

$$q_z=\frac{1.486}{n}h^{5/3}S_{fz}^{1/2}, \qquad z=x,y \tag{28}$$

Equation (28) can be rewritten as

$$q_z=-K_z\frac{\partial H}{\partial z}-K_z m_z, \qquad z=x,y \tag{29}$$

where

$$K_z=\frac{1.486}{n}h^{5/3}\Big/\left|\frac{\partial H}{\partial S}+m_S\right|^{1/2}, \qquad z=x,y \tag{30}$$

The symbol S indicates the flow direction which makes an angle of $\theta=\tan^{-1}(q_y/q_x)$ in the positive x-direction.

Values of m are assumed negligible by several investigators (Akan and Yen, 1981, Hromadka, 1984, and Xanthopoulos and Koutitas, 1976), resulting in the simple diffusion model,

$$q_z=-K_z\frac{\partial H}{\partial z}, \qquad z=x,y \tag{31}$$

The proposed 2-D DHM is formulated by substituting equation (31) into equation (24)

$$\frac{\partial}{\partial x}K_x\frac{\partial H}{\partial x}+\frac{\partial}{\partial y}K_y\frac{\partial H}{\partial y}=\frac{\partial H}{\partial t} \tag{32}$$

If the momentum term groupings were retained, equation (32) would be written as

$$\frac{\partial}{\partial x}K_x\frac{\partial H}{\partial x}+\frac{\partial}{\partial y}K_y\frac{\partial H}{\partial y}+S=\frac{\partial H}{\partial t} \tag{33}$$

where

$$S=\frac{\partial}{\partial x}(K_x m_x)+\frac{\partial}{\partial y}(K_y m_y)$$

and K_x, K_y are also functions of m_x, m_y respectively.

I.4 NUMERICAL APPROXIMATION

I.4.0 Numerical solution algorithm

The following steps are taken in the computer program where the flow path is assumed initially discretized by equally spaced nodal points with a Manning's n, an elevation, and an initial flow depth (usually zero) defined:

(1) between nodal points, compute an average Manning's n, and average geometric factors,
(2) assuming $m_x=0$, estimate the nodal flow depths for the next timestep, $(t+\Delta t)$ by using equations (20) and (21) explicitly,
(3) using the flow depths at time t and $(t+\Delta t)$, estimate the midtimestep value of m_x selected from equation (23),
(4) recalculate the conductivities K_x using the appropriate m_x values,
(5) determine the new nodal flow depths at time $(t+\Delta t)$ using equation (19), and
(6) return Step (3) until K_x matches midtimestep estimates.

The above algorithm steps can be used regardless of the choice of definition for m_x from equation (23). Additionally, the above program steps can be directly applied to a two-dimensional diffusion model with the selected (m_x,m_y) relations incorporated.

I.4.1 Numerical model formulation (grid elements)

For uniform grid elements, the integrated finite difference version of the nodal domain integration (NDI) method is used. For grid elements, the NDI nodal equation is based on the usual system shown in Fig. 3. Flow rates along the boundary Γ are estimated using a linear trial function assumption between nodal points.

For a square grid of width δ,

$$q|_{\Gamma_E}=-(K_x|_{\Gamma_E})(H_E-H_C)/\delta \tag{34}$$

where

$$K_x|_{\Gamma_E}=\begin{cases}\left(\dfrac{1.486}{n}h^{5/3}\right)_{\Gamma_E}\Big/\left|\dfrac{H_E-H_C}{\delta\cos\theta}\right|^{1/2}; & \bar{h}>0\\ 0;\ \bar{h}\leqslant 0 \text{ or } |H_E-H_C|<10^{-3}\end{cases} \tag{35}$$

In equation (35), h and n are both the average of the values of C and E, i.e., $h=(h_C+h_E)/2$ and $n=(n_C+n_E)/2$. (Additionally, the denominator of K_x is checked such that K_x is set to zero if $|H_E-H_C|$ is less than a tolerance such as 10^{-3} ft.)

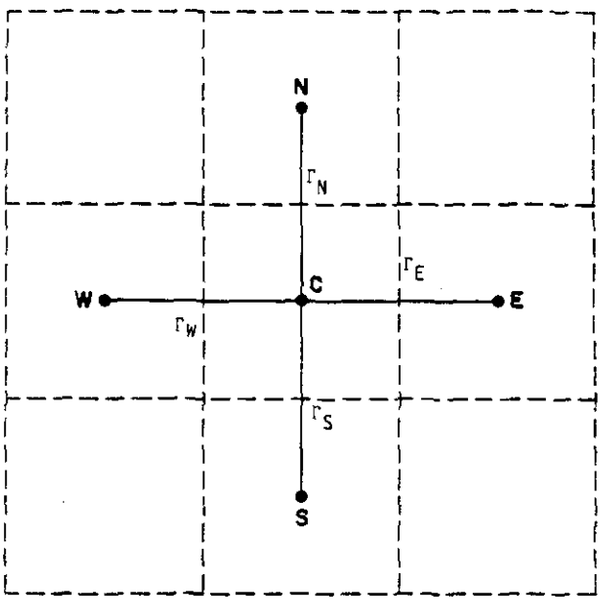

Fig. 3. Two-dimensional finite difference analog

The model advances in time by an explicit approach

$$\mathbf{H}^{i+1} = \mathbf{K}^i \mathbf{H}^i \tag{36}$$

where the assumed input flood flows are added to the specified input nodes at each timestep. After each timestep, the hydraulic conduction parameters of equation (35) are reevaluated, and the solution of equation (36) reinitiated. Using grid sizes with uniform lengths of 1000-feet, timesteps of size 5.0 sec were found satisfactory. Verification of the 2-D DHM is given in section II for the class of problems involving severe peaked flood hydrographs such as those resulting from dam-breaks.

1.4.2 Model timestep selection

The sensitivity of the model to timestep selection is dependent upon the slope of the hydrograph ($\partial Q/\partial t$) and the grid spacing. Increasing the grid spacing size introducing additional storage to a corresponding increase in nodal point flood depth values. Similarly, a decrease in timestep size allows a refined calculation of inflow and outflow values and a smoother variation in nodal point flood depths with respect to time. The computer algorithm may self-select a timestep by increments of halving (or doubling) the selected timestep size so that a proper balance of inflow–outflow to control volume storage variation is achieved. In order to avoid a matrix solution for flood depths, an explicit timestepping algorithm is used to solve for the time derivation term. For large timesteps or a rapid variation in the dam-break hydrograph (i.e., $\partial Q/\partial t$ is large), a large accumulation of flow volume will occur at the most upstream nodal point. That is, at the dam-break reservoir nodal point, the lag in outflow from the control volume can cause unacceptable error in the computation of the flood depth. One method which offset this error is the program to self-select the timestep until the difference in the rate of volume accumulation is within a specified tolerance. For the example problems considered, a timestep of about 5 to 10 seconds was found adequate.

Due to the form of the DHM in equation (22), the model can be extended into an implicit technique. However, this extension would require a matrix solution process which may become unmanageable for two-dimensional models which utilize hundreds of nodal points.

II. VERIFICATION OF DIFFUSION HYDRODYNAMIC MODEL (DHM)

INTRODUCTION

An unsteady flow hydraulic problem of considerable interest is the analysis of dam-breaks and the subsequent floodplain evolution.

The use of numerical methods to approximately solve the flow equations for the propagation of a flood wave due to an earthen dam failure has been the subject of several studies reported in the literature. Generally, the one-dimensional flow is modelled wherever there is no significant lateral variation in the flow. Land (1980 a, b) examines four such dam-break models in their prediction of flooding levels and flood wave travel time, and compares the results against observed dam failure information. In dam-break analysis studies, an assumed dam-break failure mode (which may be part of the solution) is used to develop an inflow hydrograph to the down-stream flood plain. Consequently, it is noted that a considerable sensitivity in modelling results is attributed to the dam-break failure rate assumptions. Ponce and Tsivoglou (1981) examine the gradual failure of an earthen embankment (caused by an overtopping flooding event) and present a detailed model of the total system: sediment transport, unsteady channel hydraulics, and earth embankment failure. In this section, the main objective is to evaluate the diffusion form of the flow equations for the estimation of flood depths (and the flood plain) resulting from a specified dam-break hydrograph. Consequently the dam-break failure mode is not considered in this section. Rather, the dam-break failure mode may be included as part of the model solution (such as for a sudden breach) or specified as a reservoir outflow hydrograph.

In another study, Rajar (1978) studies a one-dimensional flood wave propagation from an earthen dam failure. His model solves the St. Venant equations by means of either a first-order diffusive or a second-order Lox-Wendroff numerical scheme. A review of the literature indicates that the most often-used numerical scheme is the method of characteristics (to solve the governing flow equations) such as described in Sakkas and Strelkoff (1973), and Chen (1980 a, b).

Although many dam-break studies involve flood flow regimes which are truly two-dimensional (in the horizontal plane), the two dimensional case has not received much attention in the literature. Katopodes and Strelkoff (1978) use the method of bicharacteristics to solve the governing equations of continuity and momentum. The model utilizes a moving grid algorithm to follow the flood wave propagation, and also employs several interpolation schemes to aprroximate the nonlinearity effects. In a much simpler approach, Xanthopoulos and Koutitas (1976) use a diffusion model (i.e., the inertia terms are assumed negligible in a comparison to the pressure, friction, and gravity components) to approximate a two-dimensional flow field. The model assumes that the flood plain flow regime is such that the inertia terms (local and convective acceleration) are negligible. In a one-dimensional model, Akan and Yen (1981) also use the diffusion approache to model hydrograph confluences at channel junctions. In the latter study, comparisons of modelling results were made between the diffusion model, a complete dynamic wave model solving the total equation system, and the basic kinematic wave equation model (i.e., the inertia and pressure terms are assumed negligible in comparison to the friction and gravity terms). The comparisons between the diffusion model and the dynamic wave model were very favourable, showing only minor discrepancies.

The kinematic-wave flow model has been recently used in the computation of dam-break flood waves (Hunt, 1982). Hunt concludes in his study that the kinematic-wave solution is asympotically valid. Since the diffusion model has a wider range of applicability of bed slopes and wave periods than the kinematic model (Ponce *et al.*, 1978), then the diffusion model approach should provide an extension to the referenced kinematic model.

Because the diffusion modelling approach leads to an economic two-dimensional dam-break model (with numerical solutions based on the usual integrated finite-difference or finte element techniques), the need to include the extra components in the momentum equation must be ascertained. For example, evaluating the convective

acceleration terms in a two-dimensional flow model requires approximately an additional 50-percent of the computational effort required in solving the entire two-dimensional model with the inertia terms omitted. Consequently, including the local and convective acceleration terms increases the computer execution costs significantly. Such increases in computational effort may not be significant for one-dimensional case studies; however, two-dimensional case studies necessarily involve considerably more computational effort and any justifiable simplifications of the governing flow equations is reflected by a significant decrease in computer software requirements, costs and computer execution time.

Ponce (1981) examines the mathematical expressions of the flow equations which lead to wave attenuation in prismatic channels. It is concluded that the wave attentuation process is caused by the interaction of the local acceleration term with the sum of the terms of friction slope and channel slope. When local acceleration is considered negligible, wave attenuation is caused by the interaction of the friction slope and channel slope terms with the pressure gradient or convective acceleration terms (or a combination of both terms). Other discussions of flow conditions and the sensitivity to the various terms of the flow equations are given in Miller and Cunge (1975), Morris and Woolhiser (1980), and Henderson (1963).

It is stressed that the ultimate objective of this paper is to develop a two-dimensional diffusion model for use in estimating floodplain evolution such as occurs due to drainage system deficiencies. Prior to finalizing such a model, the requirement of including the inertia terms in the unsteady flow equations needs to be ascertained. The strategy used to check on this requirement is to evaluate the accuracy in predicted flood depths produced from a one-dimensional diffusion model with respect to the one-dimensional U.S.G.S. K-634 dam-break model which includes all of the inertia term components.

II.1 ONE-DIMENSIONAL ANALYSIS

II.1.0 Study approach

In order to evaluate the accuracy of the diffusion model of equation (22) in the prediction of flood depths, the U.S.G.S. fully dynamic flow model K-634 (Land, 1980, a, b) is used to determine channel flood depths for comparison purposes. The K-634 model solves the coupled flow equations of continuity and momentum by an implicit finite difference approach and is considered to be a highly accurate model for many unsteady flow problems. The study approach is to compare predicted: (1) flood depths, and (2) discharge hydrographs from both the K-634 and the DHM (equation (22)) for various channel slopes and inflow hydrographs.

It should be noted that different initial conditions are used for these two models. The U.S.G.S. K-634 model requires a base flow to start the simulation, i.e., the initial depth of water can not be zero. Next, the normal depth assumption is used to generate an initial water depth before the simulation starts. These two steps are not required by the DHM.

In this case study, two hydrographs are assumed; namely, peak flows of 120 000 cfs and 600 000 cfs. Both hydrographs are assumed to increase linearly from zero to the peak flow rate at time of 1-hour, and then decrease linearly to zero time of 6-hours (see Fig. 4 inset). The study channel is assumed to be a uniform rectangular section of Manning's n equal to 0.040, and various slopes S_0 in the range of $0.001 \leqslant S_0 \leqslant 0.01$. Figure 4 shows the comparison of modelling results. From the figure, various flood depths are plotted along the channel length of up to 10-miles. Two reaches of channel lengths of up to 30-miles are also plotted in Fig. 4 which correspond to a slope $S_0 = 0.0020$. In all tests, grid spacing was set at 1000-foot intervals.

From Fig. 4 it is seen that the diffusion model provides estimates of flood depths that compare very well to the flood depths predicted from the K-634 model. Differences in predicted flood depths are less than 3-percent for the various channel slopes and peak flow rates considered.

Figures 5 and 6 show good comparisons between the DHM and the K-634 model for water depths and outflow hydrographs at 5 and 10 miles downstream from the dam-break site.

II.1.1 Grid spacing selection

The choice of timestep and grid size for an explicit time advancement is a relative matter and is theoretically based on the well-known Courant condition (Basco, 1978). The choice of grid size usually depends on available topographic data for nodal elevation determination and the size of the problem. The effect of the grid size (for constant timestep for 7.2 seconds) on the diffusion model accuracy can be shown by example where nodal spacings of 1000, 2000 and 5000-feet are considered. The predicted flood depths varied only slightly from choosing the grid size between 1000-feet and 2000-feet. However, an increased variation in results occurs when a grid size of 500-feet is selected. Figure 7 shows the computed flood

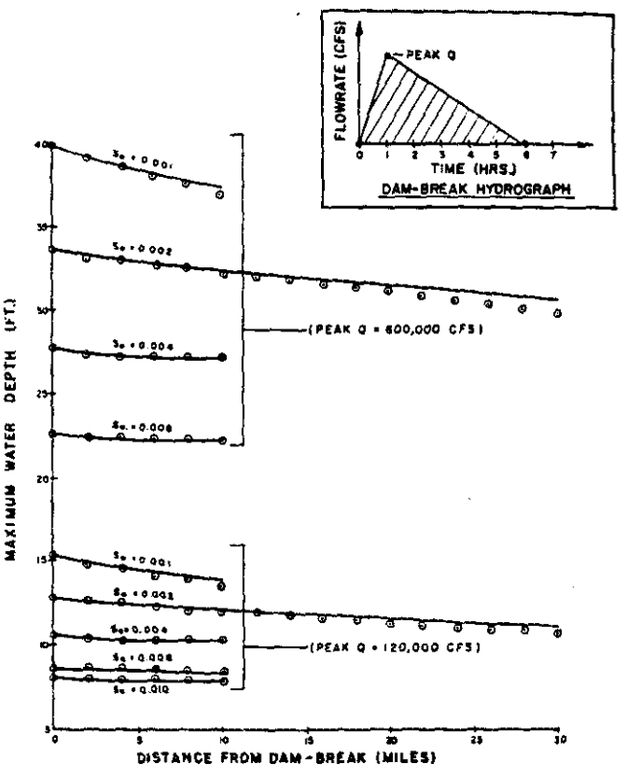

Fig. 4. Diffusion model (⊙) and K-634 model results (solid line) for 1000-foot width channel, Manning's $n = 0.040$, and various channel slopes, S_0

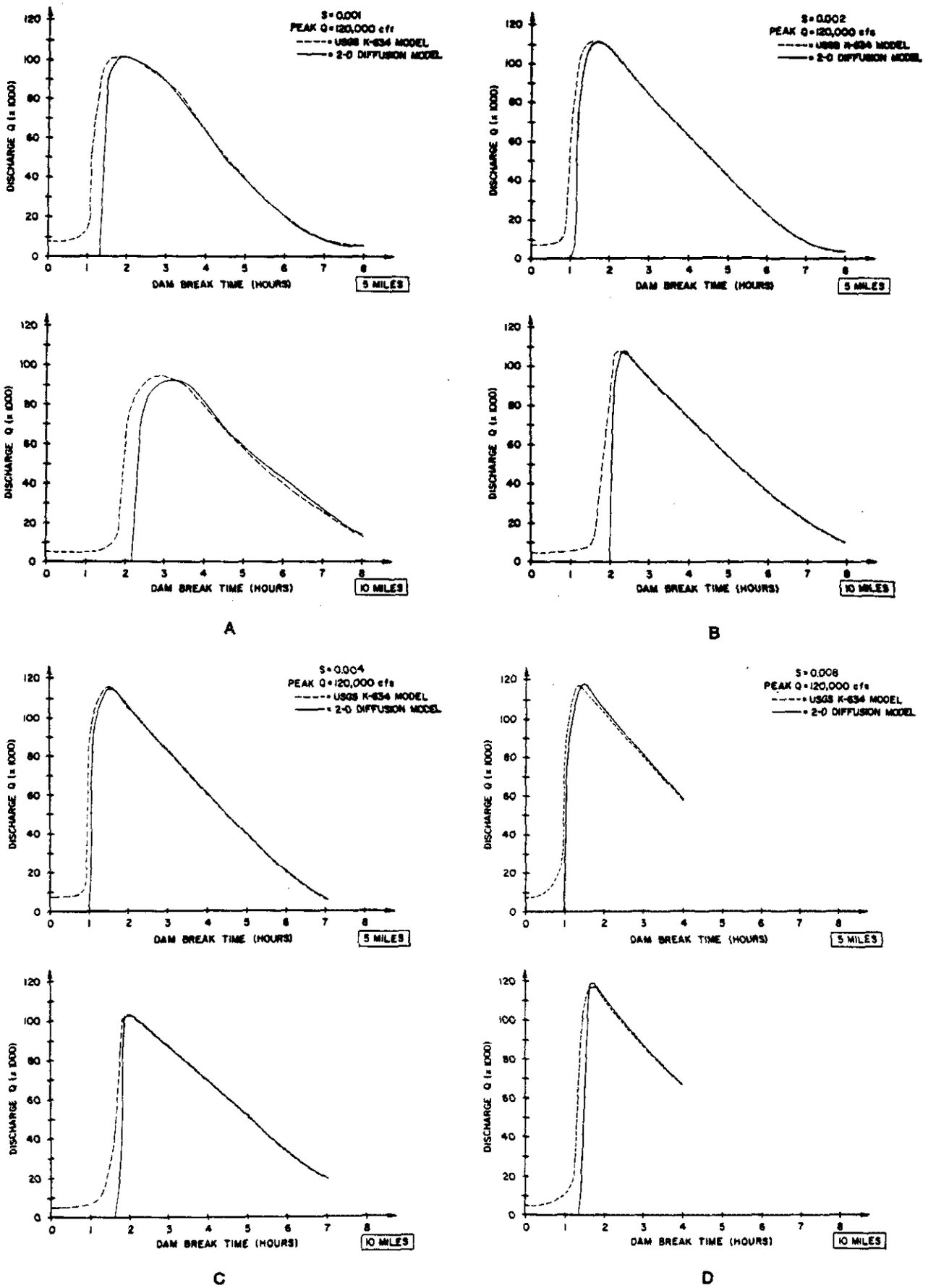

Fig. 5. Comparisons of outflow hydrographs at 5 and 10 miles downstream from the dam-break site

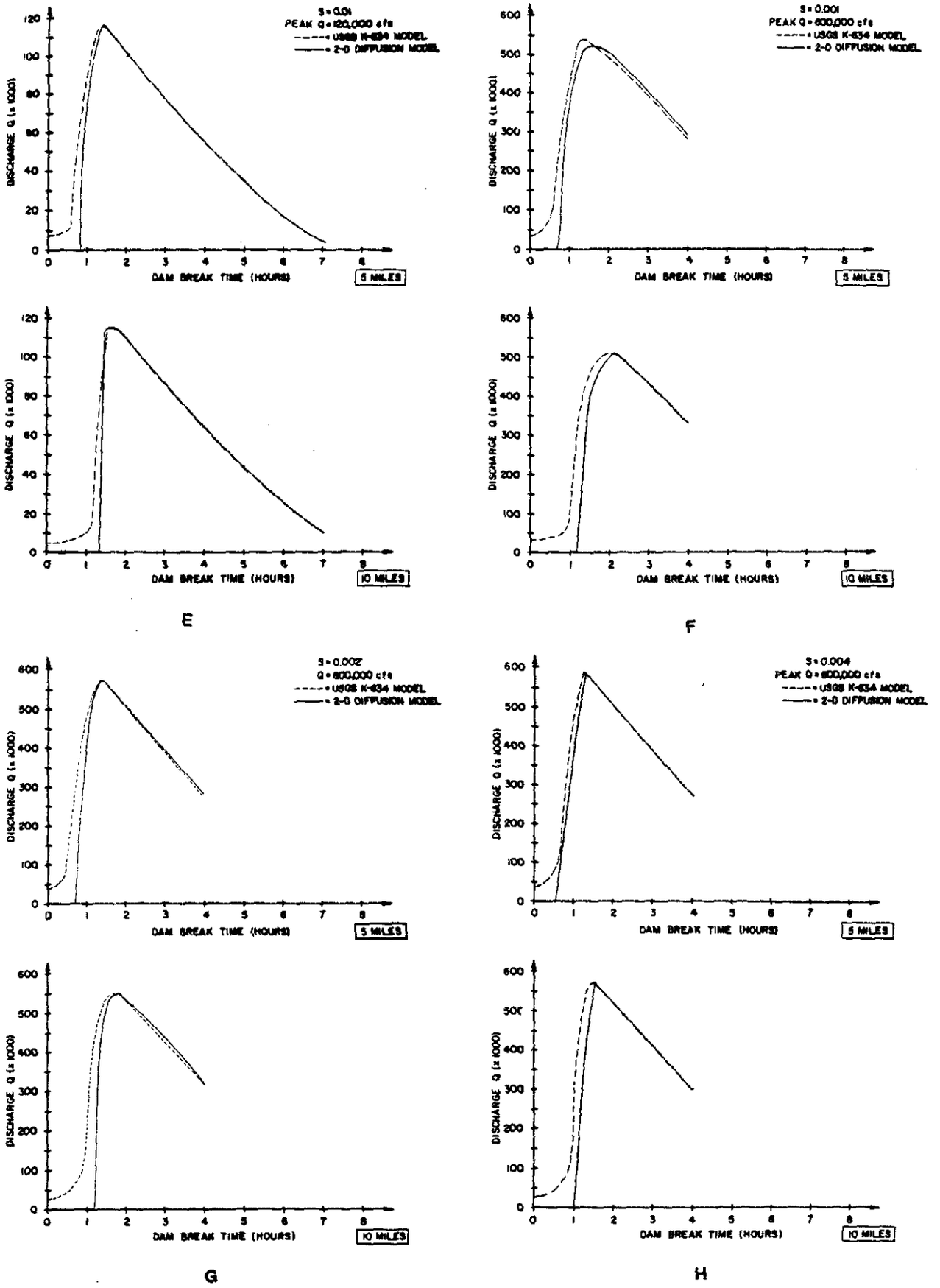
S = 0.01
PEAK Q = 120,000 cfs
USGS K-634 MODEL
2-D DIFFUSION MODEL
DISCHARGE Q (x 1000)
DAM BREAK TIME (HOURS)
5 MILES
S = 0.001
PEAK Q = 600,000 cfs
USGS K-634 MODEL
2-D DIFFUSION MODEL
DISCHARGE Q (x 1000)
DAM BREAK TIME (HOURS)
5 MILES
DISCHARGE Q (x 1000)
DAM BREAK TIME (HOURS)
10 MILES
E
DISCHARGE Q (x 1000)
DAM BREAK TIME (HOURS)
10 MILES
F
S = 0.002
Q = 600,000 cfs
USGS K-634 MODEL
2-D DIFFUSION MODEL
DISCHARGE Q (x 1000)
DAM BREAK TIME (HOURS)
5 MILES
S = 0.004
PEAK Q = 600,000 cfs
USGS K-634 MODEL
2-D DIFFUSION MODEL
DISCHARGE Q (x 1000)
DAM BREAK TIME (HOURS)
5 MILES
DISCHARGE Q (x 1000)
DAM BREAK TIME (HOURS)
10 MILES
G
DISCHARGE Q (x 1000)
DAM BREAK TIME (HOURS)
10 MILES
H

Fig. 5.—cont.

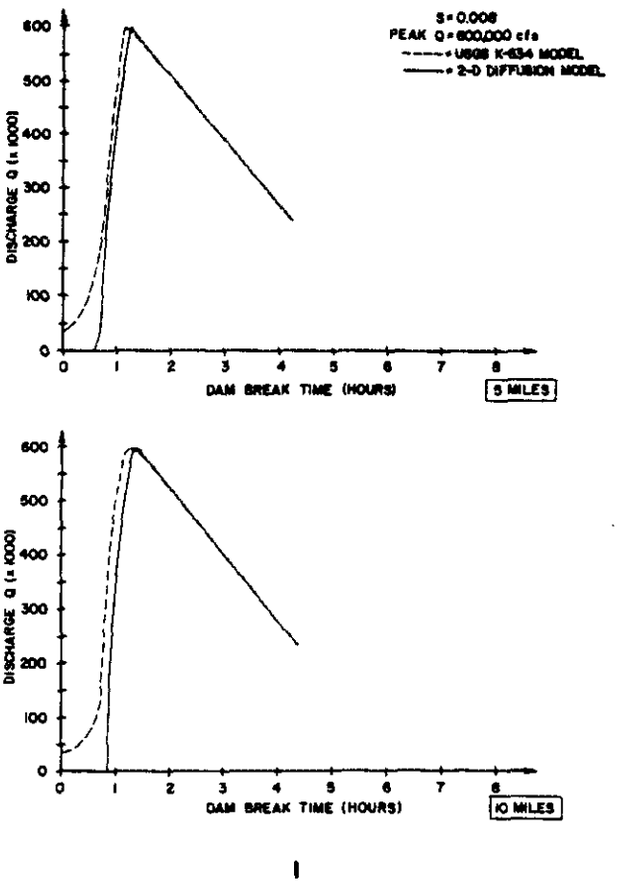

Fig. 5.—cont.

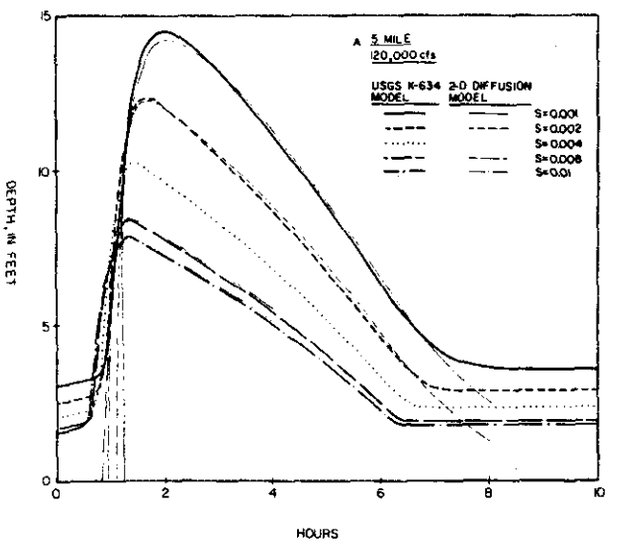

Fig. 6. Comparisons of depths of water at 5 and 10 miles downstream from the dam-break site

depths in comparison to the K-634 modelling results (Fig. 4) for the considered grid sizes, and the peak flow rate test hydrograph of 600 000 cfs.

Because the algorithm presented is based upon an explicit timestepping technique, the modelling results may become inaccurate should the timestep size *versus* grid size ratio become large. A simple procedure to eliminate this instability is to half the timestep size until convergence in computed results is achieved. Generally, such a timestep adjustment may be directly included in the dam-break model computer program. For the cases considered in this section, timestep sizes of 7.2 seconds was found to be adequate when using the 1000-feet to 5000-feet grid sizes.

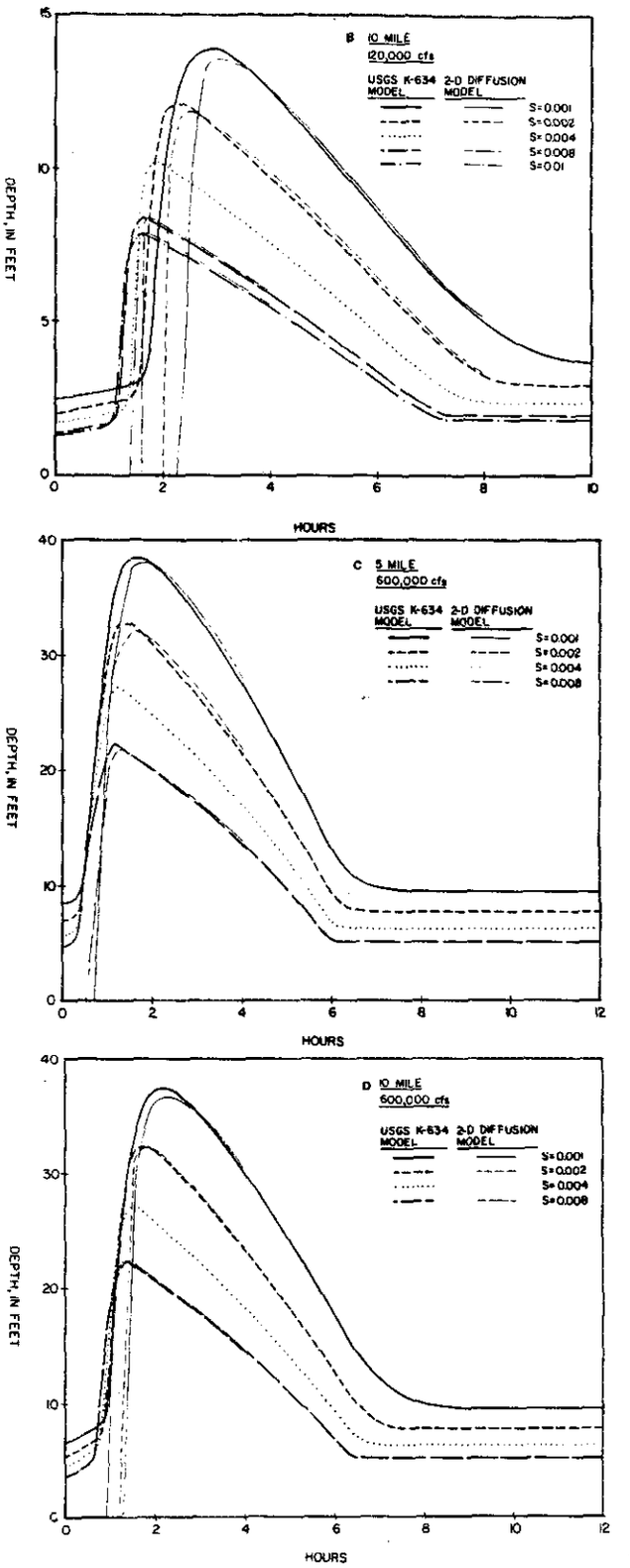

Fig. 6.—cont.

II.1.2 Conclusions and discussions

For the dam-break hydrographs considered and the range of channel slopes modelled, the simple diffusion dam-break model of equation (22) provides estimates of flood depths and outflow hydrographs which compare favourably to the results determined by the well-known K-634 one-dimensional dam-break model. Generally speaking, the difference between the two modelling approaches is found to be less than a 3 percent variation in predicted flood depths.

The presented diffusion dam-break model is based upon a straightforward explicit timestepping method which allows the model to operate upon the nodal points without the need to use large matrix systems. Consequently, the model can be implemented on most currently available microcomputers.

The diffusion model of equation (22) can be directly extended to a two-dimensional model by adding the y-direction terms which are computed in a similar fashion as the x-direction terms. The resulting two-dimensional diffusion model is tested by modelling the considered test problems in the x-direction, the y-direction, and along a 45-degree trajectory across a two-dimensional grid aligned with the x-y coordinate axis. Using a similar two-diemsional model, Xanthopoulos and Koutitas (1976) conceptually verify the diffusion modelling technique by considering the evolution of a two-dimensional flood plain which propagates radially from the dam-break site.

From the above conclusions, use of the diffusion approach of equation (22) in a two-dimensional DHM may be justifiable due to the low variation in predicted

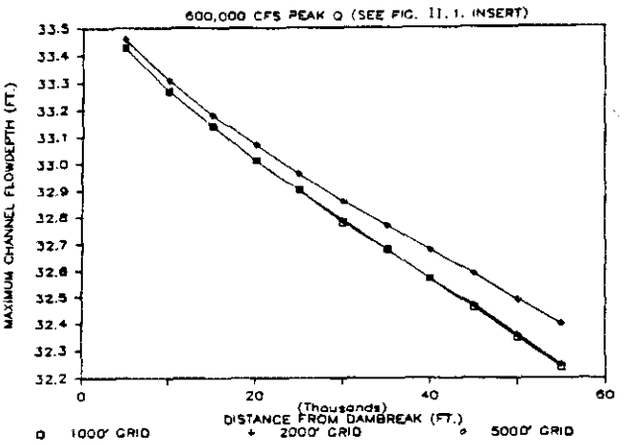

Fig. 7. Effects of differing grid size

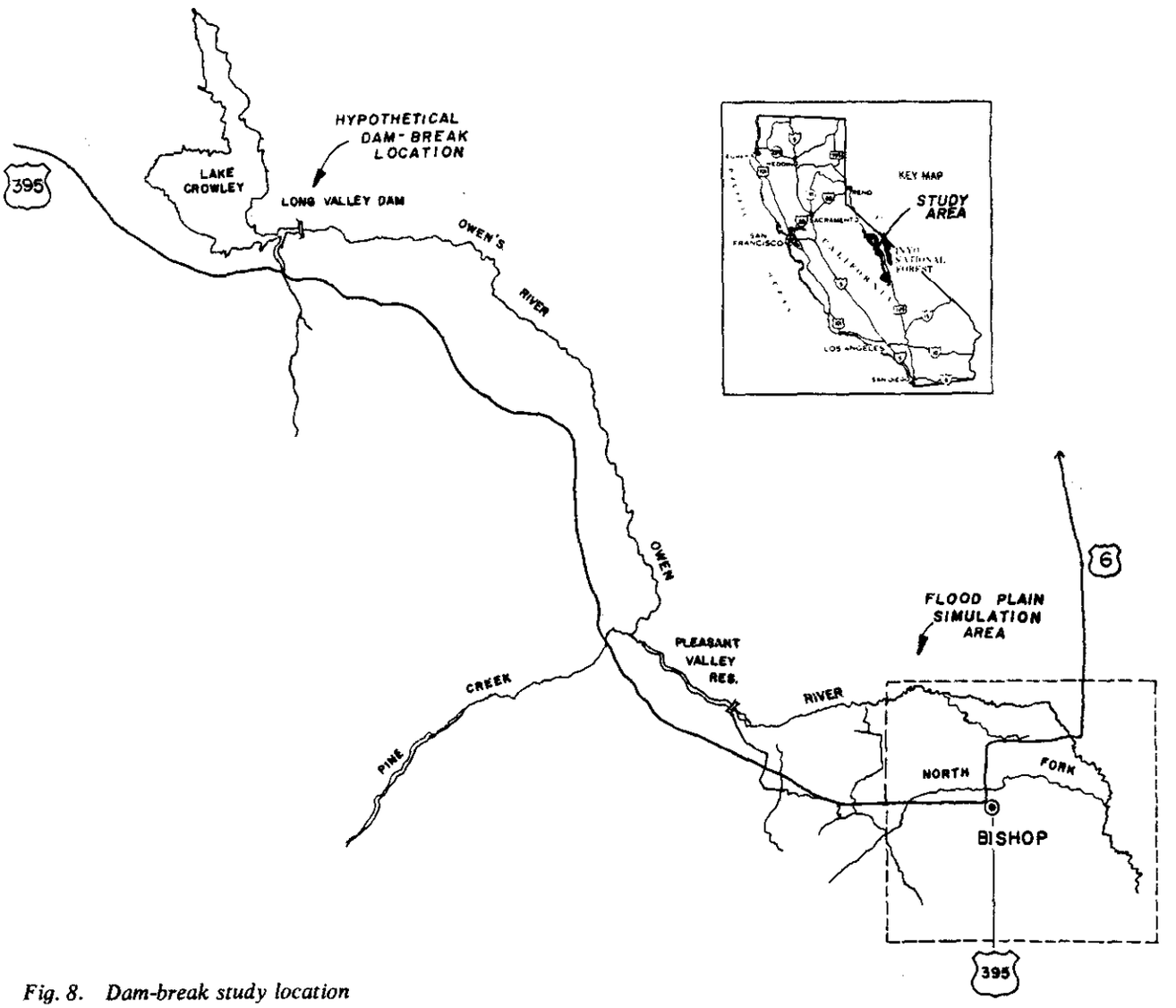

Fig. 8. Dam-break study location

flooding depths (one-dimensional) with the exclusion of the inertia terms. Generally speaking, a two-dimensional model would be employed when the expansive nature of flood flows is anticipated. Otherwise, one of the available one-dimensional models would suffice for the analysis.

II.2 TWO-DIMENSIONAL ANALYSIS

II.2.0 Introduction

In this section, a two-dimensional DHM is developed. The model is based on a diffusion approach where gravity, friction, and pressure forces are assumed to dominate the flow equations. Such an approach has been used earlier by Xanthopoulos and Koutitas (1975) in the prediction of dam-break flood plains in Greece. In those studies, good results were also obtained in the use of the two-dimensional model in predicting one-dimensional flow quantities. The preceding section considers a one-dimensional diffusion model and concludes that for most velocity flow regimes (i.e., less than approximately 25 feet/sec), the diffusion model is a reasonable approximation of the full dynamic wave formulation.

An integrated finite difference grid model is developed which equates each cell-centrered node to a function of the four neighbouring cell nodal points. To demonstrate the model's flood plain predictive capacity, a study of a hypothetical dam-break of the Crowley Lake dam near the City of Bishop, California (Fig. 8) is considered (Hromadka *et al.*, 1985).

II.2.1 K-634 modelling results and discussion

Using the K-634 model for computing the two-dimensional flow was attempted by means of the one-dimensional nodal spacing shown in Fig. 9. Cross sections were obtained by field survey, and the elevation data used to construct nodal point flow-width *versus* stage diagrams. A constant Manning's friction factor of 0.04 was assumed for study purposes. The assumed dam-break failure reached a peak flow rate of 420 000 cfs within one hour, and returned to zero flow 9.67 hours later. The resulting K-634 flood plain limits is shown in Fig. 10. To model the flow break-out, a slight gradient was assumed for the topography perpendicular to the main channel. The motivation for such a lateral gradient is to limit the channel floodway section in order to approximately conserve the one-dimensional momentum equations. Consequently, fictitious channel sides are included in the K-634 model study which results in an artificial confinement of the flows. Hence, a narrower flood plain is delineated (such as shown in Fig. 10) where the flood flows are falsely retained within a hypothetical channel confine. An examination of the flood depths given in Fig. 12 indicates that at the widest flood plain expanse of Fig. 10, the flood depth is about 6-feet, yet the flood plain is not delineated to expand southerly, but is modelled to terminate based on the assumed gradient of the topography towards the channel. Such complications in accommodating an expanding flood plain when using a one-dimensional model are obviously avoided by using a two-dimensional approach.

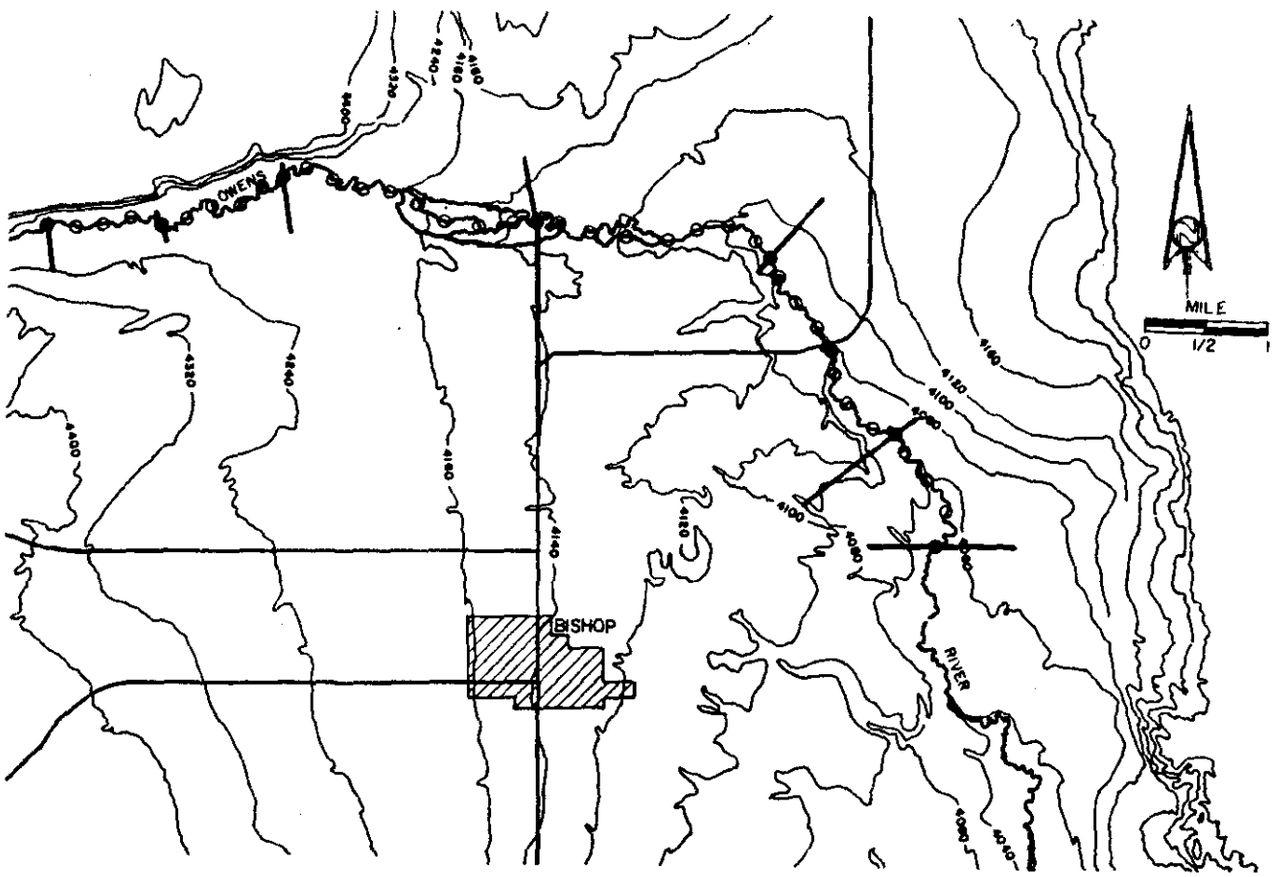

Fig. 9. Surveyed cross section locations on Owens River for use in K-634 model

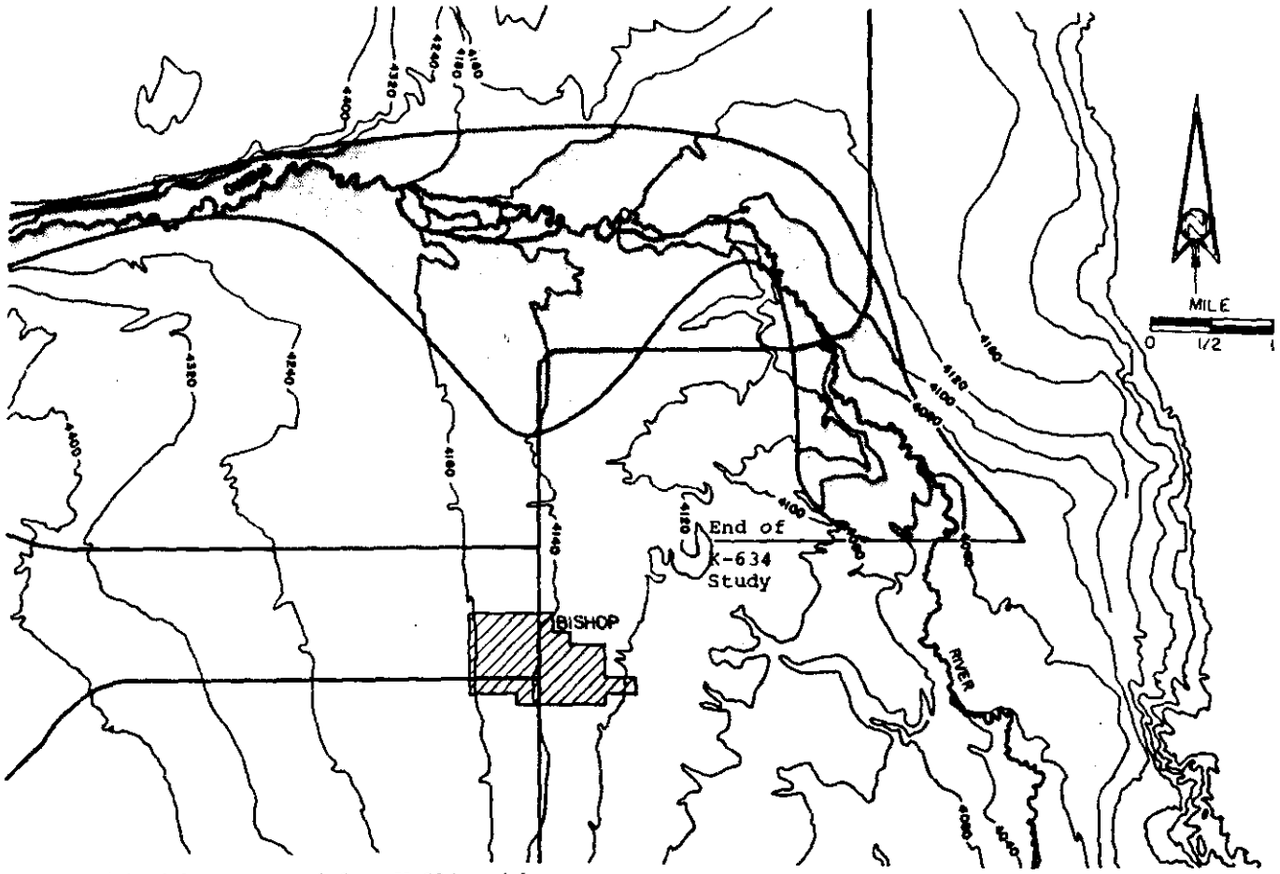

Fig. 10. Floodplain computed from K-634 model

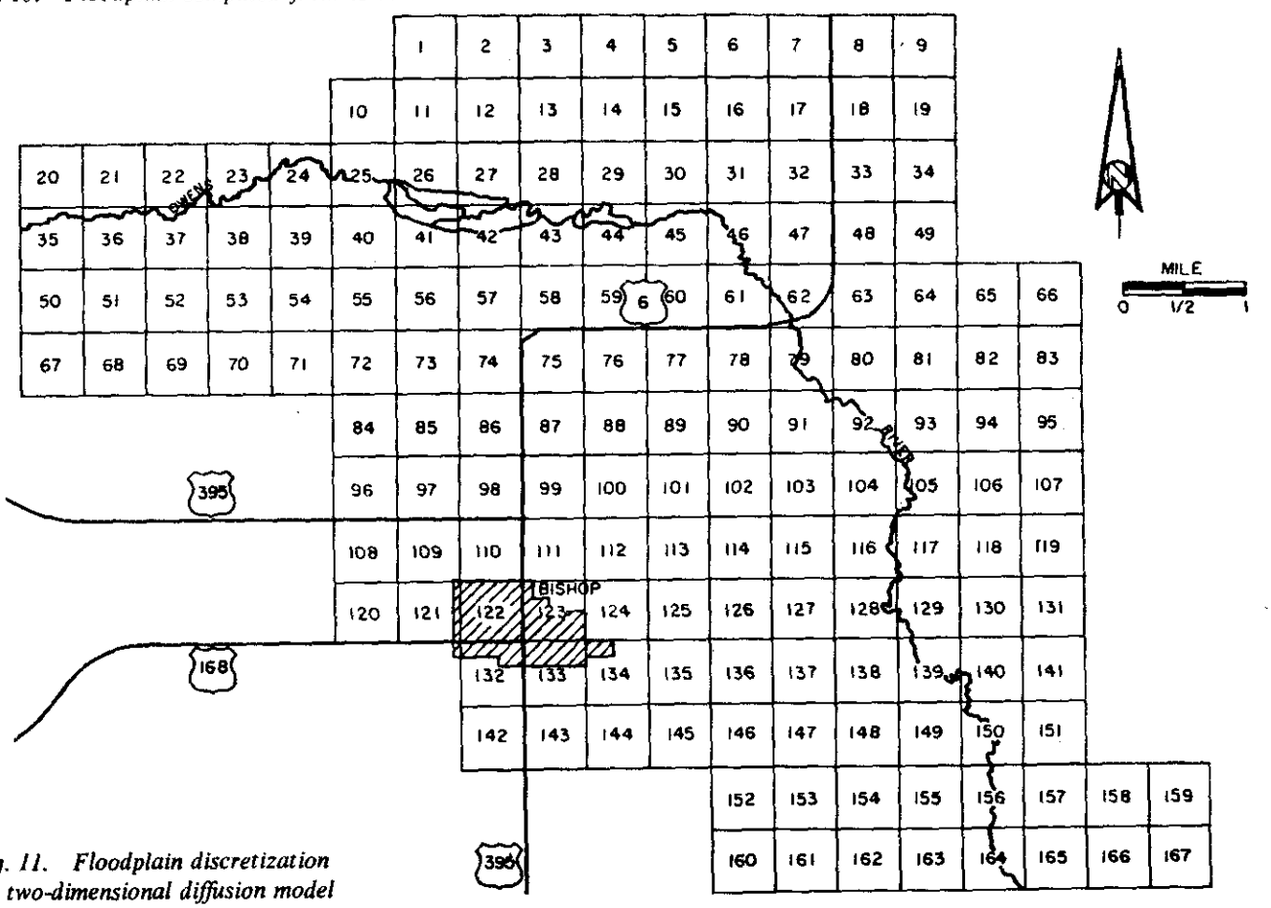

Fig. 11. Floodplain discretization for two-dimensional diffusion model

The two-dimensional DHM is now applied to the hypothetical dam-break problem using the grid discretization shown in Fig. 11. The same inflow hydrograph produced by the K-634 model is used for the DHM. Again, the Manning's friction factor of 0.04 was used. The resulting flood plain is shown in Fig. 13 for the $\frac{1}{4}$-square-mile grid model.

Comparisons of predicted maximum water elevations are shown in Fig. 12 which plots K-634 modelling results and the two-dimensional modelling results. The two approaches are comparable except at points shown as A and B in the figure. Point A corresponds to the predicted breakout of flows away from the Owens River channel with flows travelling southerly towards the City of Bishop. As discussed previously, the K-634 predicted flood depth corresponds to a flow depth of 6 feet (above natural ground) which is actually unconfined by the channel. The natural topography will not support such a flood depth and, consequently, there should be southerly breakout flows such as predicted by the two-dimensional model. With such breakout flows included, it is reasonable that the two-dimensional model would predict a lower flow depth at point A.

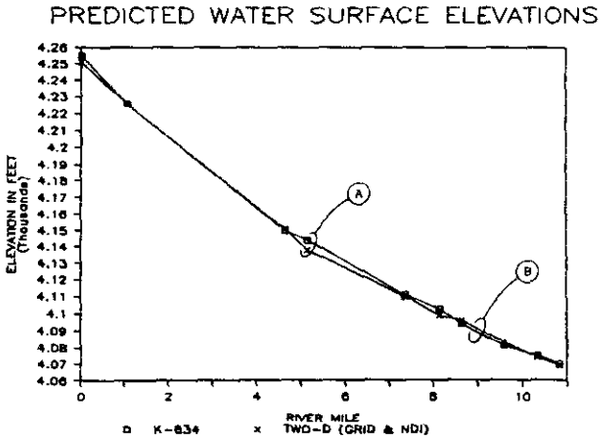

Fig. 12. Comparison of modelled water surface elevations

At point B, the K-634 model predicts a flood depth of approximately 2 feet less than the two-dimensional model. However at this location, the K-634 modelling results are based on cross-sections which traverse a 90-degree bend. In this case K-634 model will over-estimate the true channel storage, resulting in an underestimation of flow depths.

In comparing the various model predicted flood depths and delineated plains, it is seen that the two-dimensional DHM produced more reasonable predictions of the flood plain characteristics which are associated with broad, flat plains such as found at the study site than the one-dimensional model. The DHM model affords approximation of channel bends, channel expansions and contractions, flow breakouts, and the general area of inundation. Additionally, the DHM approach allows for the inclusion of return flows (to the main channel) which result due to upstream channel breakout flows, and other

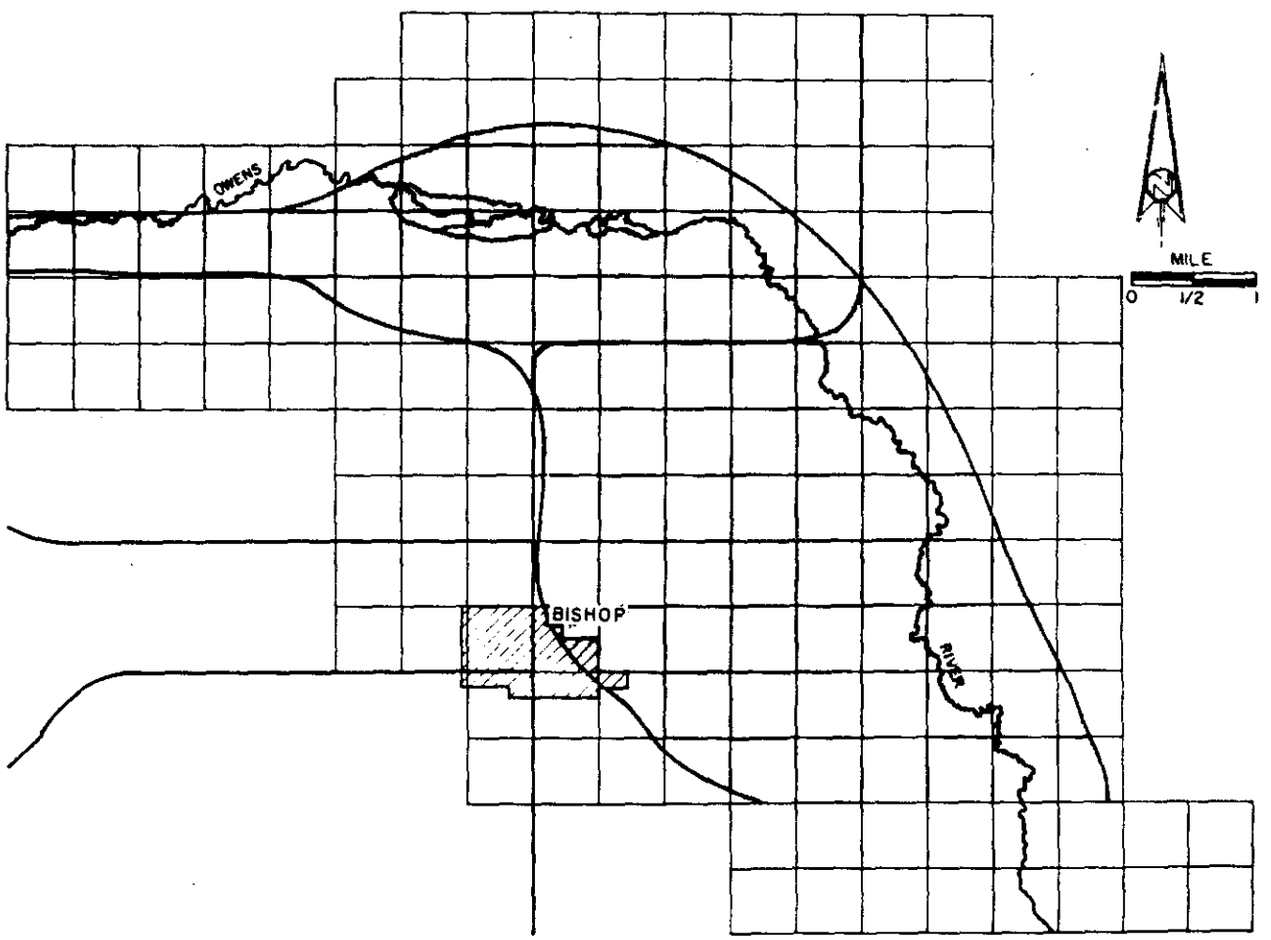

Fig. 13. Floodplain for two-dimensional diffusion model

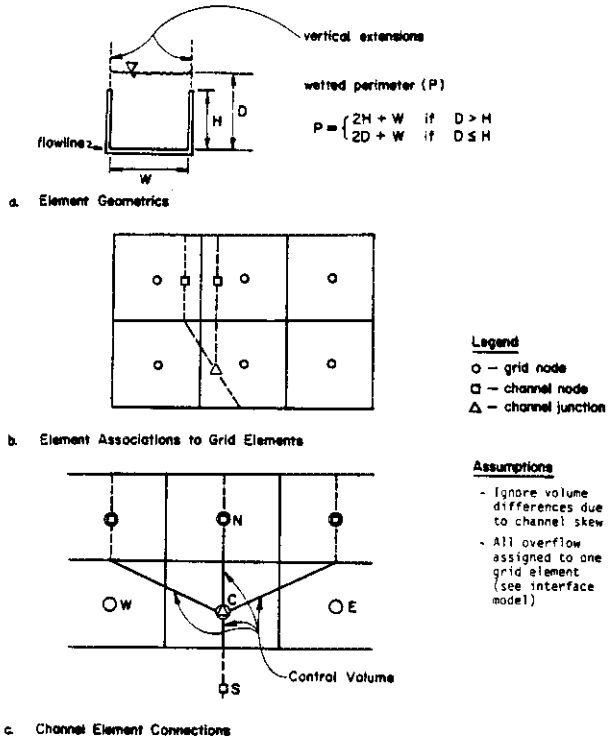

Fig. 14. DHM one-dimensional channel elements

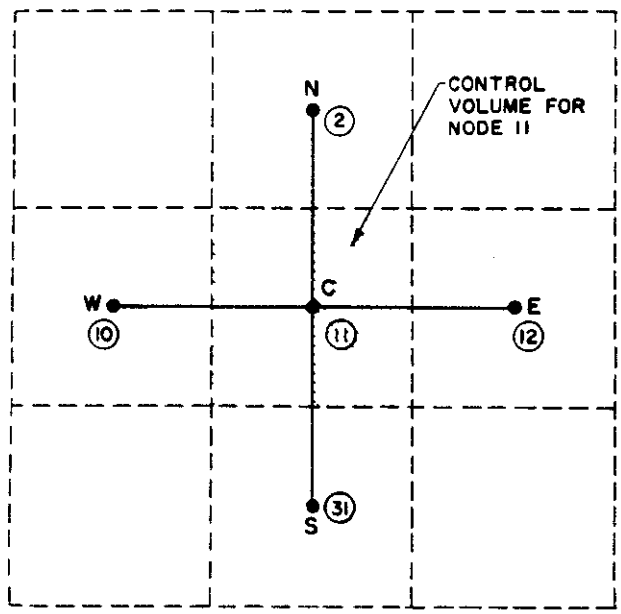

Fig. 15. Grid element nodal molecule

two-dimensional flow effects without the need for special modelling accommodations which would be required when using a one-dimensional model.

III. PROGRAM DESCRIPTIONS OF DHM MODEL

INTRODUCTION

A computer program for the two-dimensional diffusion hydrodynamic model which is based on the diffusion form of the St. Vincent equations where gravity, friction, and pressure forces are assumed to dominate the flow equation will be discussed in this section.

The DHM model consists of a 1-D channel and 2-D flood plain models, and an interface sub-model. The one-dimensional channel element utilizes the following assumptions:

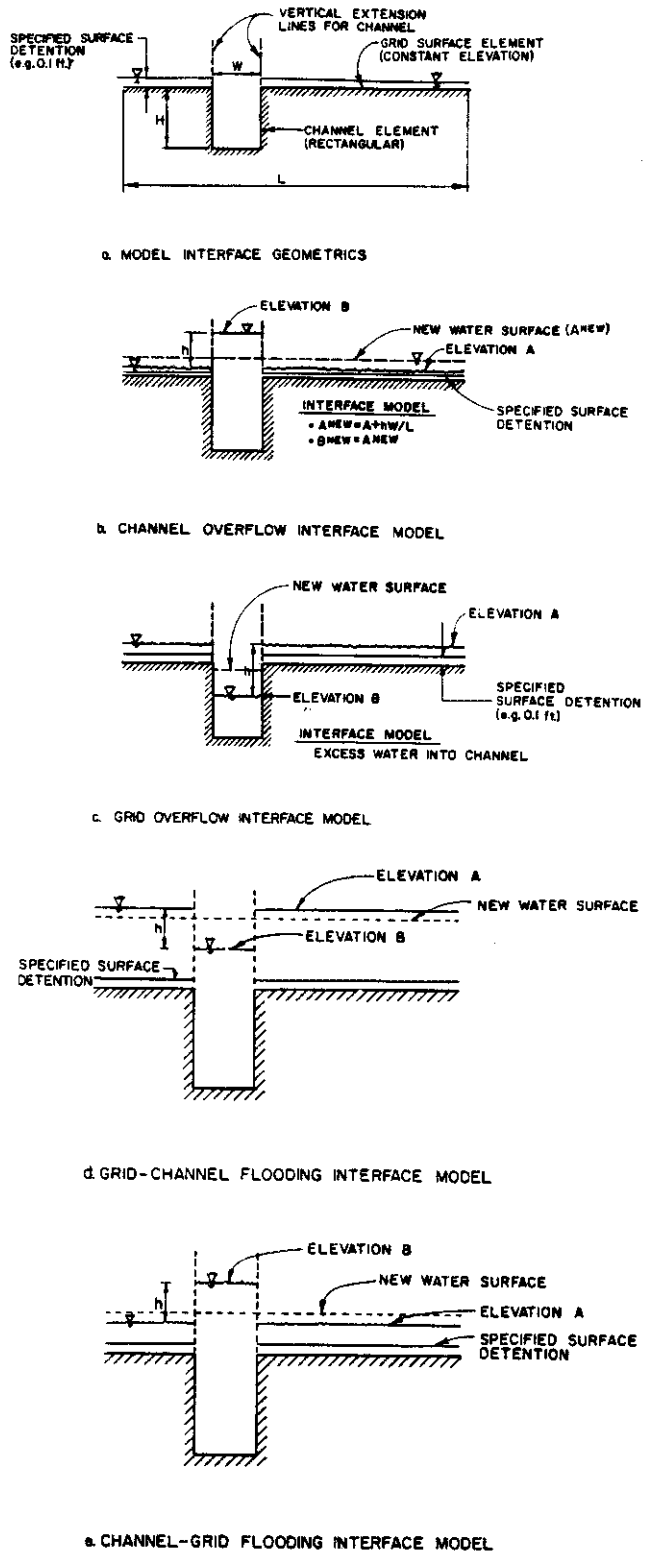

Fig. 16. DHM interface model

(1) infinite vertical extensions on channel walls (Fig. 14a),
(2) wetted perimeter is calculated as shown on Fig. 14b,
(3) volumes due to channel skew is ignored (Fig. 14c), and
(4) all overflow water is assigned to one grid element (Fig. 15).

The interface model calculates the excess amount of water either from the channel element or from the flood plain element. This excess water is redistributed to the flood plain element or the channel element according to the water surface elevation.

This FORTRAN program has the capabilities to simulate both one- and two-dimensional surface flow problems, such as the presented one-dimensional open channel flow and two-dimensional dam-break problems. Engineering applications of the program will be presented in the next section.

III.1 INTERFACE MODEL

Introduction

The interface model modifies the water surface elevations of grid (flood plain) and channel elements at specified time intervals (update intervals). There are three cases of interface situations: (1) channel overflow, (2) grid overflow, and (3) flooding of channel and grid elements.

III.1.1 Channel overflow

When the channel is overflowing, the excess water is temporarily stored in the vertical extension area (Fig. 16b). This excess water ($h \cdot w \cdot L$) is subsequently uniformly distributed over the grid element. In other words, the new grid water surface elevation is equal to the old water surface elevation plus a depth of hw/L, and the channel water surface elevation now matches the parent grid water surface elevation.

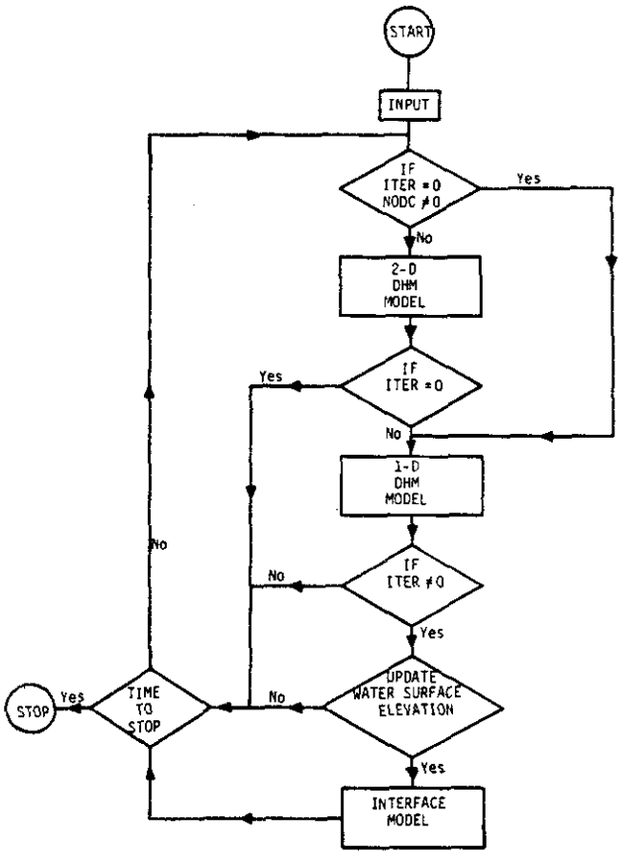

Fig. 17a. Flow chart for DHM model

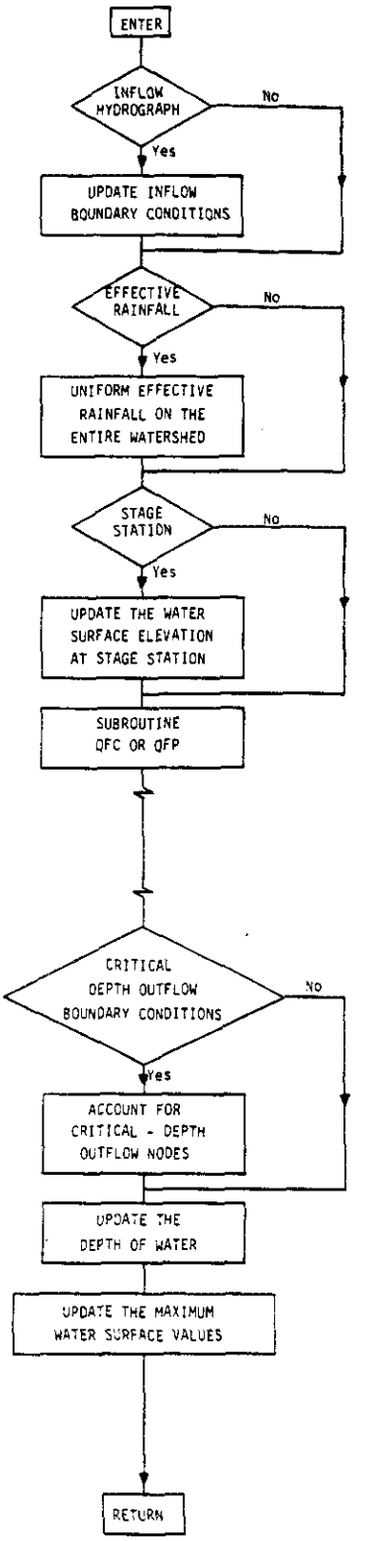

Fig. 17b. Flow chart for channel and floodplain DHM models

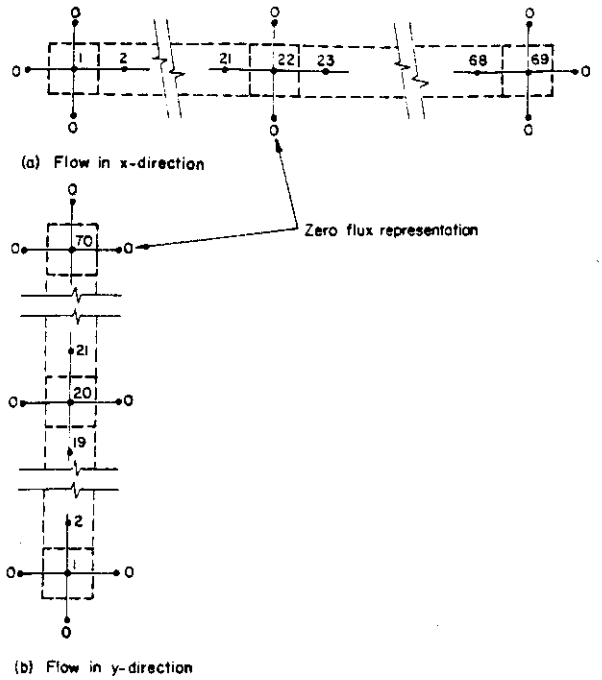

Fig. 18. One-dimensional grid element

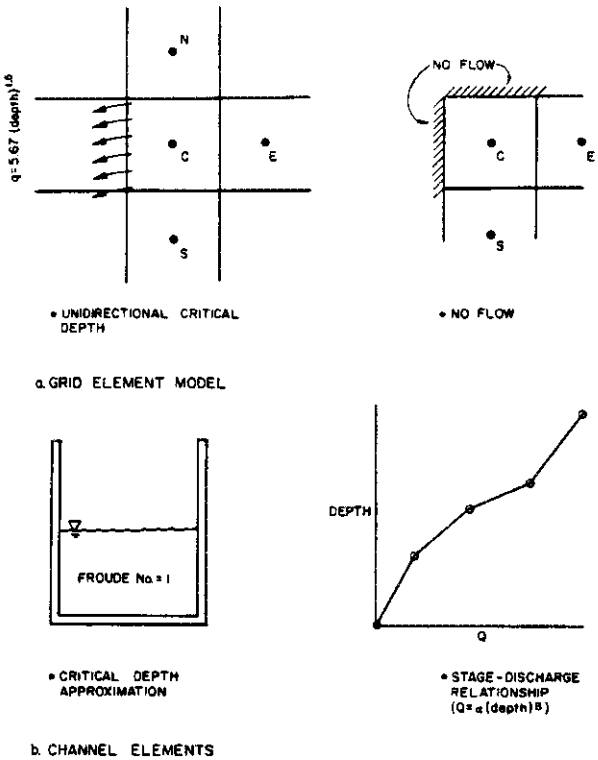

Fig. 19. DHM boundary conditions models

III.1.2 Grid overflow

When the surface water elevation of the grid element is greater than a specified surface detention (Fig. 16a), the excess water drains into the channel element and the new surface water elevation is changed according to the following two conditions (Fig. 16c), (a) If $v > v'$, where v denotes the excess volume of water per unit length and v' denotes the available volume per unit length, the new water surface of the grid element is $A^{NEW} = A^{OLD} - (v - v')/L$ and the new water surface elevation of the channel element is also equal to A^{NEW}; (b) If $v \leqslant v'$, the new water surface elevation of the grid element is $A^{NEW} = A^{OLD} - h$ and the new water surface elevation of the channel element is $B^{NEW} = B^{OLD} + v/w$.

III.1.3 Flooding of channel and grid

When flooding occurs, the water surface elevations of the grid and channel elements are both greater than the specified surface detention elevation. Two cases have to be considered as follows:

(1) If $A > B$ (Fig. 16d), the new water surface elevation of the grid element is $A^{NEW} = A^{OLD} - h(L - w)/L$ and the new water surface elevation of the channel element is equal to A^{NEW}.
(2) If $A < B$ (Fig. 16e), the new water surface elevation of the grid element is $A^{NEW} = A^{OLD} + h \cdot w/L$ and the new water surface elevation of the channel element is equal to A^{NEW}.

III.2 COMPUTER PROGRAM

III.2.0 Introduction

Figures 17a and 17b depict the simple flow chart for the DHM Model. The listings of the computer program and an example input file are included in the appendix.

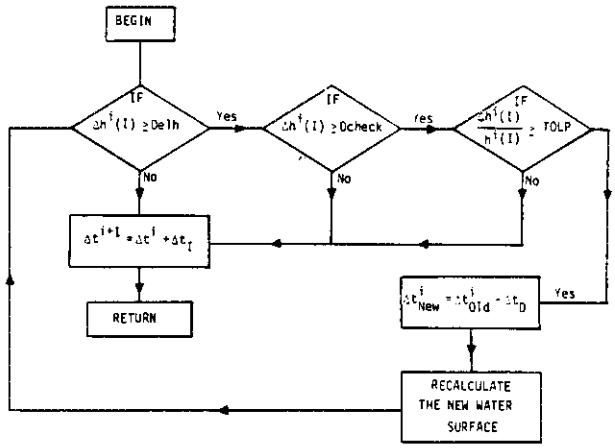

Fig. 20. Algorithm for the variable time step

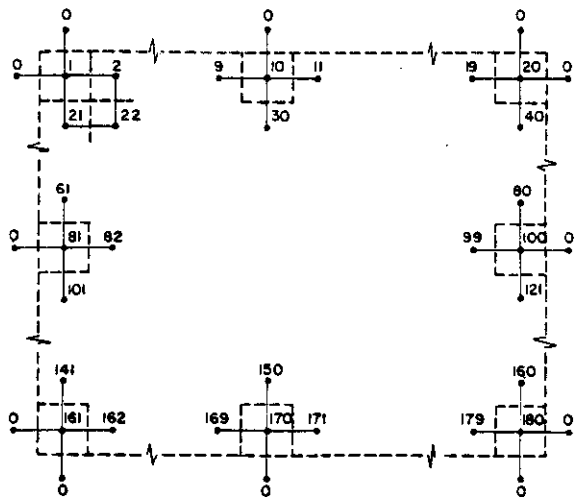

Fig. 20. No flux boundary nodes

III.2.1 Input file descriptions

The DHM model calls for the following data entries:

Line	*Variables*
1	DTMIN,DTMAX,DTI,DTD,SIMUL,ITER,TOUT,KODE,KMODEL
2	NNOD,NODC,SIDE,TOL,DTOL,DTOLP,TI,TO
3	FP(1,J),J = 1,7
⋮	⋮
NNOD + 2	FP(NNOD,J)J = 1,7
NNOD + 3	NERI
NNOD + 4	(R(I,J),J = 1,2),I = 1,NERI
NNOD + 5	NFPI,NPFPI
NNOD + 6	KINP(1),(HP(1,J,1),HP(1,J,2),J = 1,NPFPI)
⋮	⋮
NNOD + 5 + NFPI	KINP(NFPI),(HP(NFPI,J,1),HP(NFPI,J,2),J = 1,NPFPI)
NNOD + NFPI + 6	NDC
NNOD + NFP + 7	NODDC(I),I = 1,NDC
NNOD + NFPI + 8	NFLUX,NFOUT
NNOD + NFPI + 9	NODFX(I),I = 1,NFLUX
NNOD + NFPI + 10	KK,(FC(KK,J),J = 1,5)
⋮	⋮
NNOD + NFPI + NODC + 9	KK,(FC(KK,J),J = 1,5)
NNOD + NFPI + NODC + 10	NCHI,NPCHI,NCHO,NPCHO,NSTA,NPSTA
NNOD + NFPI + NODC + 11	KIN(1),((H(1,J,1),H(1,J,2)),J = 1,NPCHI)
⋮	⋮
NNOD + NFPI + NODC + NCHI + 10	KIN(NCHI),((H(NCHI,J,1),H(NCHI,J,2)),J = 1,NPCHI)
NNOD + NFPI + NODC + NCHI + 11	KOUT(1),(HOUT(1,J,1),HOUT(1,J,2), HOUT(1,J,3),J = 1,NPCHO)
⋮	⋮
NNOD + NFPI + NODC + NCHI + NCHO + 10	KOUT(NCHO),(HOUT(NCHO,J,1),HOUT(NCHO,J,2), HOUT(NCHO,J,3),J = 1,NPCHO)
NNOD + NFPI + NODC + NCHI + NCHO + 11	NOSTA(1),(STA(1,J,1),STA(1,J,2),J = 1,, NPSTA)
⋮	⋮
NNOD + NFPI + NODC + NCHI + NCHO + 10 + NSTA	NOSTA(NSTA),(STA(NSTA,J,1),STA(NSTA,J,2), J = 1,NPSTA)

where

DTMIN	is the minimum allowable timestep in second,
DTMAX	is the maximum allowable timestep in second,
DTI	is the increment of timestep in second,
DTD	is the decrement of timestep in second,
SIMUL	is the total simulation time in hour,
ITER	is the update interval (timestep) that interface model is called,
TOUT	is the output period in hour,
KODE	$\begin{cases} 0, & \text{supress the efflux velocities} \\ 1, & \text{output the efflux velocities} \end{cases}$
KMODEL	$\begin{cases} 1, & \text{kinematic routing technique} \\ \text{otherwise}, & \text{diffusion hydrodynamic model} \end{cases}$
NNOD	is the total number of nodal points for floodplain,
NODC	is the number of channel element,
SIDE	is the dimension of the uniform grid side in feet,
TOL	is the specified surface detention in feet,
DTOL	is the minimum change of water depth in feet for each timestep,
DTOLP	is defined as $\text{DTOLP} = \frac{\text{change of water depth}}{\text{pervious water depth}} \times 100\%$
FP(I,1)	is the northern nodal point of node I,
FP(I,2)	is the eastern nodal point of node I,
FP(I,3)	is the southern nodal point of node I,
FP(I,4)	is the western nodal point of node I,

FP(I,5)	is the averaged Manning's friction factor for node I,
FP(I,6)	is the averaged surface elevation for node I in feet,
FP(I,7)	is the initial water depth for node I in feet,
NERI	is the number of uniform effective rainfall rate data pairs,
R(I,1)	is the time (hour) corresponding to the effective rainfall rate,
R(I,2)	is the effective rainfall intensity (in/hr) ordinate for effective rainfall rate,
NFPI	is the number of input nodal points for the flood plain,
NPFPI	is the number pair of inflow hydrograph rate entires,
KINP(I)	is the array that stores the inflow boundary condition nodal points,
HP(I,J,1)	is the time (hour) corresponding to the inflow hydrograph,
HP(I,J,2)	is the inflow rate (cfs) ordinate for the inflow hydrograph,
NDC	is the number of critical-depth outflow nodal points,
NODDC(I)	is the array which stores the critical-depth outflow nodal points,
NFLUX	is the number of nodal points where outflow hydrographs are being printed,
NFOUT	is the interval for outflow hydrograph (in timesteps),
NODF(I)	is the array which stores the nodal points where outflow hydrographs are being printed,
KK	is the nodal point for channel element,
FC(KK,1)	is the array which stores the averaged Manning's coefficient of the channel elements,
FC(KK,2)	is the array which stores the width of the channel elements,
FC(KK,3)	is the array which stores the depth of the channel elements,
FC(KK,4)	is the array which stores the bottom elevation of the channel elements,
FC(KK,5)	is the array which stores the initial water depth of the channel elements,
NCHI	is the number of the inflow boundary conditions for the channel system,
NPCHI	is the pair of inflow hydrograph entries of the channel system,
NCHO	is the number of the outflow boundary conditions for the channel system,
NPCHO	is the pair of outflow hydrograph entries of the channel system,
NSTA	is the number of the stage station nodal points,
NPSTA	is the pair of stage curve entries,
KIN(I)	is the array which stores the nodes of inflow hydrograph of the channel system,
H(I,J,1)	is the time (hour) corresponding to the inflow hydrograph for the channel system,
H(I,J,2)	is the inflow rate (cfs) ordinate for the inflow hydrograph for the channel system,
KOUT(I)	is the array which stores the nodes of outflow hydrograph of the channel system,
HOUT(I,1)	is the array which stores the depth that a specified stage-discahrge curve is used,
HOUT(I,2)	is the array which stores the multiplier of a stage-discharge curve,
HOUT(I,3)	is the array which stores the exponent of a stage-discharge curve,
NOSTA(I)	is the array which stores the node of stage curve for the channel system,
STA(I,J,1)	is the array which stores the time (hour) corresponding to the time-stage curve,
STA(I,J,2)	is the array which stores the water surface elevation (feet) of the time-stage curve.

Note:

1. If any value of NERI, NFPI, NDC, NFLUX and NODC is equal to zero, then the values for the corresponding array need not be entered in the input file. For example, if NERI = 0 then R(I,J) needs not be included in the input file.
2. If NODC equals to zero, then entire channel element information need not be entered in the input file.

III.3 USER'S INSTRUCTIONS

Introduction

The DHM model has the capabilities to perform: (1) one-dimensional analysis, (2) two-dimensional analysis and (3) one- and two-dimensional interface analysis.

III.3.1 One-dimensional analysis

For one-dimensional analysis, a zero value should be entered for variable ITER. The entries for array FP(I,J) should reflect the one-dimensional representation as shown in Fig. 18.

III.3.2 Two-dimensional analysis

For two-dimensional analysis, zero values should be assigned to variables ITER and NODC. The entire data entries for the channel system can be neglected in the input file.

III.3.3 One- and two-dimensional interface model

When variables ITER and NODC are not equal to zero, the interface model is called at each update interval to calculate the new surface water elevations for both the grid and channel elements. A negative sign should be used in the Manning's coefficient to indicate a channel element passing through a grid element.

III.3.4 Inflow boundary conditions

Inflow boundary conditions are described by a linear time-inflow rate hydrograph for each specified inflow grid or channel element.

III.3.5 Outflow boundary conditions

Outflow boundary conditions for channel element (Fig. 19a) are:

(1) unidirectional critical depth assumption, i.e., discharge per unit length is $q = 5.67\ (\text{depth})^{1.5}$, and
(2) no flow boundary conditions (Fig. 20).

Outflow boundary condition for channel system is described by the following equation (Fig. 19b) as:

$$Q = \begin{cases} 0 & \text{If } 0 \leqslant \text{depth of water} \leqslant \text{specified surface detention} \\ \alpha_1\ (\text{depth})^{\beta_1} & \text{If specified surface detention} < \text{depth of water} \leqslant d_1 \\ \alpha_2\ (\text{depth})^{\beta_2} & \text{If } d_1 < \text{depth of water} \leqslant d_2 \\ \vdots & \vdots \end{cases}$$

where d_1, d_2, ..., are the pre-determined values from a stage-discharge station and up to 10 set of data can be used to represent the stage-discharge relationship for each station.

III.3.6 Variable time step

Variable time step dramatically reduces the computational time. The algorithm of the variable time step is depeicted in Fig. 20.

where

$\Delta h^i(I)$	is the change of water depth for Node I at timestep i,
Delh	is the user specified tolerance,
Δt^i	is the interval for timestep i,
Δt_I	is the user specified incremental time interval,
Δt_D	is the user specified decremental time interval,
TOLP	is the user specified percentage of water depth, and
Dcheck	is the user specified percentage of water depth, and Dcheck is defined as Delh/TOLP.

III.3.7 Kinematic routing technique

The kinematic routing technique is also included in the DHM model. By setting KMODEL to 1, the kinematic routing is evoked. A comparison study between the kinematic routing technique and the diffusion model is presented in section V.

IV. APPLICATIONS OF THE DHM ONE-DIMENSIONAL MODEL

Application 1: Steady flow in an open channel

Because the DHM is anticipated for use in modelling watershed phenomena, it is important that the channel models represent known flow characteristics. Unsteady flow is examined in the previous section. For steady flow, a steady-state, gradually varied flow problem is simulated by the 2-D diffusion model. Figure 21 depicts both the water levels from the 2-D diffusion model and from the flow resistance equation. For an 8000 cfs constant inflow rate, the surface water profiles from both the 2-D diffusion model and the flow resistance equation match quite well. The discrepancies of these profiles occur at the break points where the upstream channel slope and downstream channel slope is equal to 0.001 and the downstream channel slope is equal to 0.005, the surface water level is assumed to be equal to the critical depth. However, Henderson (1966), notes that brink flow is typically less than the critical depth (Dc). The DHM water surface closely matches the 0.72 Dc brink depth.

It is clear to see that the DHM cannot simulate the hydraulic jump, but rather smooths out the usually assumed 'shock front'. However, when considering unsteady flow, the DHM may be a reasonable approach for approximating jump profile. For a higher inflow rate, 20 000 cfs, the surface water levels differ in the most upstream reach. Again, this is due to the downstream control, critical depth, of the flow resistance equation.

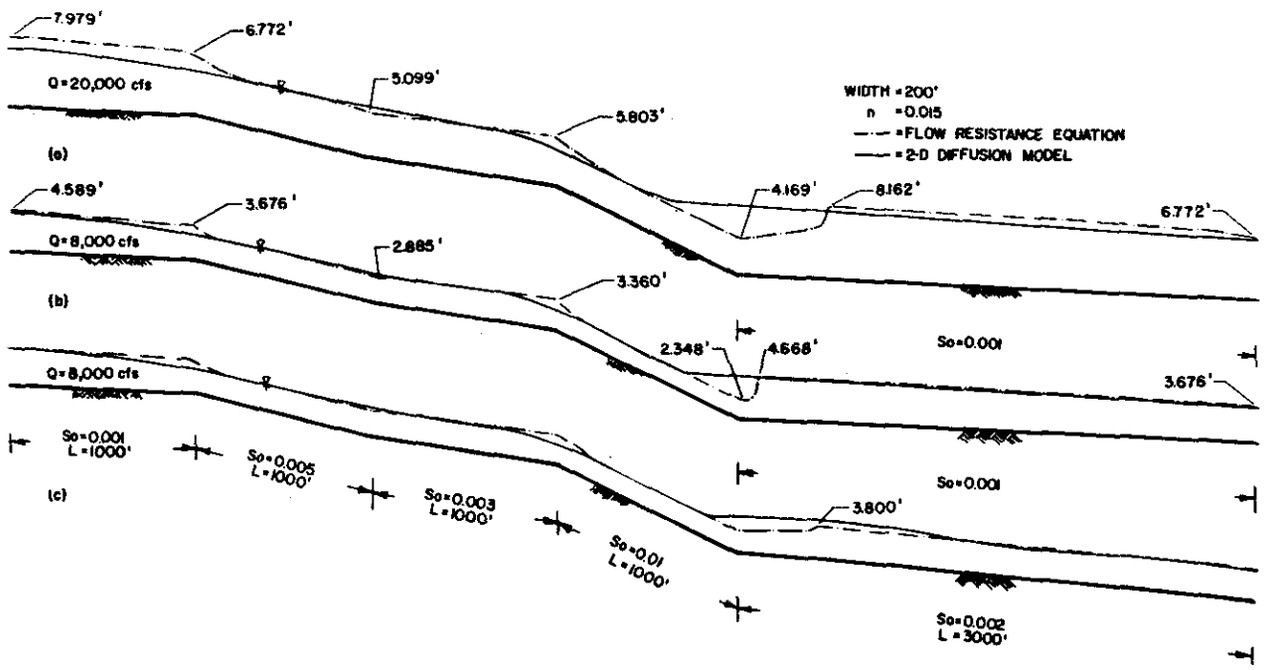

Fig. 21. Gradually varied flow profiles (Note DHM smoothing of hydraulic jumps and 'brink' flow depths less than critical depth)

IV.1 TWO-DIMENSIONAL APPLICATIONS

Application 2: Rainfall-runoff model

The DHM can be used to develop a runoff hydrograph given the time distribution of effective rainfall. To demonstrate the DHM runoff hydrograph generation, the DHM is used to develop a synthetic *S*-graph for a watershed where overland flow is the dominating flow effect.

To develop the *S*-graph, a uniform effective rainfall is assumed to uniformly occur over the watershed. For each timestep (e.g., 5-seconds), an incremental volume of water is added directly to each grid-element based on the assumed constant rainfall intensity, resulting in an equivalent increase in the nodal point depth of water. Runoff flows to the point of concentration according to two-dimensional diffusion hydrodynamics.

The following applications show *S*-graphs developed for several hypothetical watersheds with various cross-slopes, channel slopes, areas, and friction factors. Figure 22 shows the watershed discretization used for the *S*-graph development shown in Fig. 23. Included for comparison purposes in Fig. 23 are the S.C.S. *S*-graphs for a triangular and a curvilinear unit hydrograph representations. It is seen that the DHM runoff *S*-graph closely matches the equivalent S.C.S. *S*-graph. Fig. 24 shows other *S*-graphs developed for different watershed configurations and conditions. From the figure, all *S*-graphs have a strong similarity to the S.C.S. *S*-graph.

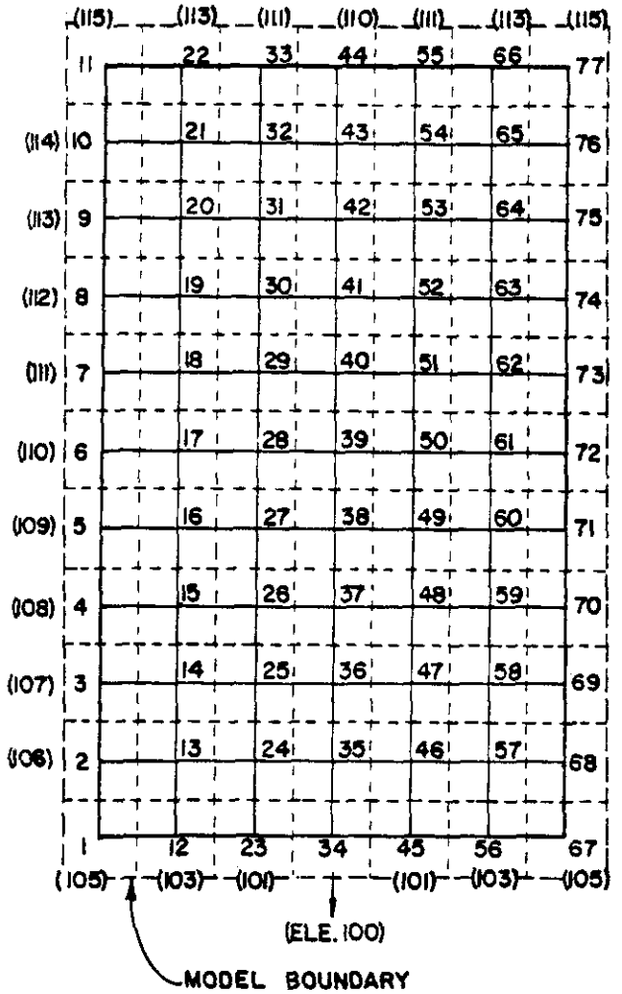

Fig. 22. Test watershed discretization

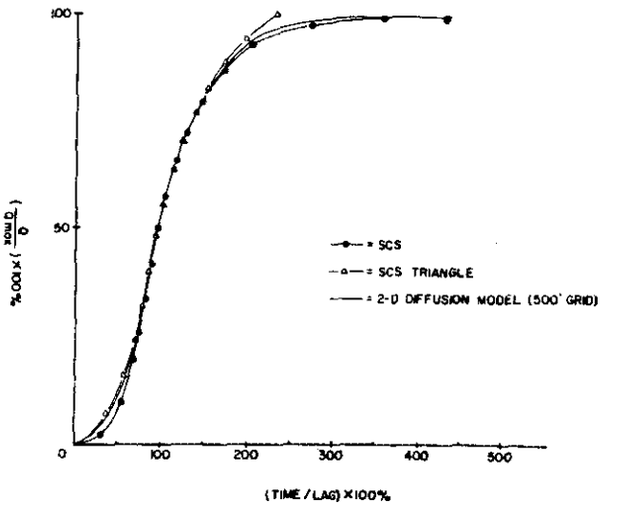

Fig. 23. Diffusion model produced S-graph and S.C.S. S-graphs

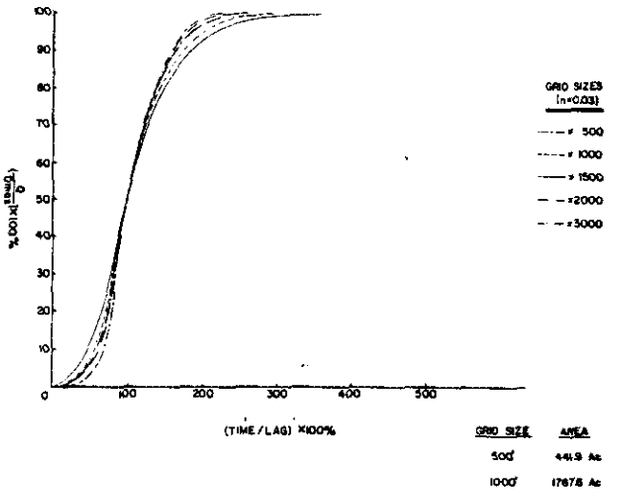

Fig. 24a. Diffusion model produced S-graphs for various grid sizes (nodal elevations held constant)

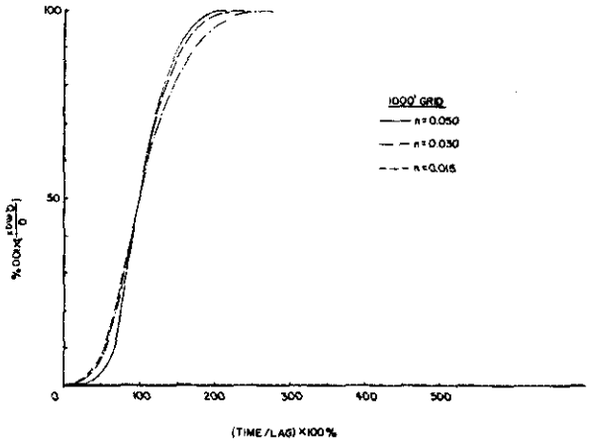

Figure 24b. Diffusion model produced S-graph for various Manning's friction factors

Application 3: Rainfall-runoff model

The 10 square mile Cucamonga Creek watershed (California) is shown discretized by 1000-foot grid elements in Fig. 25. A design storm (Fig.26a) applied by the U.S. Army Corps of Engineers and resulting runoff

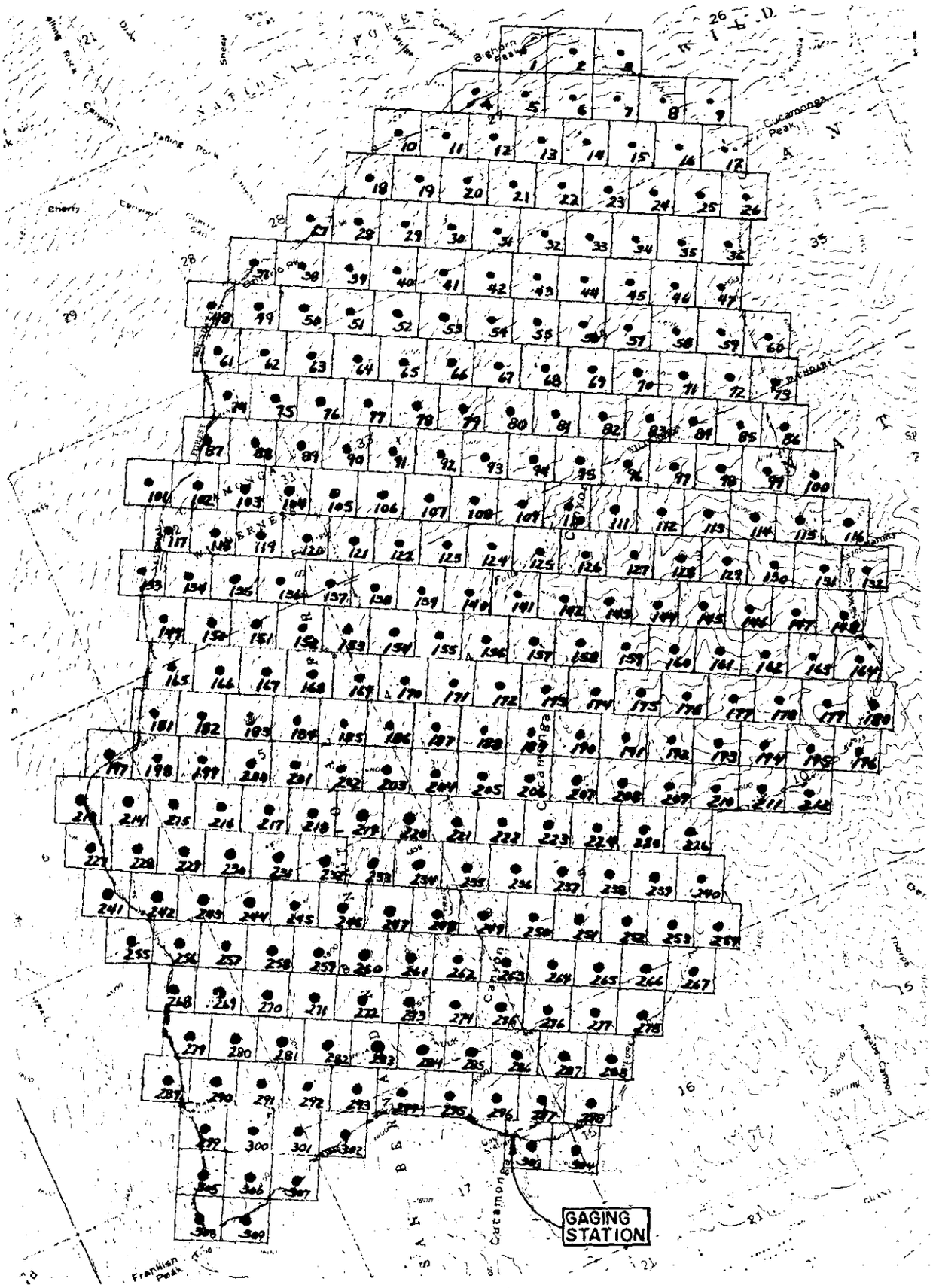

Fig. 25. Cucamonga Creek discretization

hydrograph is shown in Fig. 26b. Also shown in Fig. 26b is the corresponding DHM runoff hydrograph. From the figure, the diffusion model develops runoff quantities which are in good agreement with the values computed using unit hydrograph (S-graph) derived from stream gage data.

Application 4: Small-scale dam-break floodplain analysis

The DHM is applied to a hypothetical dam-failure of the Orange County Reservoir located north of the City of Brea, Orange County, California (see Fig. 27). The study site (Fig. 28) includes the area between the Orange County Reservoir (north of the City of Brea) and the proposed Brea Mall development. This application of the DHM illustrates its use in a municipal setting where flood flow patterns are impacted by railroads, bridge undercrossings, and other man-made obstacles to flow.

Using current U.S.G.S. topographic quadrangle maps (photo-revised, 1981) a 500-foot grid control volume discretization was constructed as shown in Fig. 29.

In each grid, an area-averaged ground elevation was estimated based on the topographic map. A Manning's friction factor of $n = 0.040$ was used throughout the study. (Canyon reaches, $n = 0.030$; grassy plains, $n = 0.050$).

Major assumptions used in this DHM application are as follows:

(1) Friction effects are modelled by Manning's equation as used in the DHM.
(2) All storm drain systems provide negligible draw off of the dam-break flows. This assumption accommodates a design storm in progress during the dam failure. This assumption also implies that storm water runoff provides a negligible increase to the dam-break flow hydrograph.
(3) All canyon damming effects due to culvert crossings provide negligible attenuation of dam-break flows. This assumption is appropriate due to the concurrent design storm assumption, and due to sediment deposition from transport of the reservoir earthen dam materials.
(4) The reservoir failure conforms to an outflow hydrograph such as shown in Fig. 30.

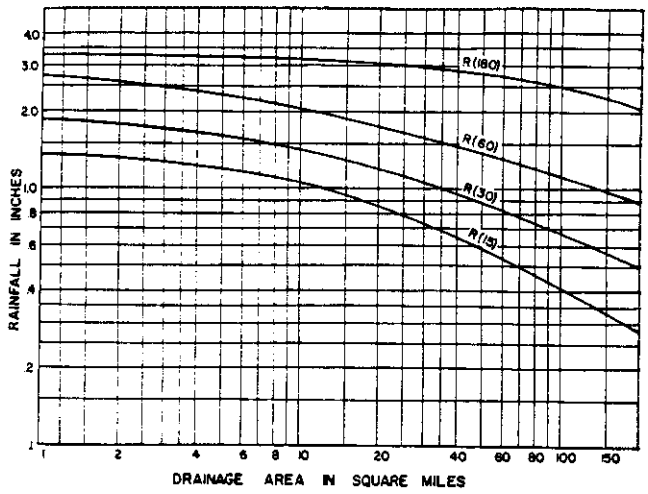

HYETOGRAPH COMPUTATION

UNIT PERIOD	AMOUNT	
1	.07	(R(180)-R(60))
2	.05	(R(180)-R(60))
3	.11	(R(180)-R(60))
4	.05	(R(180)-R(60))
5	.20	(R(180)-R(60))
6	.22	(R(180)-R(60))
7	.14	(R(180)-R(60))
8	.16	(R(180)-R(60))
9	.48	(R(60)-R(30))
10	.52	(R(60)-R(30))
11	1.00	(R(15))
12	1.00	(R(30)-R(15))

LOCAL PROJECT STORM
DEPTH AREA DURATION CURVES

Fig. 26a. Design storm

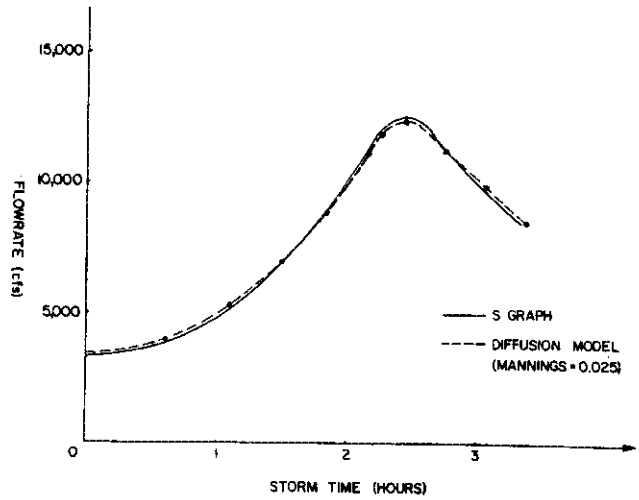

Fig. 26b. Modelled runoff hydrographs

The Orange County Reservoir is an earthen dam lined (along the interior) with concrete. In the improbable event of a failure, an erosive process will initiate which allows the escape flowrate to increase gradually rather than suddenly as would occur due to failure of a rigid structure.

Due to the low volume (200 acre-feet) retained in the reservoir, the outlet hydrograph assumed is a significant function of the remaining reservoir storage. That is, the reservoir volume is quickly depleted by low-to-moderate flows out of the reservoir.

To estimate a reasonable peak outlet flow, Q_p, an iteration method is used until a balance between the estimated outlet hydrograph Q_p is made to the resulting flowrate as a function of the remaining stored waters.

The ultimate outlet geometry is assumed to be a V-shaped massive failure with side slopes at a 45-degree incline. Flows are then based on critical depth, with a free outlet to the steep downstream canyon reaches. Backwater effects to the dam outlet are assumed negligible due to the steep terrain, and to also assume a more conservative condition.

Based on the above assumptions, the outlet flowrate for a ponded depth H (feet) is given (for the ultimate dam-break failure geometry) by $Q_p = 2.472\,H^{2.5}$ cfs. The reservoir rating curve relating basin depth to volume is shown in Table 1. For the assumed outlet hydrograph shape width Q_p occuring at 20-minutes after dam-failure, the volume drained by time 20-minutes is given by $V_d = 0.01377 Q_p$ (acre-feet). The estimate of Q_p is provided by the iteration shown in Table 2.

From the table, it is seen that Q_p is strongly influenced by the quick depletion of the reservoir's stored waters. It

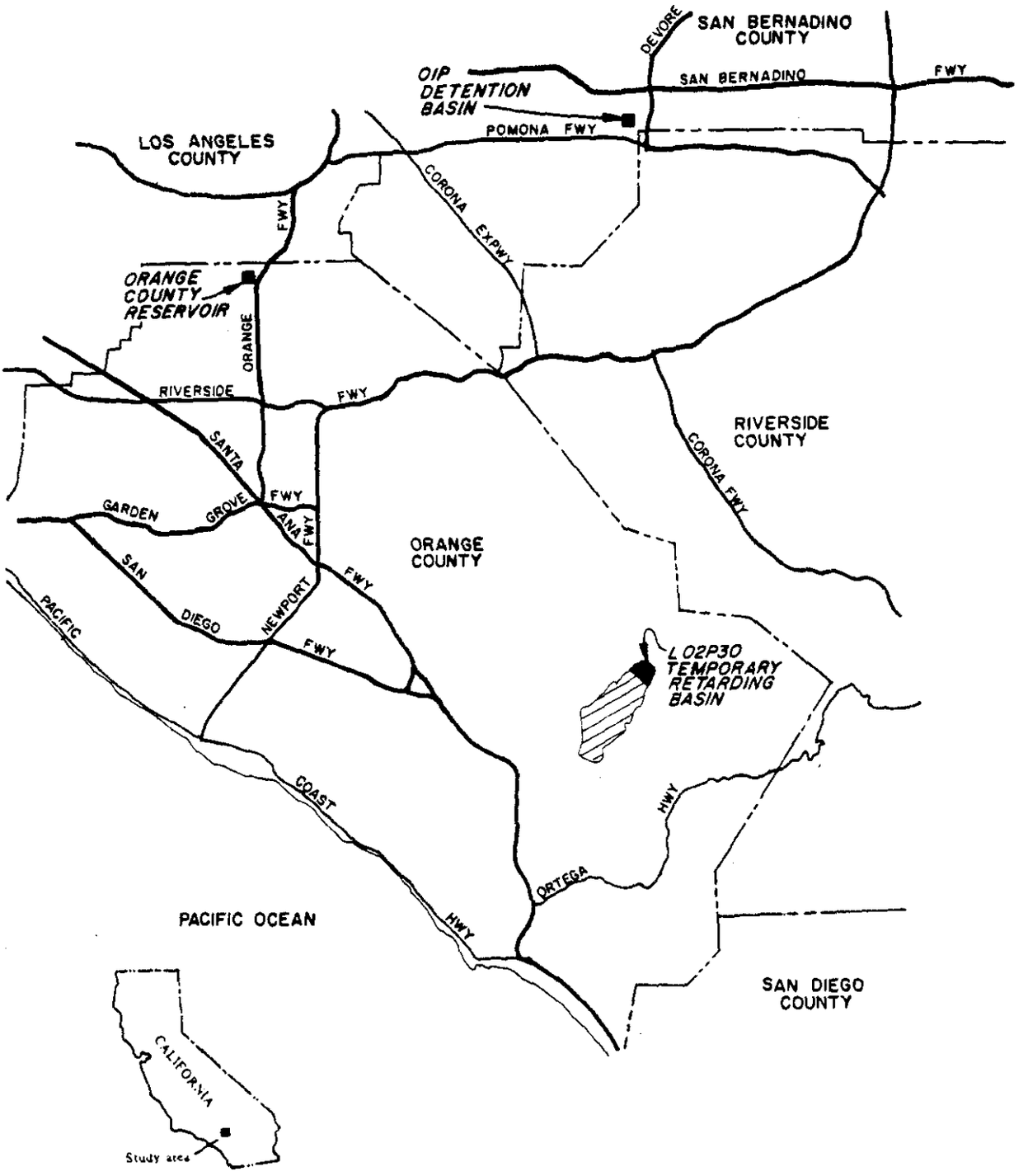

Fig. 27. Vicinity map for dam-break analyses

is also noted that the peak Q_p is assumed to occur at model time of 20-minutes which indicates a severe erosion rate that destroys a substantial earthen berm structure (lined with concrete on the basin interior) with flow velocities less than about 30 fps. Consequently, the estimated Q_p may be considered conservative.

The dam-break hydrograph of Fig. 30 was used on the inflow hydrograph to the grid network of Fig 29. The resulting flood-plain (using the DHM) is shown in Fig 31. From Figure 31 it is seen that the northeasterly portion of the Brea Mall is predicted to be subject to approximately 1.5-foot depth of flooding. This portion of the mall represents a lower level of the complex with parking lots located between the mall and the neighbouring boulevard.

It is noted, however, that the uncertainty in modelling results may be significant due to the modelling effort being based upon 20-foot contour U.S.G.S. topographic maps. To aid in reducing this uncertainty, several site examinations were conducted in order to verify the grid

schematic representation of the problem domain and the reasonableness in modelling results. The model discretization was adjusted when considered appropriate to better represent field conditions and subsequent modelling results rechecked by additional field investigations.

In order to develop more refined modelling results, detailed survey information would be required to reduce the uncertainty in elevations determined from the cited topographic maps.

Comparison of the flood plain to a previous study (Metropolitan Water District of Southern California, 1973) is shown in Fig. 32. The main differences in estimated flood plains is due to the dynamic nature of the diffusion model which accounts for the storage effects due to flooding, and the attenuation of a flood wave due to two-dimensional routing effects.

To examine the sensitivity in modelling results, the dam-break was assumed to occur at node 6 (neglecting canyon routing), and also the peak outflow was doubled to $Q_p = 18\,000$ cfs (at a time of 20 minutes). To allow this new Q_p to occur, the basin volume was doubled to over 400 acre-feet. The resulting flood plain is shown in Fig. 33. From this figure, it is seen that with doubling the basin capacity, only the northeastern portion of the Brea Mall site is still estimated to be affected by the hypothetic dam-

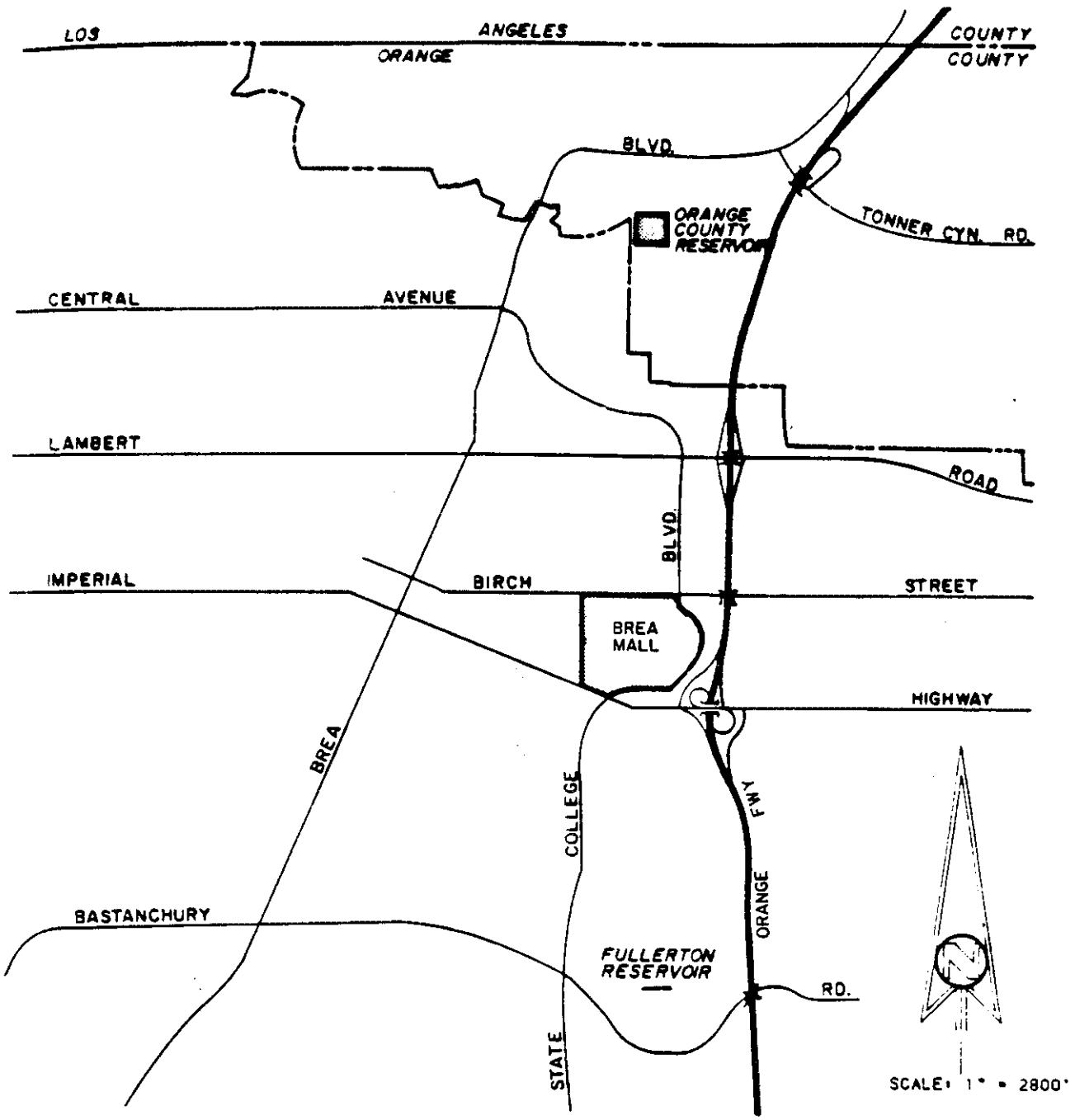

Fig. 28. Location map for the Orange County reservoir dam-break problem

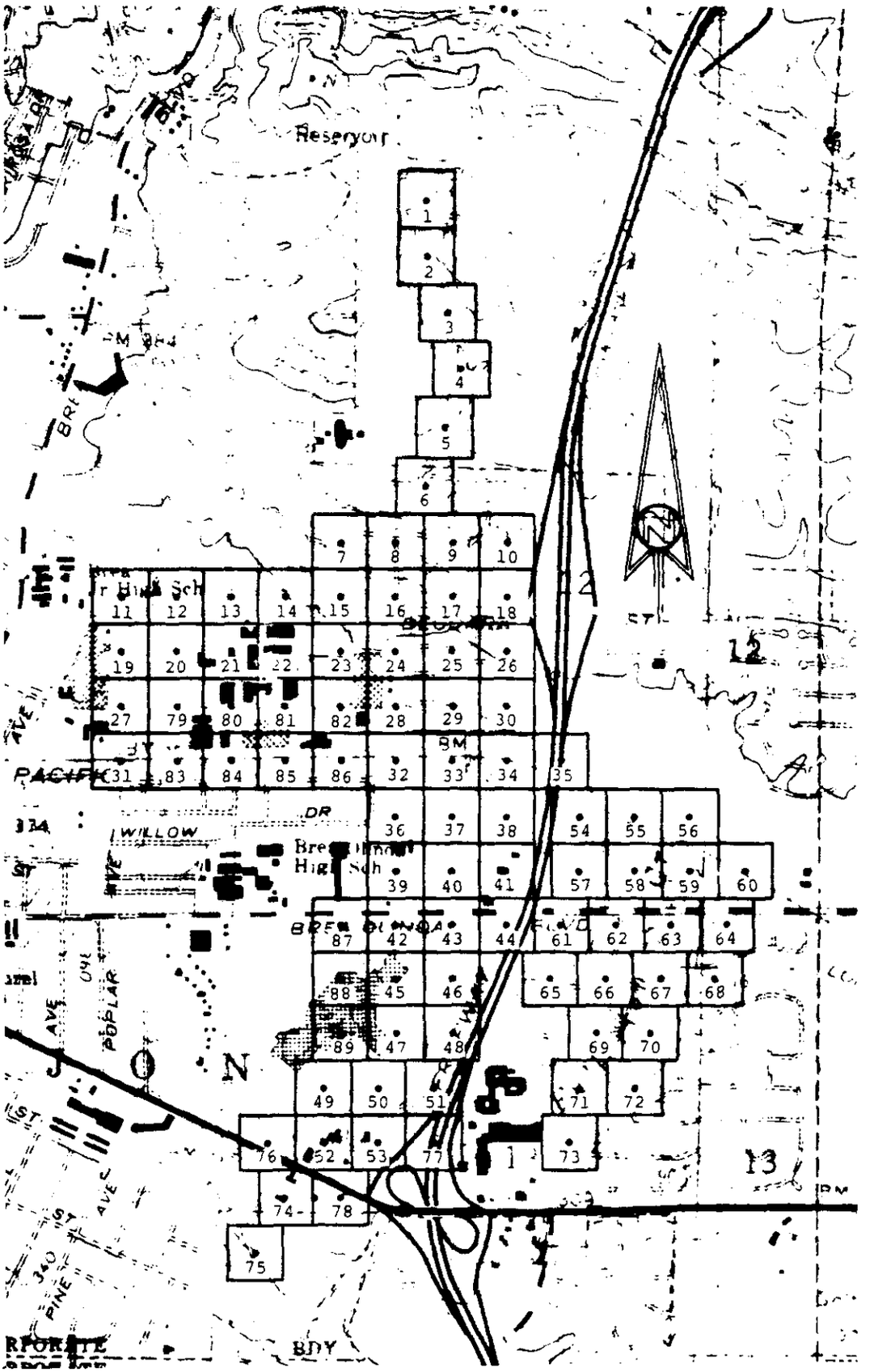

Fig. 29. Domain discretization for Orange County reservoir

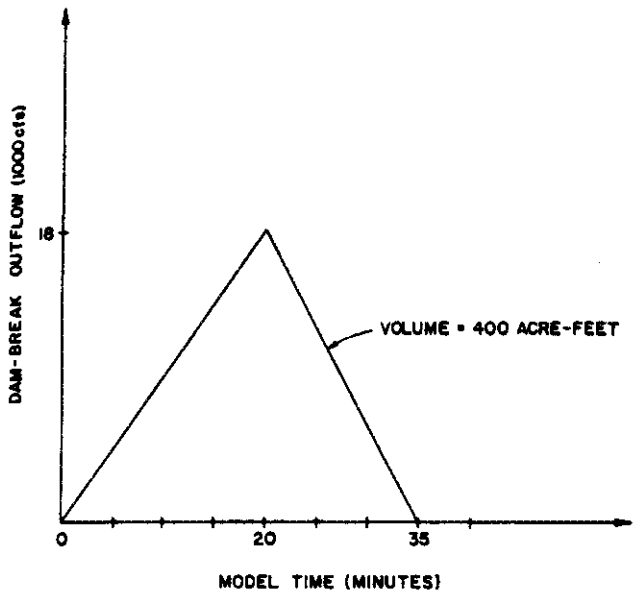

Fig. 30. Study dam-break outflow hydrograph

failure of the Orange County Reservoir. In this second analysis, the flooding depth is estimated to increase to about 2.5 feet.

Figure 34 shows lines of arrival times for the second (volume doubled) basin test study.

Application 5: Small-scale flows onto a flat plain

A common civil engineering problem is the use of temporary detention basins to offset the effect of urbanization on watershed runoff. A problem, however, is the analysis of the basin failure; especially, when the floodflows enter a wide expanse land surface with several small channels. This application is to present study conclusions in estimating the flood plain which may result from a hypothetical dam-failure of the L02P30 Temporary Retarding Basin. The results of this study are to be used to study the potential impacts of the area if the retention basis berm were to fail.

The study site includes the area south of Plano Trabuco, Phase I. It is bounded on the north by L02P30 Retarding Basin Berm, on the east and south of Portola Parkway and on the west by the Arroyo Trabuco bluffs (see Fig. 35).

Using a $1''=300'$ topographic map, a 200-foot grid control volume discretization was constructed as shown in Fig. 36. In each grid, an area-averaged ground elevation was estimated based on the topographic map. A Manning's friction factor of $n=0.030$ was used throughout the study.

Due to the low volume (80.5 acre-feet) retained in the reservoir, the outlet hydrograph assumed is a significant function of the remaining reservoir storage. That is, the reservoir volume is quickly depleted by low-to-moderate flows out of the reservoir.

To estimate a reasonable peak outlet flow, Q_p, an iteration method is used until a balance between the estimated outlet hydrograph Q_p is made to the resulting flowrate as a function of the remaining stored waters.

The ultimate outlet geometry is assumed to be a 90-foot wide rectangular broad crested spillway.

Based on the above assumptions, the outlet flowrate for a ponded depth H (feet) is given (for the ultimate dam-break failure geometry) by $Q_p=270\,H^{1.5}$ cfs. The rating curve relating basin depth to volume is shown in Table 3. For the assumed outlet hydrograph shape width Q_p occurring at 15-minutes after dam-failure, the volume drained by time 15-minutes is given by $V_d=0.01033Q_p$ (acre-feet). The estimate of Q_p is provided by the iteration shown in Table 4.

The dam-break hydrograph of Fig. 37 was used as seen in the inflow hydrograph to the grid network of Fig 36. The resulting flood-plain using the dam-break model is shown in Fig. 38. It is seen from Fig. 38 that the floodplain continues south across the Portola Parkway in some areas and also spreads westerly and eventually flows down the Arroyo Trabuco bluffs.

The profile of Portola varies approximately 2 feet above and below the adjacent land. Consequently, minor ponding may occur where Portola Parkway is high and sheet flow across Porthola Parkway will occur at low points. It should be noted that depths along Portola Parkway are less that 1 foot. Figure 39 shows lines of arrival times for the basin study.

Directly below the location of the dam-break at grid no. 3, the water depth is the greatest reading 1.3 feet, but the maximum depth of Portola Parkway is 0.8 feet. It is

Table 1. Orange County reservoir volume and dam-break outflow

Depth (ft)	Volume (af)	Q_p (Dam-break) (cfs)
2	4.6	14
4	9.5	79
6	14.8	218
8	20.3	447
10	26.4	782
12	32.7	1 233
14	39.4	1 813
16	46.5	2 530
18	54.1	3 400
20	62.0	4 420
22	70.3	5 611
24	79.2	7 000
26	88.5	8 520
28	96.2	10 300
30	108.4	12 200
32	119.1	14 300
34	130.2	16 700
36	141.9	19 200
38	154.0	22 000
40	166.7	25 000
42	179.9	28 300
44	193.8	31 800
46	211.0	35 500

Table 2. Estimating dam-break Q_p for Orange County reservoir (20-minute peak time)

Assumed depth (ft)	Q_p[1] (cfs)	Volume drained[2] (af)	Volume left[3] (af)	Depth (ft)
20.0	4 420	60.9	151.0	37.0
26.0	8 520	117.3	94.7	27.5
26.5	8 936	123.1	88.9	26.0

NOTES:
1: $Q_p=2.472H^{2.5}$
2: $V_d=0.1377Q_p$ AF
3: $V_{left}=(212-V_d)$ AF

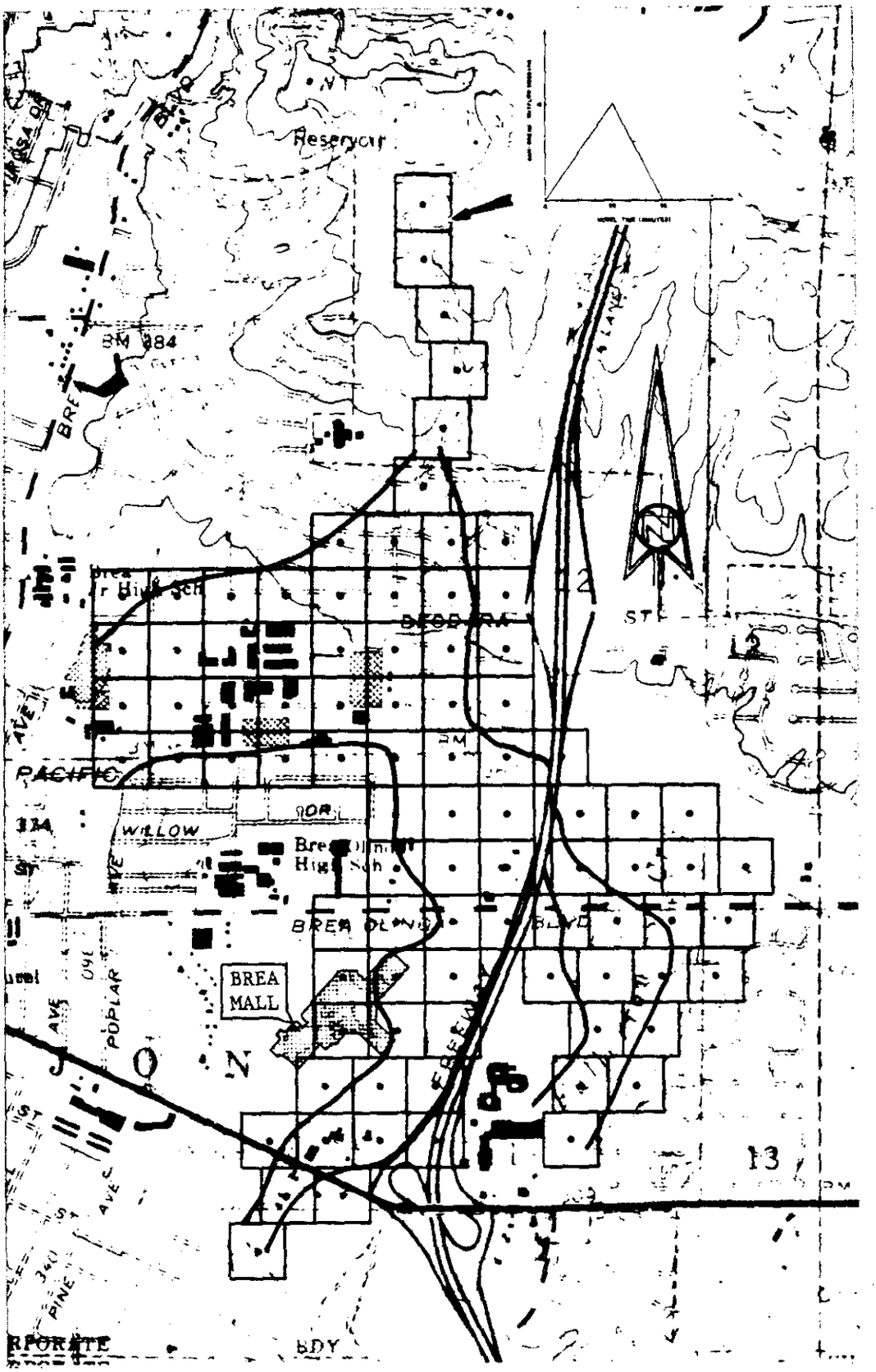

Fig. 31. Flood plain for 200 A.F. basin test for Orange County reservoir

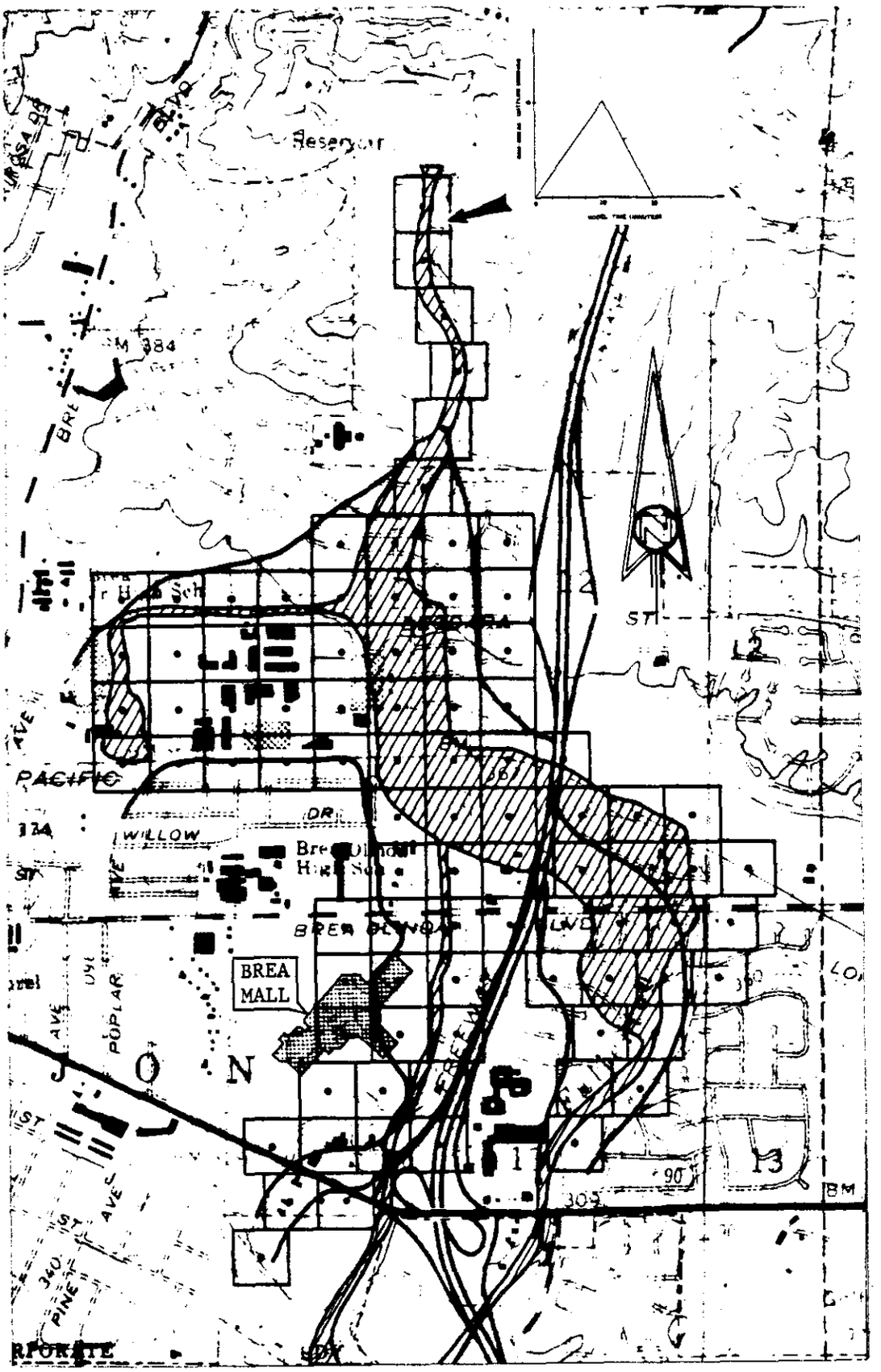

Fig. 32. Comparison of flood plain results

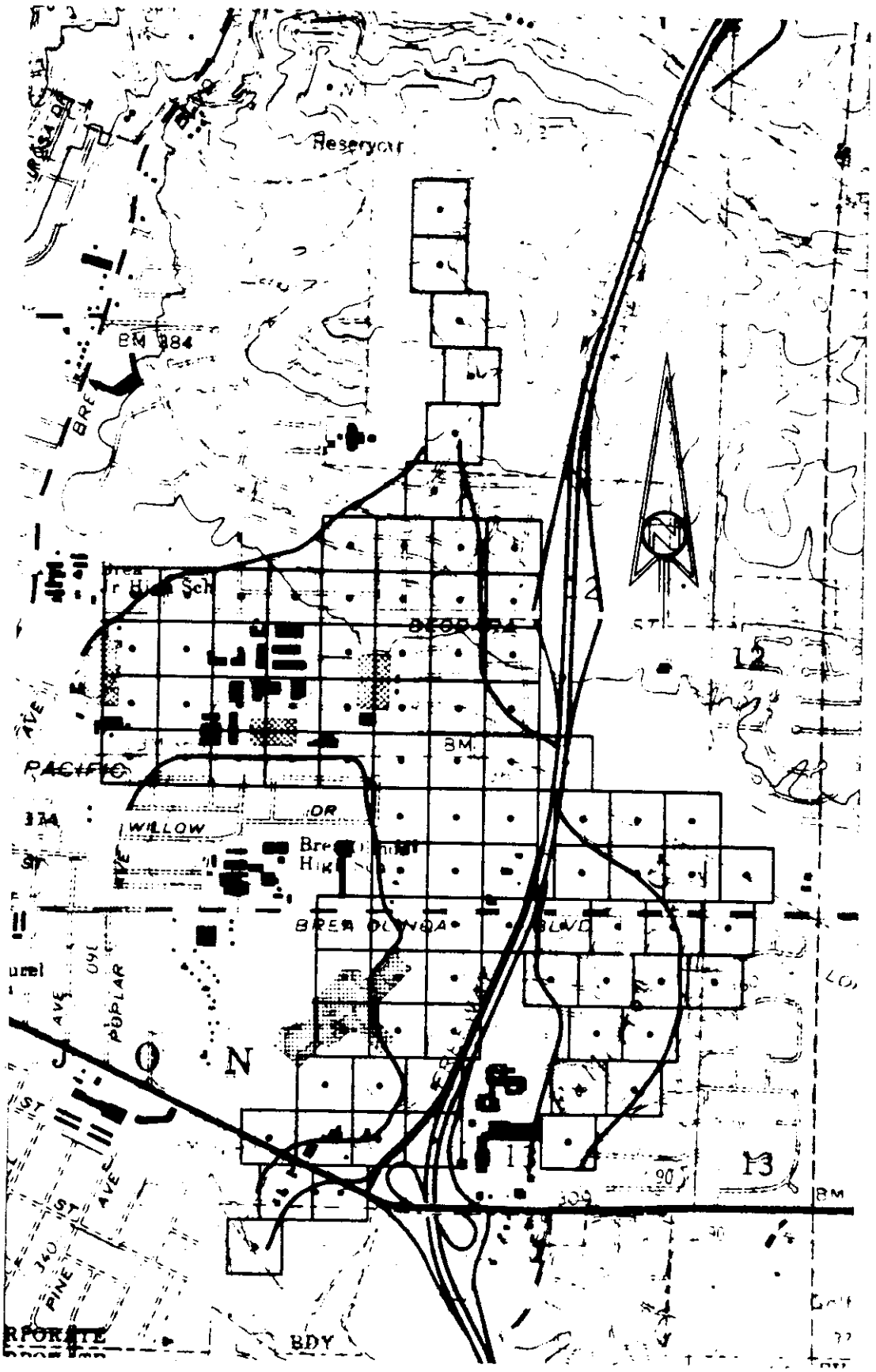

Fig. 33. Flood plain for 400 A.F. basin test for Orange County reservoir

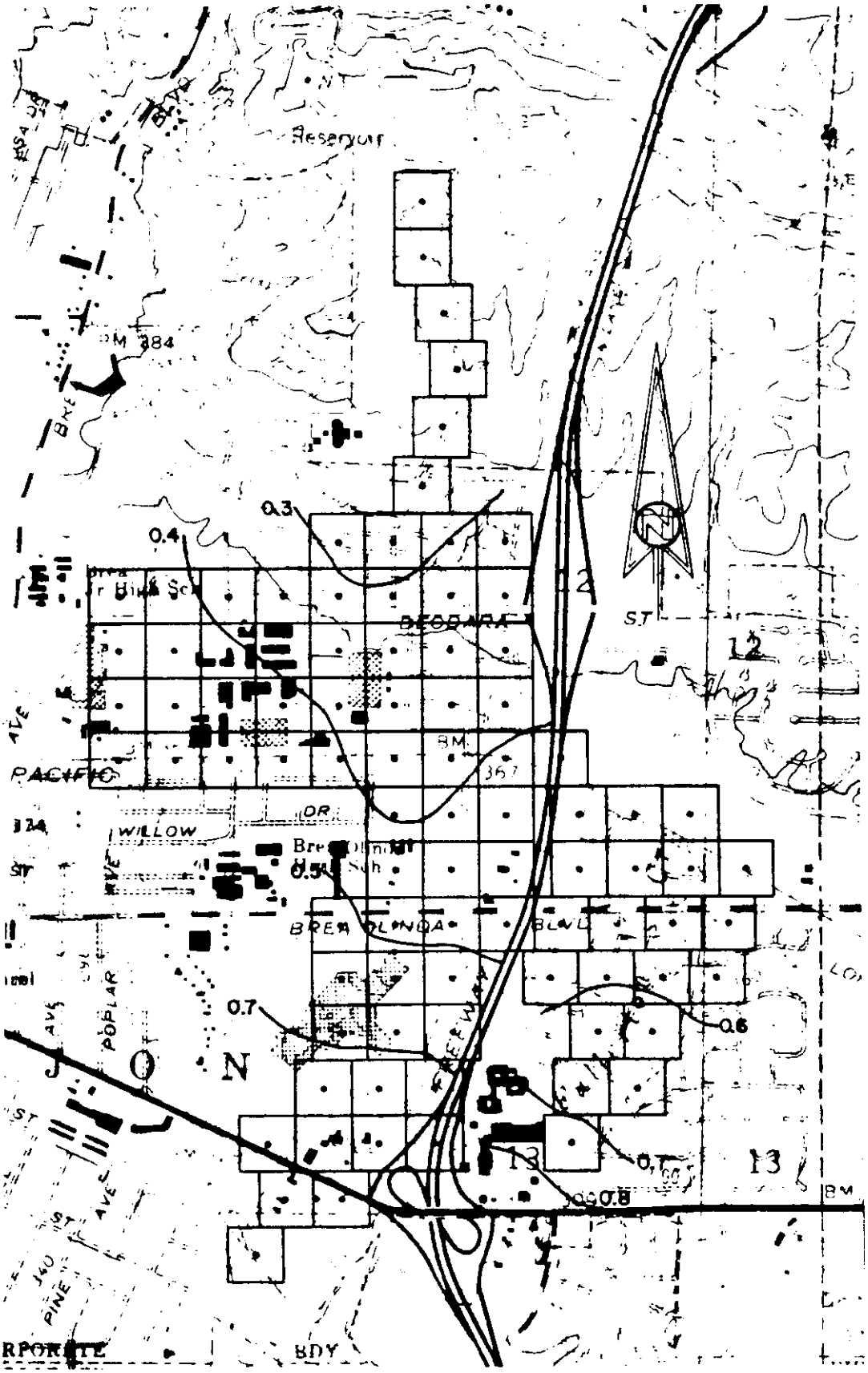

Fig. 34. Time (hours) of maximum flooding depth (400 A.F. basin test) for Orange County reservoir

concluded that Portola Parkway is essentially unaffected by a hypothetical failure of the L02P30 Temporary Retarding Basin.

Application 6: Two-dimensional floodflows around a large obstruction

In another temporary detention basin site, floodflows (from a dam-break) would pond upstream of a landfill site, and then split, when waters are deep enough, to flow on either side of the landfill. An additional complication is a railroad berm located downstream of the landfill, which forms a channel for floodflows. The study site (see Fig. 40) is bounded on the north by a temporary berm approximately 300 feet north of the Union Pacific Railroad, bounded on the east by Milliken Avenue, bounded on the south by the Union Pacific Railroad and bounded on the west by Lower Deer Creek.

In this problem, a four-foot berm is to represent the

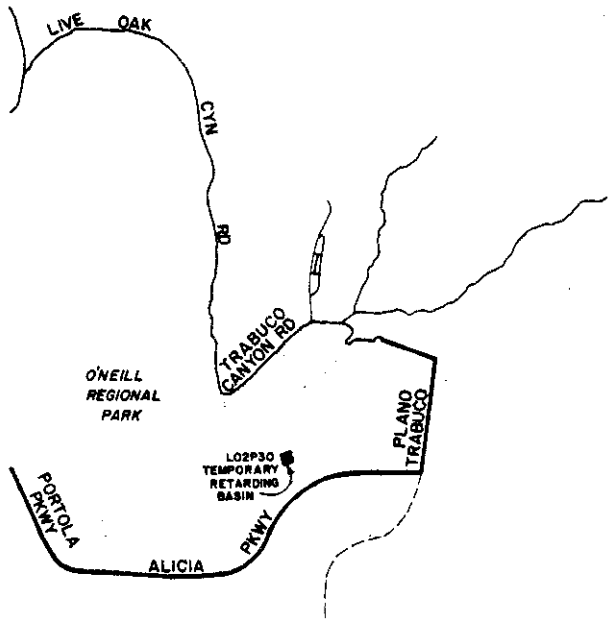

Fig. 35. Location map for L02P30 Temporary Retarding Basin

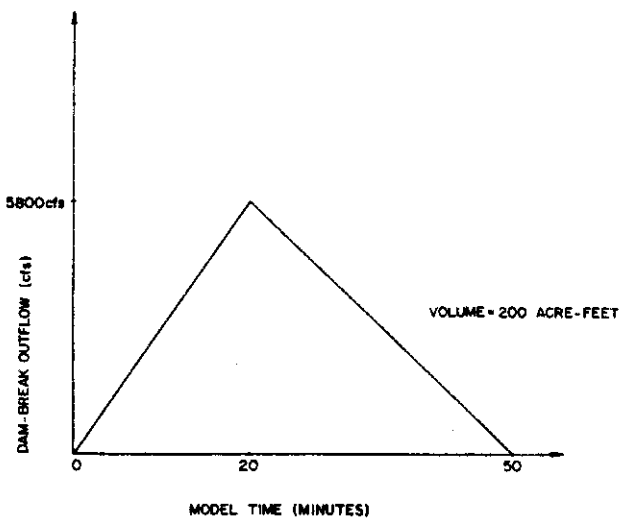

Fig. 37. Study dam break outflow hydrograph for the L02P30 Temporary Retarding Basin

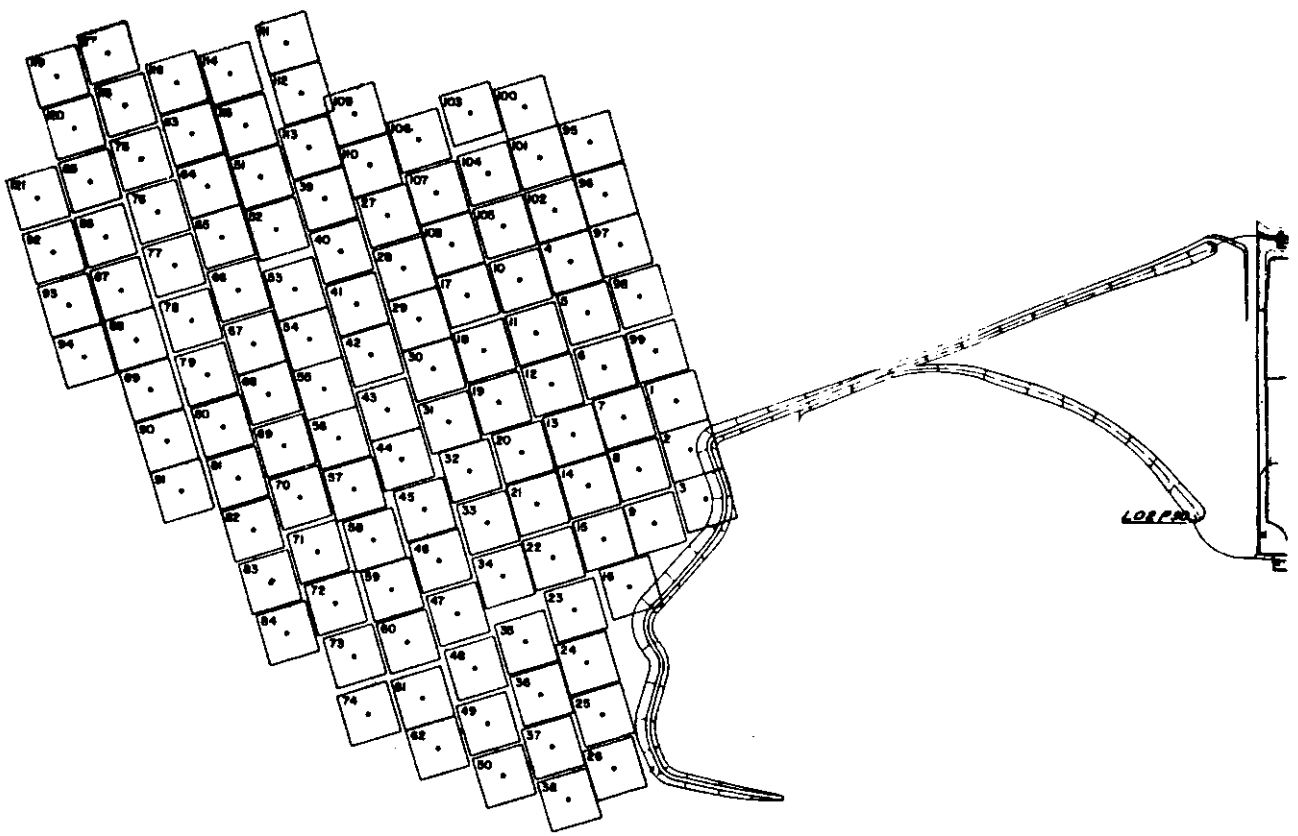

Fig. 36. Domain discretization of L02P30 Temporary Retarding Basin

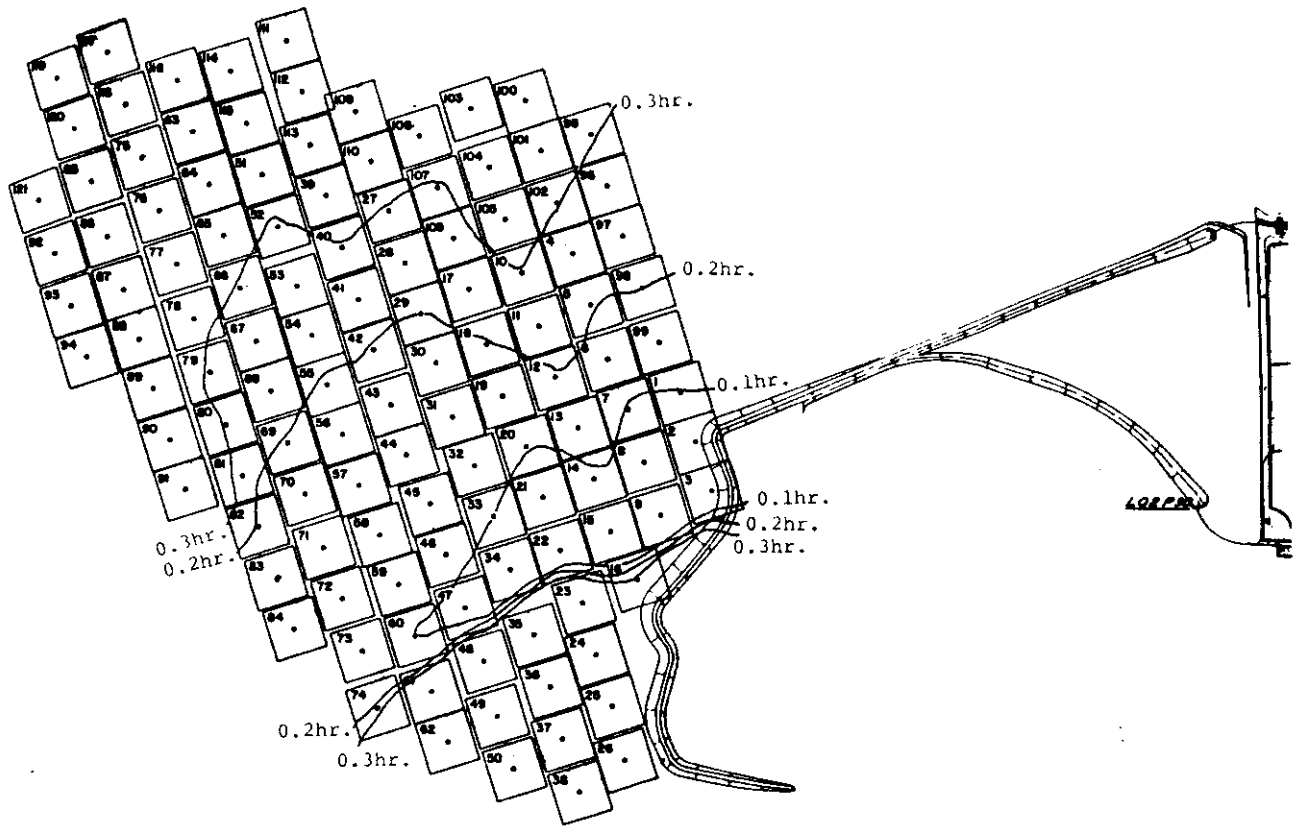

Fig. 38. Time of maximum flooding depth (80.5 A.F. basin test) for L02P30 Temporary Retarding Basin

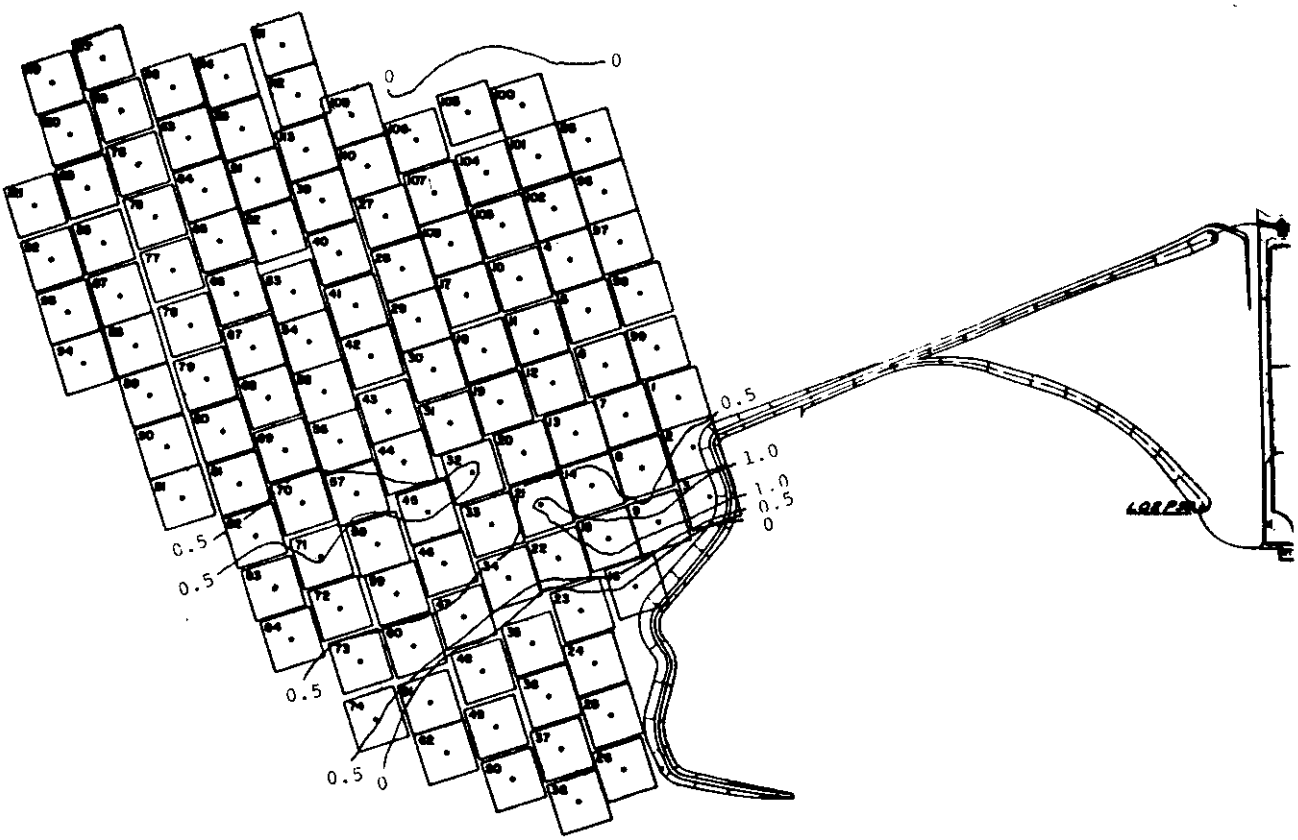

Fig. 39. Flood plain for 80.5 A.F. basin test for L02P30 Temporary Retarding Basin

railroad's floodplain capacity. A 200-foot grid control volume discretization was constructed as shown in Fig. 41.

In each grid, an area-averaged ground elevation was estimated based on the topographic map, except for the railroad boundary where a four-foot berm is imposed. A Manning's friction factor of $n=0.030$ was used throughout the study.

The O.I.P. Temporary Detention Basin is an earthen dam approximately 15 feet high and 30 feet deep. It is assumed that the flowrate reaches its peak in 20 minutes and then residues over the proceeding 30 minutes. The estimated outflow hydrograph is shown in Fig. 42.

Table 3. L02P30 temporary retarding basin volume and dam-break outflow

Depth (ft)	Volume (af)	Q_p (Dam-break) (cfs)
0.5	9.9	95
1.0	15.1	270
1.5	20.3	496
2.0	25.5	764
2.5	30.7	1 067
3.0	37.6	1 403
3.5	44.6	1 768
4.0	51.5	2 160
4.5	58.4	2 577
5.0	65.4	3 019
5.5	72.3	3 483
6.0	80.5	3 968

Table 4. Estimating dam-break Q_p for L02P30 temporary retarding basin (15-minute peak time)

Assumed depth (ft)	Q_p[1] (cfs)	Volume drained[2] (af)	Volume left[3] (af)	Depth (ft)
4.0	2 160	22.3	58.2	4.5
4.5	2 577	26.6	53.9	4.2
4.3	, 2 407	24.9	55.6	4.3

NOTES:
$Q_p = 3LH^{1.5}$ where $L = 90'$
$Q_p = 270H^{1.5}$ cfs
2: $V_d = 0.01033 Q_p$ AF
$V_{left} = (80.5 - V_d)$ AF

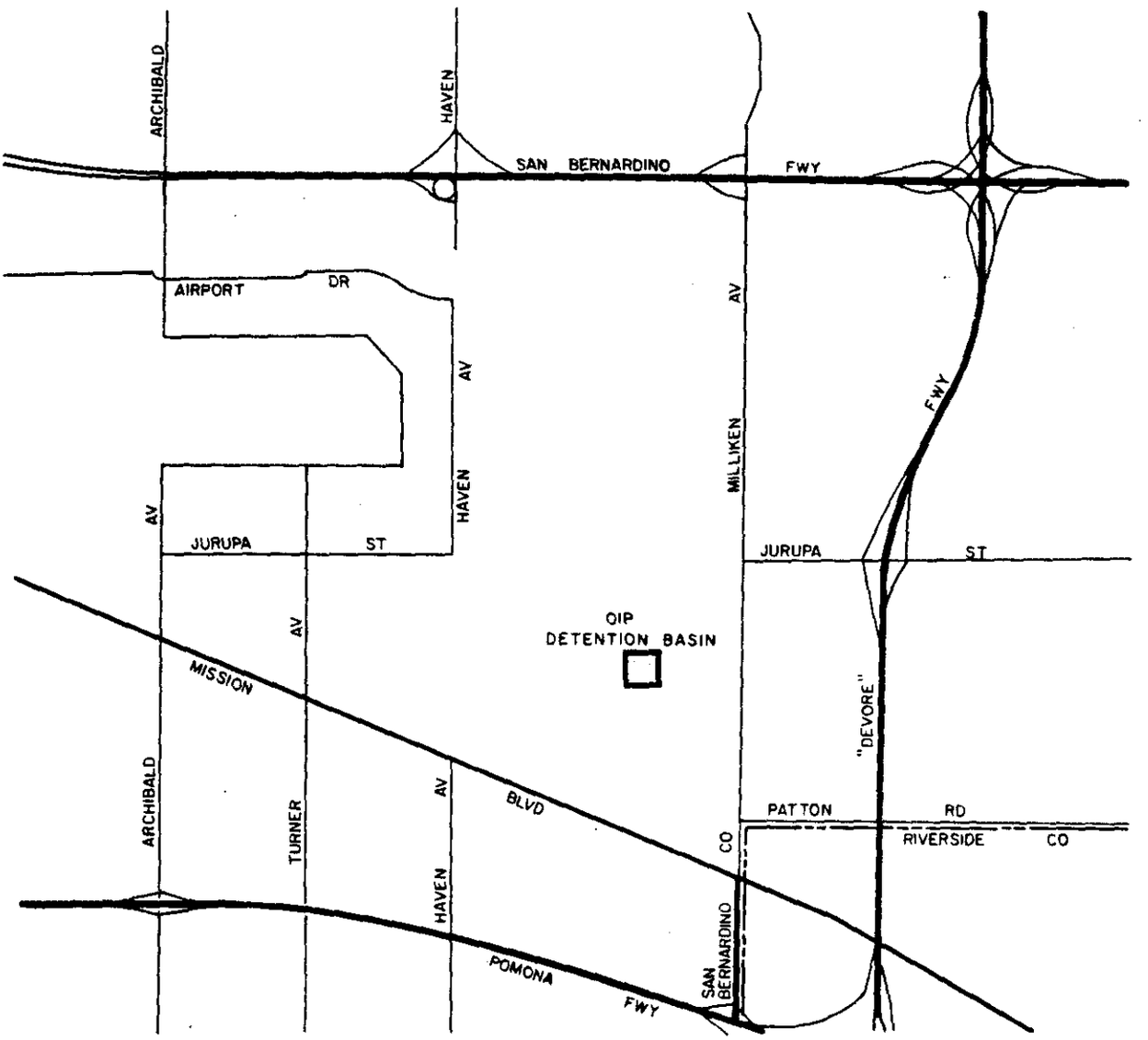

Fig. 40. Location map for O.I.P. Temporary Detention Basin

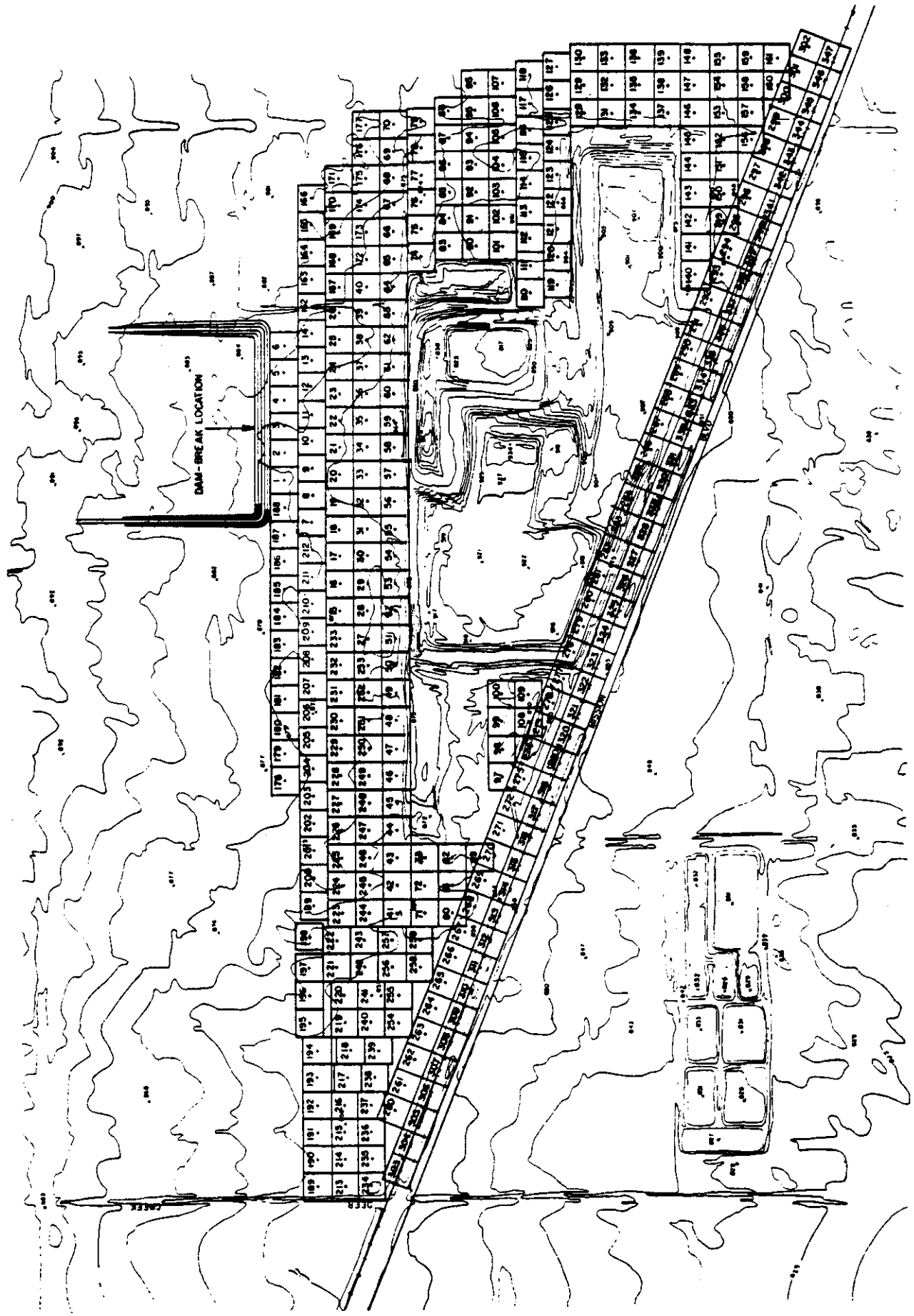

Fig. 41. Domain discretization for O.I.P. Detention Basin

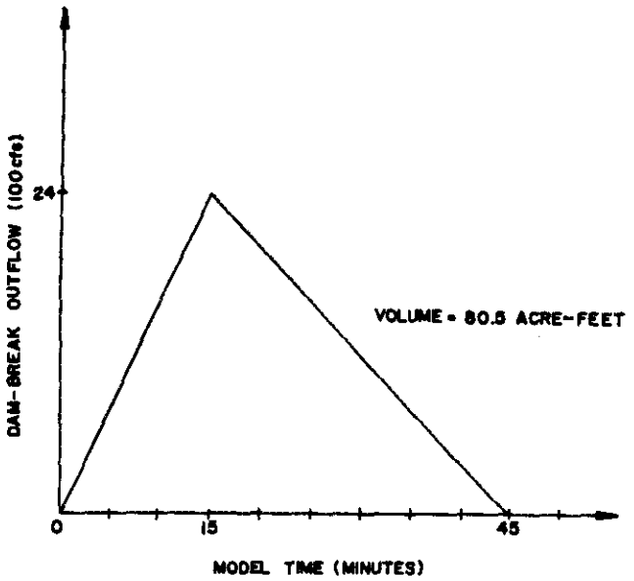

Fig. 42. Study dam-break outflow hydrograph for O.I.P. Temporary Detention Basin

The ultimate outflow geometry is assumed to be a 40 foot break in a 15 foot high, 30 foot wide berm. Based on the said conditions $Q_p = 3.09\ LH^{1.5}$ cfs. For the assumed outlet hydrograph shape with Q_p occuring at 20-minutes after the dam failure, the volume drained by peak time is given by $V_d = 0.01377 Q_p$ (acre feet).

From the table, it is seen that Q_p is strongly influenced by the quick depletion of the reservoir's stored waters. It is also noted that the Q_p is assumed to occur at model time of 20-minutes which indicates a severe erosion rate that destroys a substantial earthen berm structure. Consequently, the estimated Q_p may be considered conservative.

The dam-break hydrograph of Fig. 42 is used for the inflow hydrograph to the grid network of Fig. 41. The resulting floodplain (using the dam-break model) is shown in Fig. 43. (This floodplain is simply representative of the flow 2.5 hours after the dam-break.) From Fig. 43, it is seen that the floodplain spreads out laterally and flows around the landfill. The flow ponds up around the landfill; along the north side of the landfill, the water ponds as high as 9.2 feet, and along the sides of the landfill, the water ponds up to 5.1 feet high. As the flow travels south, it ponds up to a depth of 4.8 feet against the railroad near Milliken Avenue. Because the water spreads laterally, Milliken Avenue runs the risk of becoming flooded; however, the water only ponds to 0.6 feet along the street. A more in-depth study is needed to see if the water would remian in the gutter or flood Milliken Avenue.

By observing the arrival times of the floodplain in Fig. 44, it is seen that the floodplain changes very little on the west side of the landfill once it reaches the railroad (0.6 hours after the dam-break). But on the east side of the landfill it takes 2.0 hours to reach the railroad.

Application 7: Estuary modelling

A hypothetical bay is shown in Fig. 45 and is schematized in Fig. 46. Stage hydrographs are available at seven stations as marked in Fig. 45 and are numbered 1 through 7 (counterclockwise). Stage values in this application are expressed by sinusoidal equations which are shown in Table 5. Some DHM-predicted flow patterns in the estuary are shown in Figs. 47 to 49. The flow patterns appear reasonable by comparing the fluctuations of the water surface to the stage hydrographs. DHM computed flow patterns compare well to a similar study prepared by Lai (1976).

IV.2 APPLICATION FOR CHANNEL AND FLOODPLAIN INTERFACE MODEL

Application 8: Channel-floodplain model

Figure 50 depicts a discretization of a two-dimensional hypothetical watershed with three major channels crossing through the floodplain.

Figure 51 depicts the inflow and outflow boundary conditions for the hypothetical watershed model. Figures 52 through 57 show the evolutions of the floodplain. The shaded areas indicate which grid element are flooded. From Fig. 52, it is seen that the outflow rate is less than the inflow rate which results in a flooding situation adjacent to the neighbouring grid elements and the junction of channel B and B′ is also flooded. At the end of the peak inflow rate (Fig. 55), about 1/3 of the floodplain is flooded. After 10 hours of simulation, Fig. 57 indicates a flooding situation along bottom of the model. Figure 58 shows the maximum depth of water at 4 downstream cross-sections. It is needed to point out that the water surface elevations are not necessarily incurred at the same time. Finally, Figs 59 and 60 show the outflow hydrographs for both the channel system and the floodplain system.

IV.3 DISCUSSION

As shown in the previous examples, the DHM model is capable to simulate the one- and two-dimensional problems, separatively. Up till now, no existing numerical model can be used successfully to simulate or predict the evolution of the channel-flood plain interface problem. The proposed DHM model uses a simple diffusion model and interface model to simulate the channel-flood plain interface problem. Results from the hypothetical channel-flood plain interface model show an acceptable floodplain evolution.

Table 5. Boundary values for flow computation in a hypothetical bay

Node	a (ft)	ξ (sec)	M (ft)
63	5	0	0
70	4.95	60	0
74	4.85	180	0
75	4.85	180	0
46	4.75	1200	0.3
39	4.725	1260	0.35
33	4.7	1320	0.4
5	4.5	1800	0.7
4	4.45	1860	0.75

Boundary value equation:

$$z = a \sin\left[\frac{2\pi(t-\xi)}{T}\right] + M + 100$$

in which

a = amplitude, t = time, in second.
ξ = phase lag, T = tidal period = 12.4 hr.
M = mean water level, = 44640 sec.

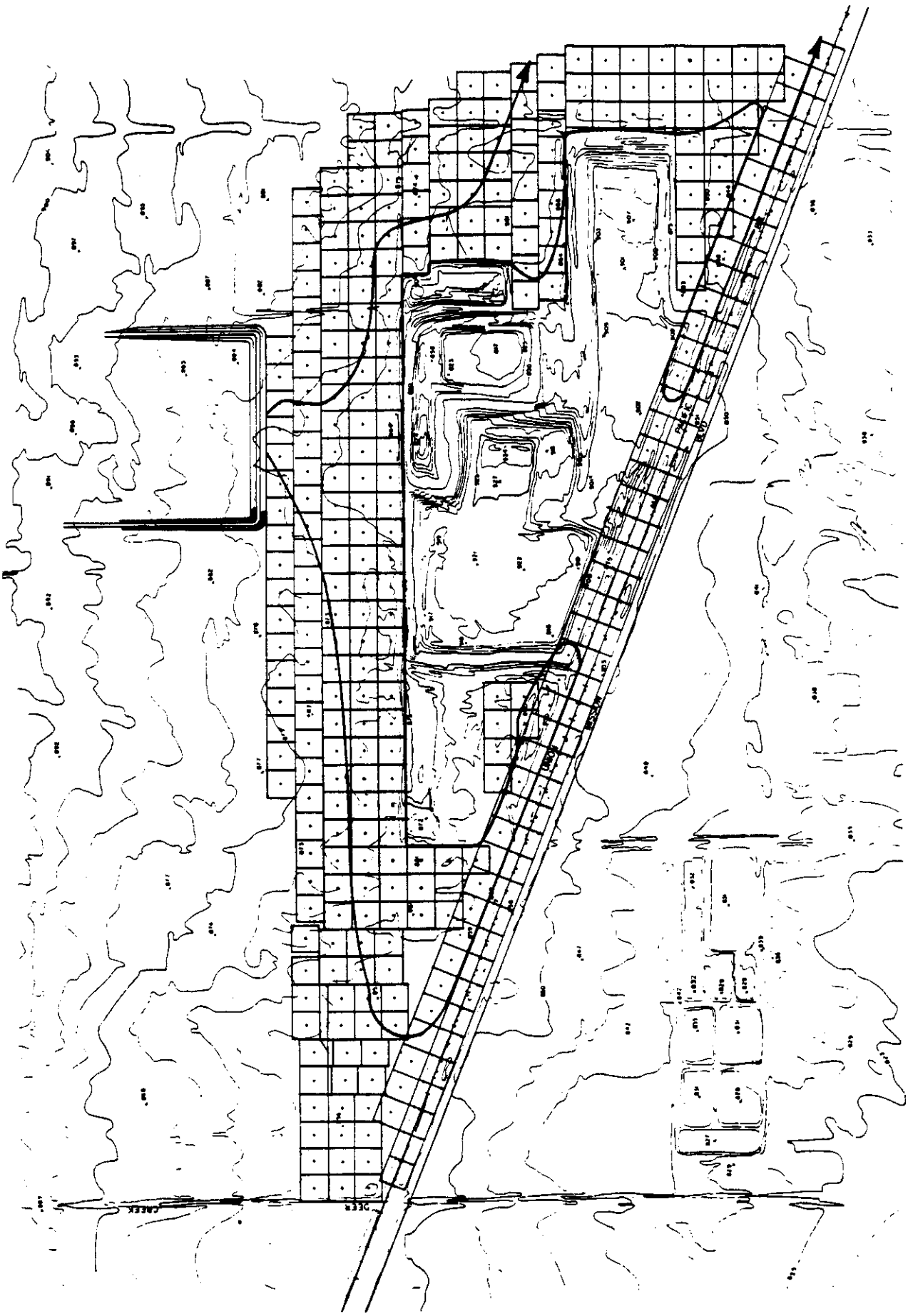

Fig. 43. Time (hours) of maximum flooding depth for O.I.P. Detention Basin

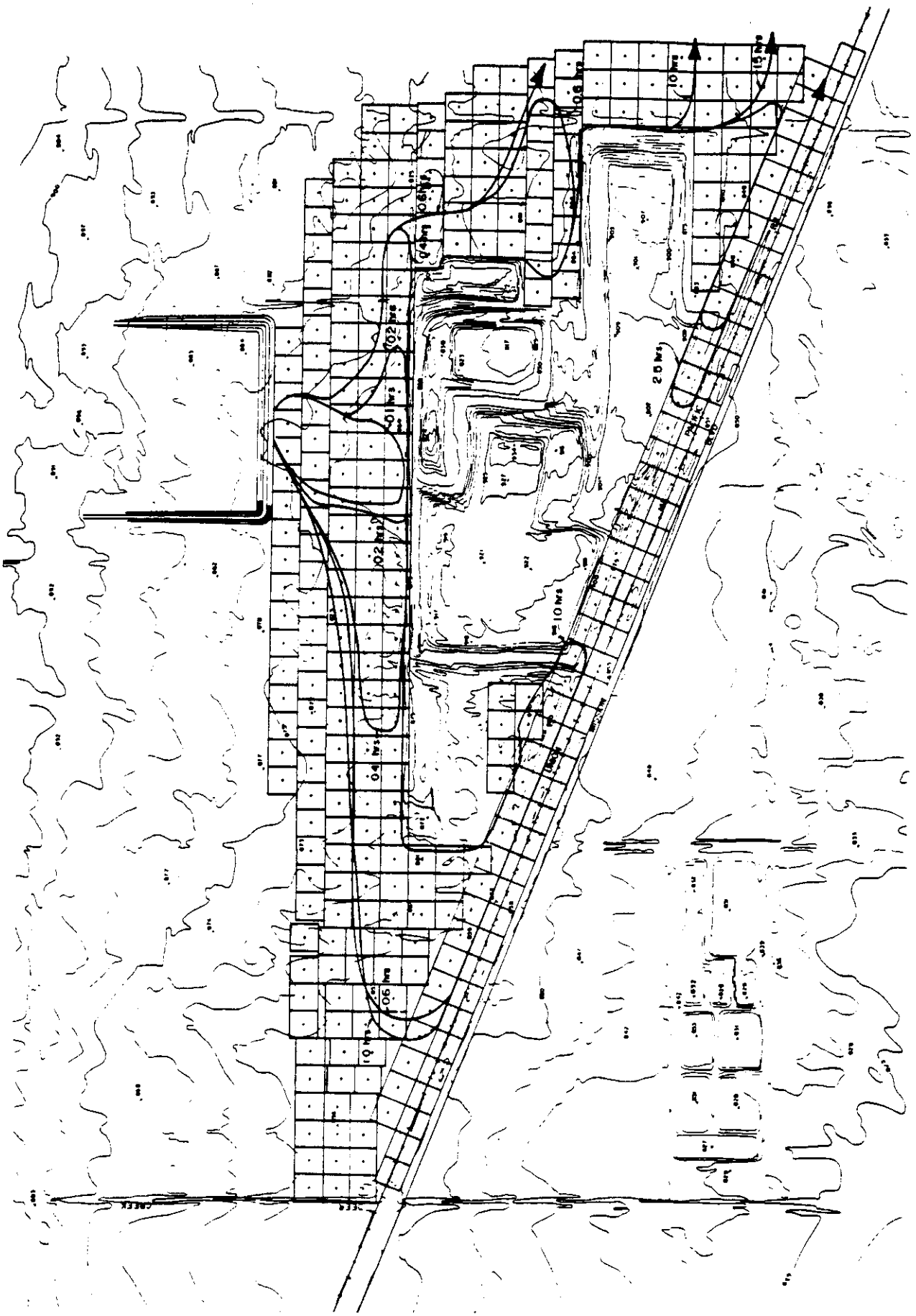

Fig. 44. Flood plain for O.I.P. Detention Basin

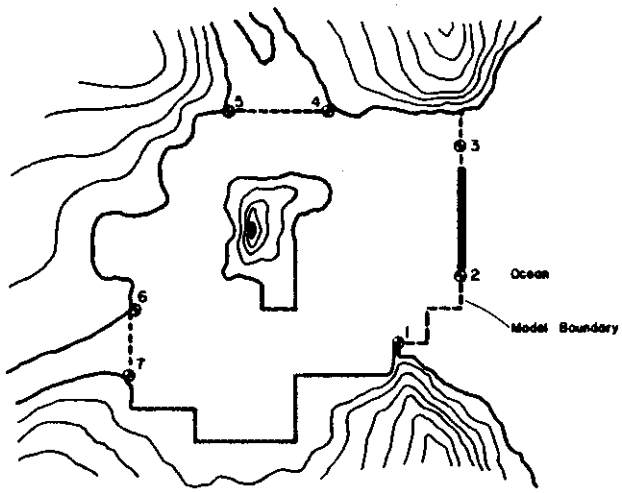

Fig. 45. A hypothetical bay

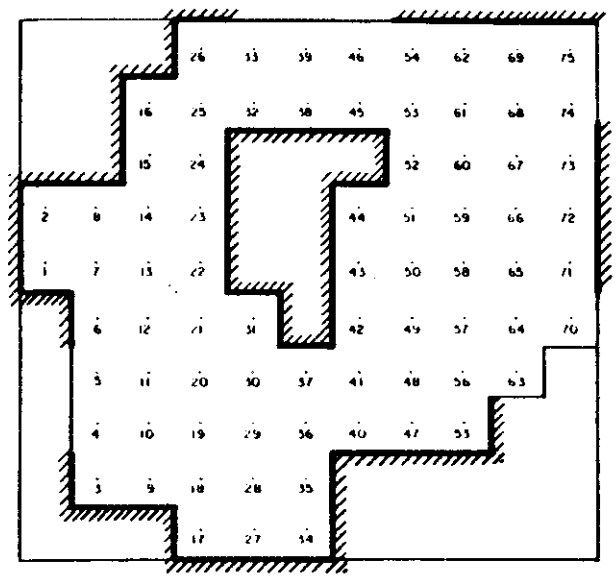

Fig. 46. The schematization of a hypothetical bay shown in Fig. 45

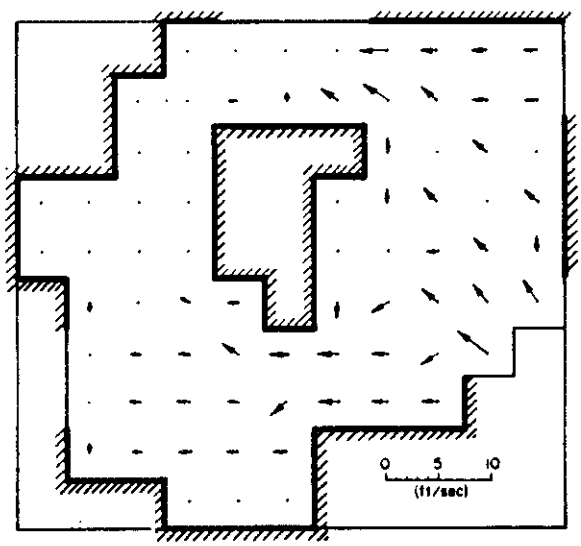

Fig. 47a. Mean velocity at 1-hour

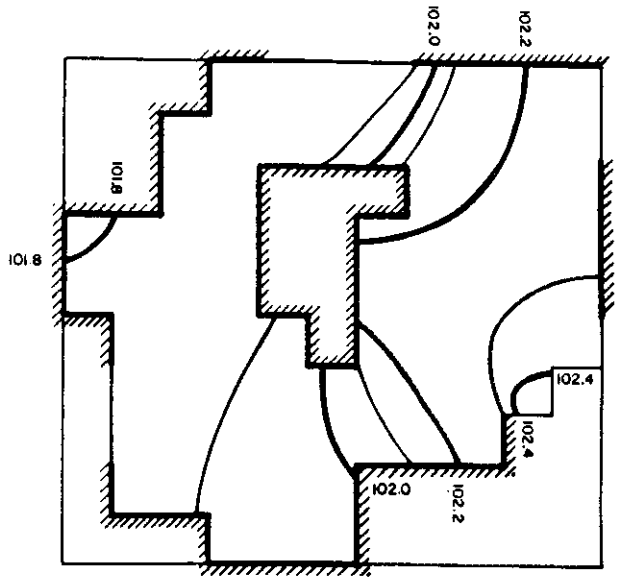

Fig. 47b. Mean water surface profile at 1-hour

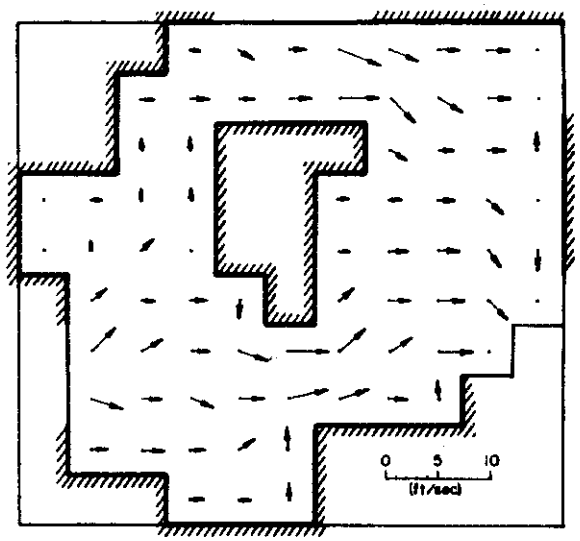

Fig. 48a. Mean velocity profile at 5-hours

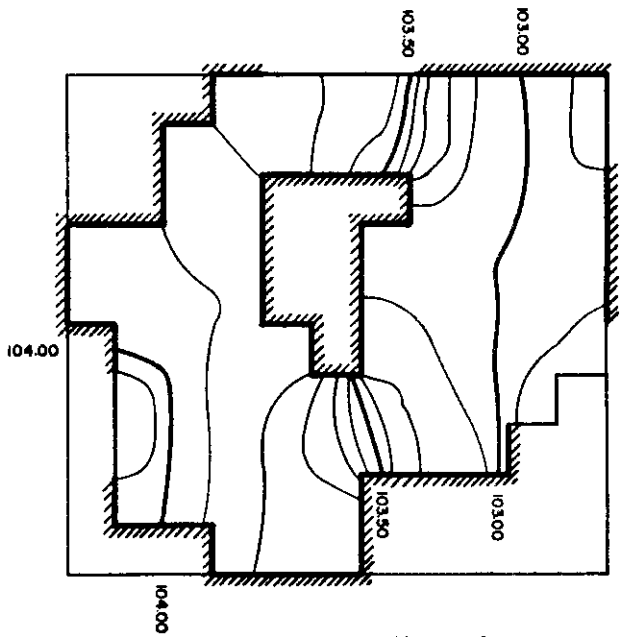

Fig. 48b. Mean water surface profile at 5-hours

V. COMPARISON BETWEEN KINEMATIC ROUTING TECHNIQUE AND DHM MODEL

Introduction

The two-dimensional DHM formulation of equation (32) can be simplified into a kinematic wave approximation of the two-dimensional equations of motion by using the slope of the topographic surface rather than the slope of the water surface as the friction slope in equation (28). That is flowrates are driven by Manning's equation, and backwater effects, reverse flows, and ponding effects are entirely ignored. As a result, the kinematic wave routing approach cannot be used for flooding situations such as considered in the previous chapter. Flows which escape from the channels cannot be modelled to pond over the surrounding land surface nor move over adverse slopes, nor are backwater effects being

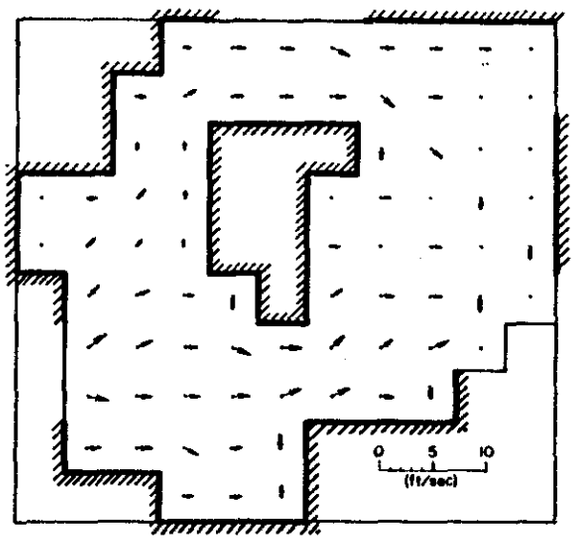

Fig. 49a. Mean velocity at 10-hours

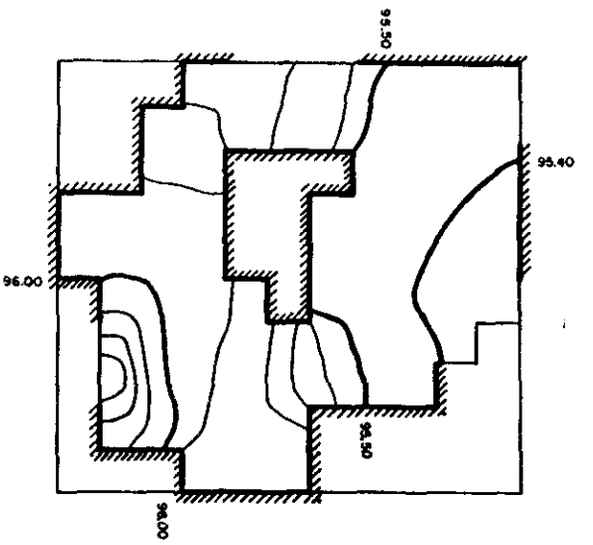

Fig. 49b. Mean water surface at 10-hours

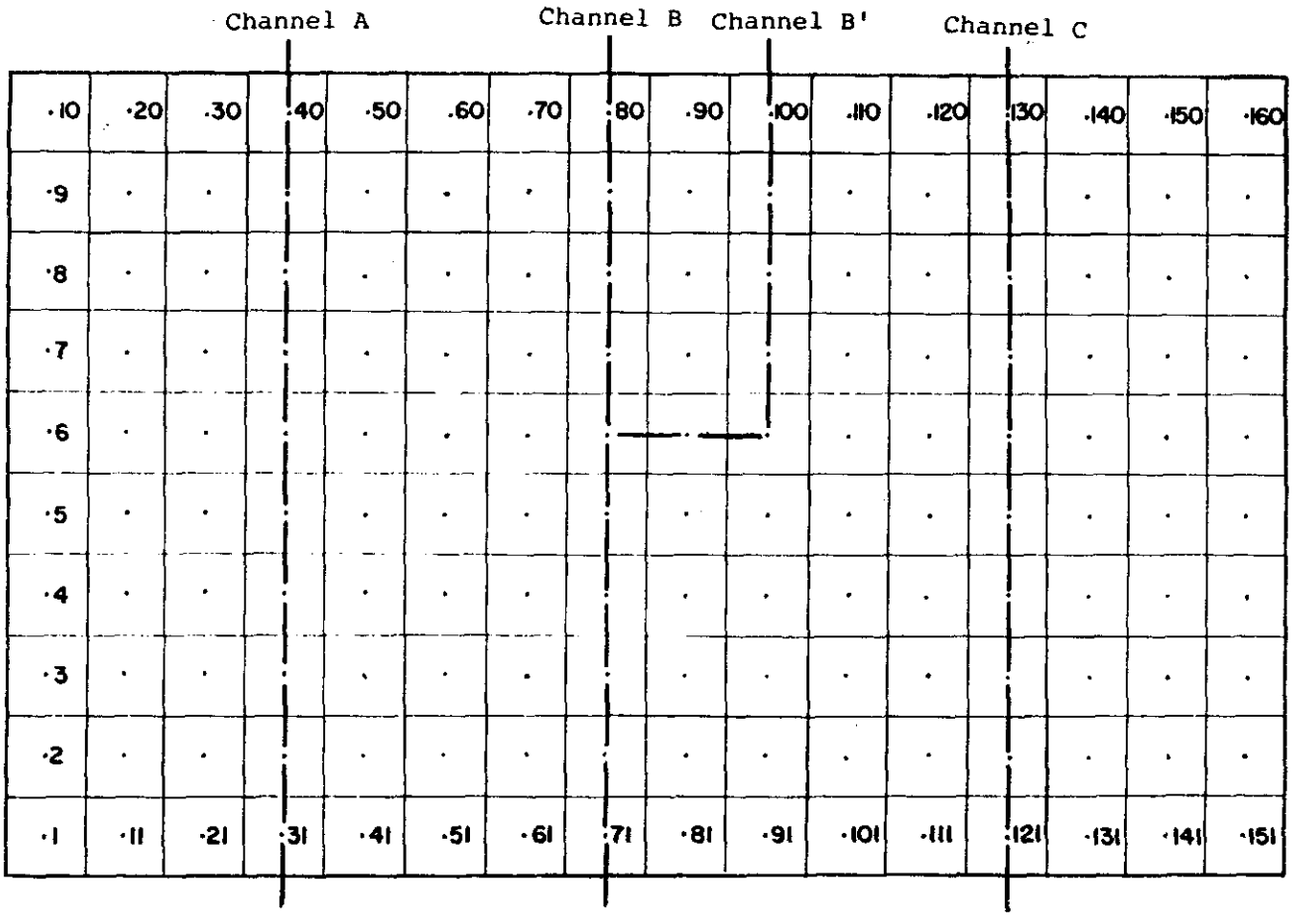

Fig. 50. DHM model discretization of a hypothetical watershed

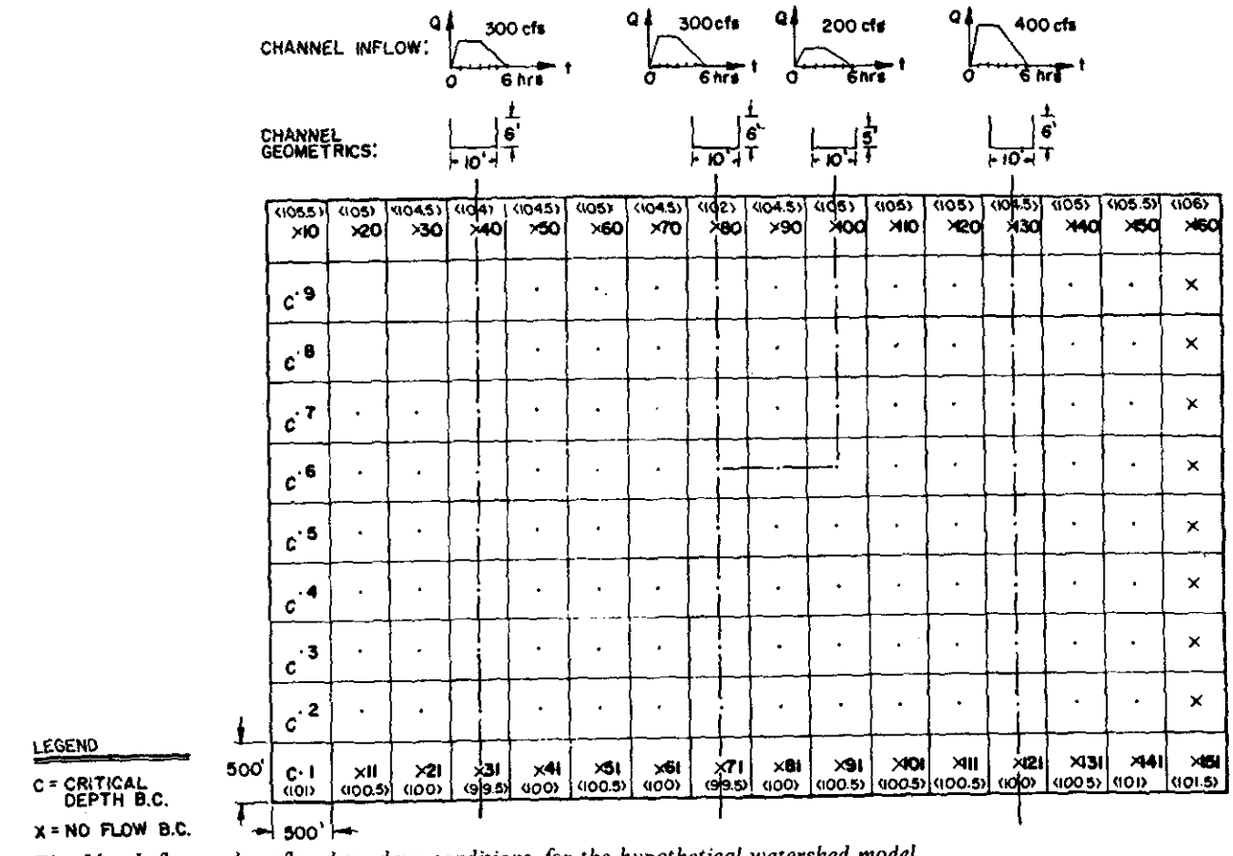

Fig. 51. Inflow and outflow boundary conditions for the hypothetical watershed model

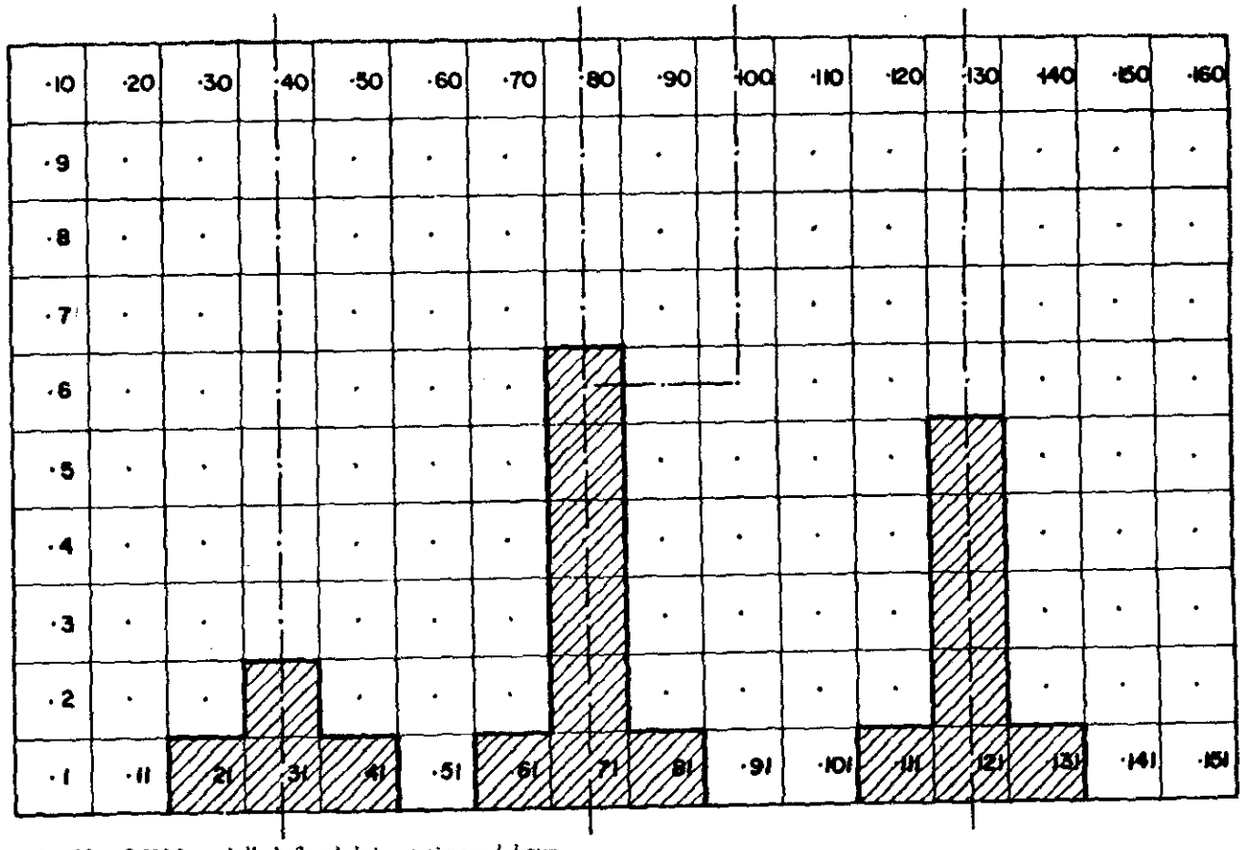

Fig. 52. DHM modelled floodplain at time = 1-hour

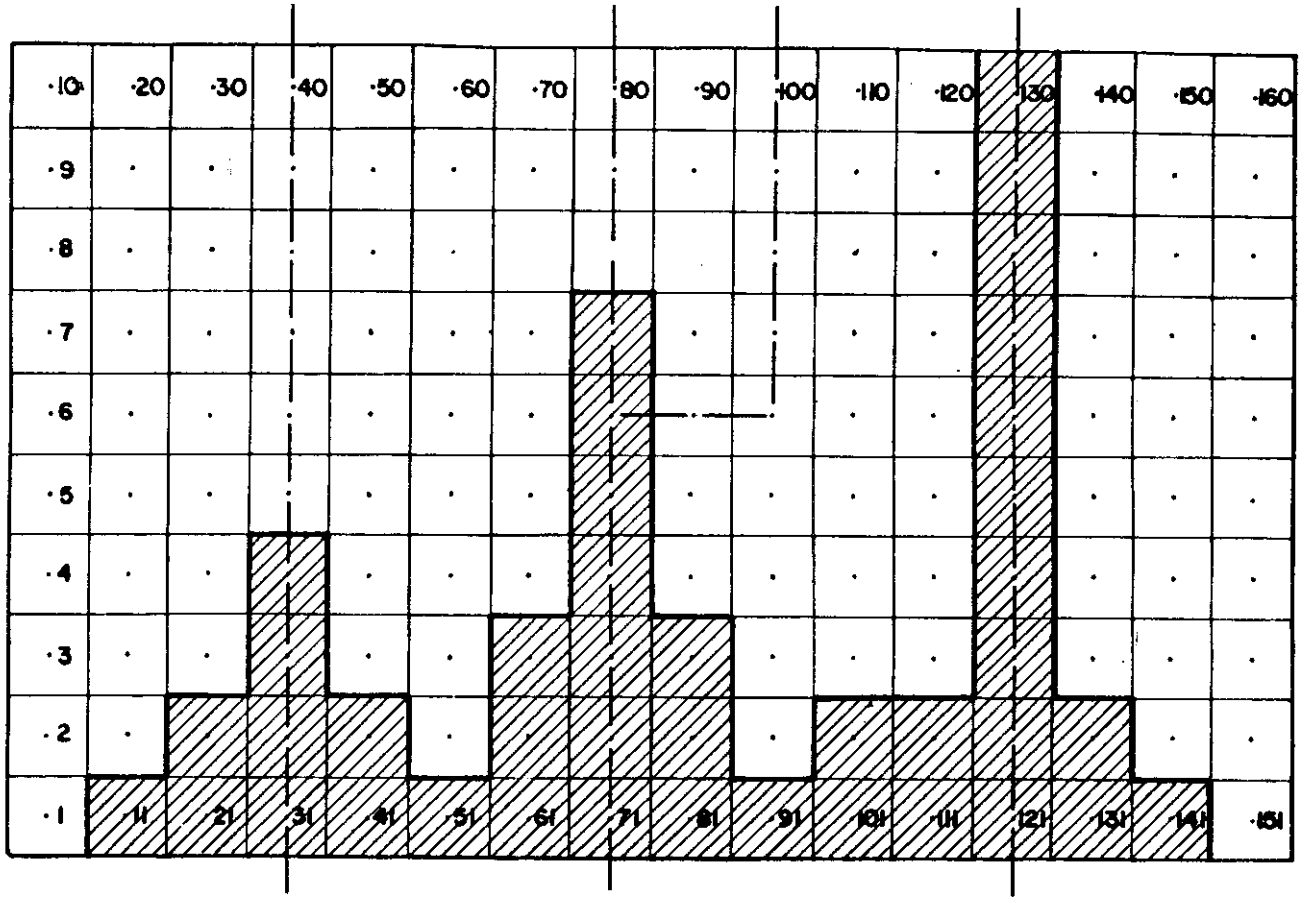

Fig. 53. DHM modelled floodplain at time = 2-hours

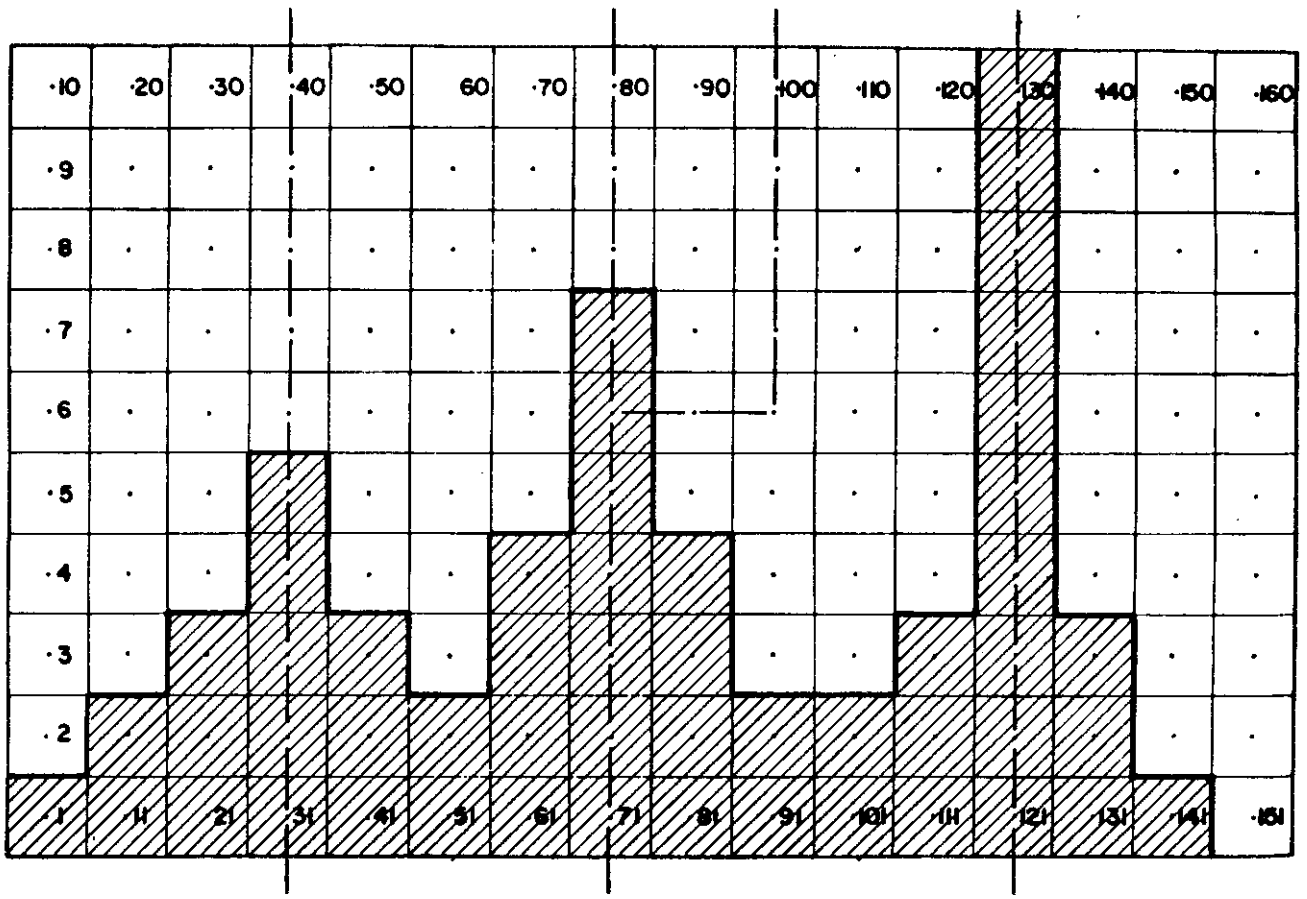

Fig. 54. DHM modelled floodplain at time = 3-hours

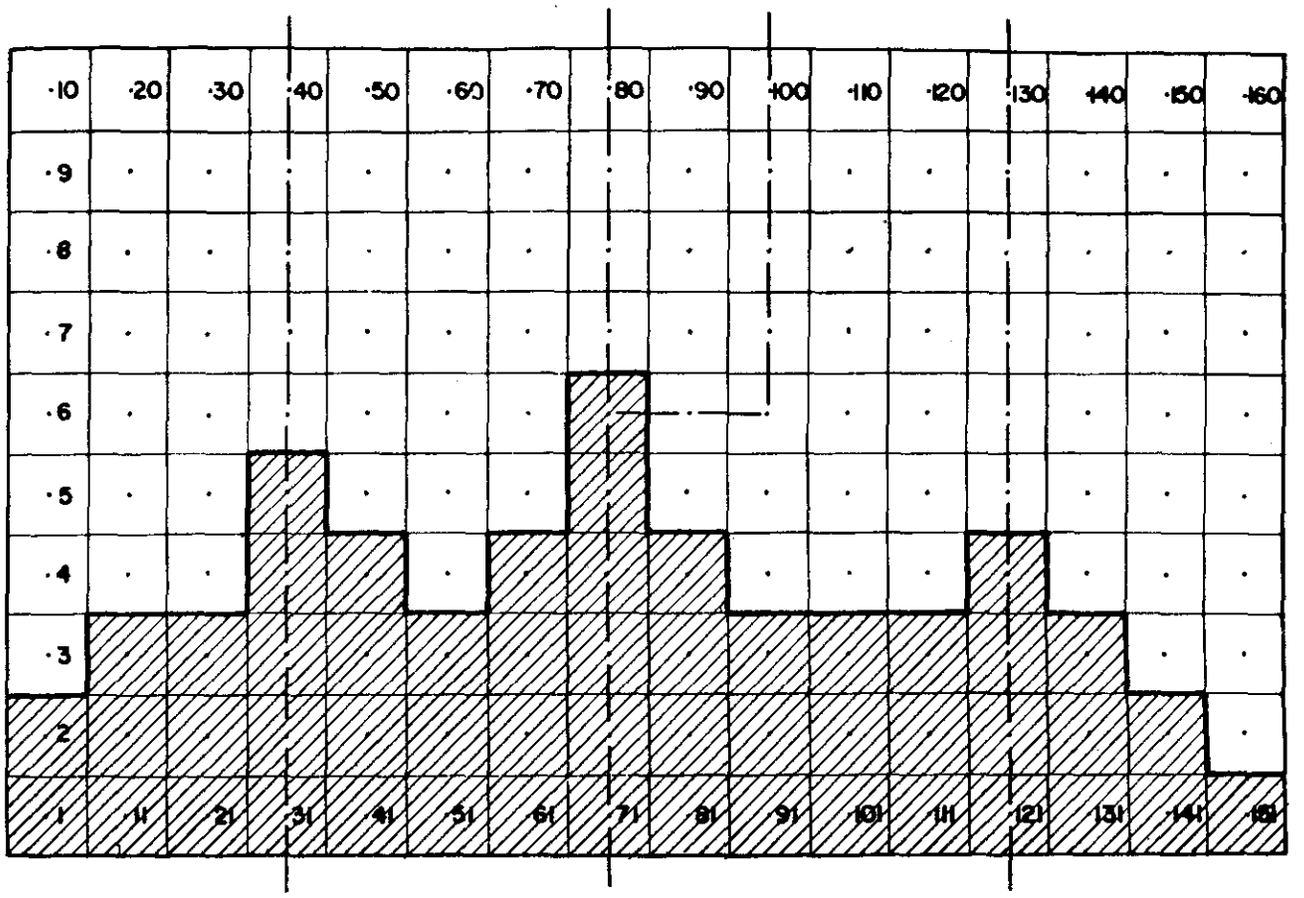

Fig. 55. DHM modelled floodplain at time = 5-hours

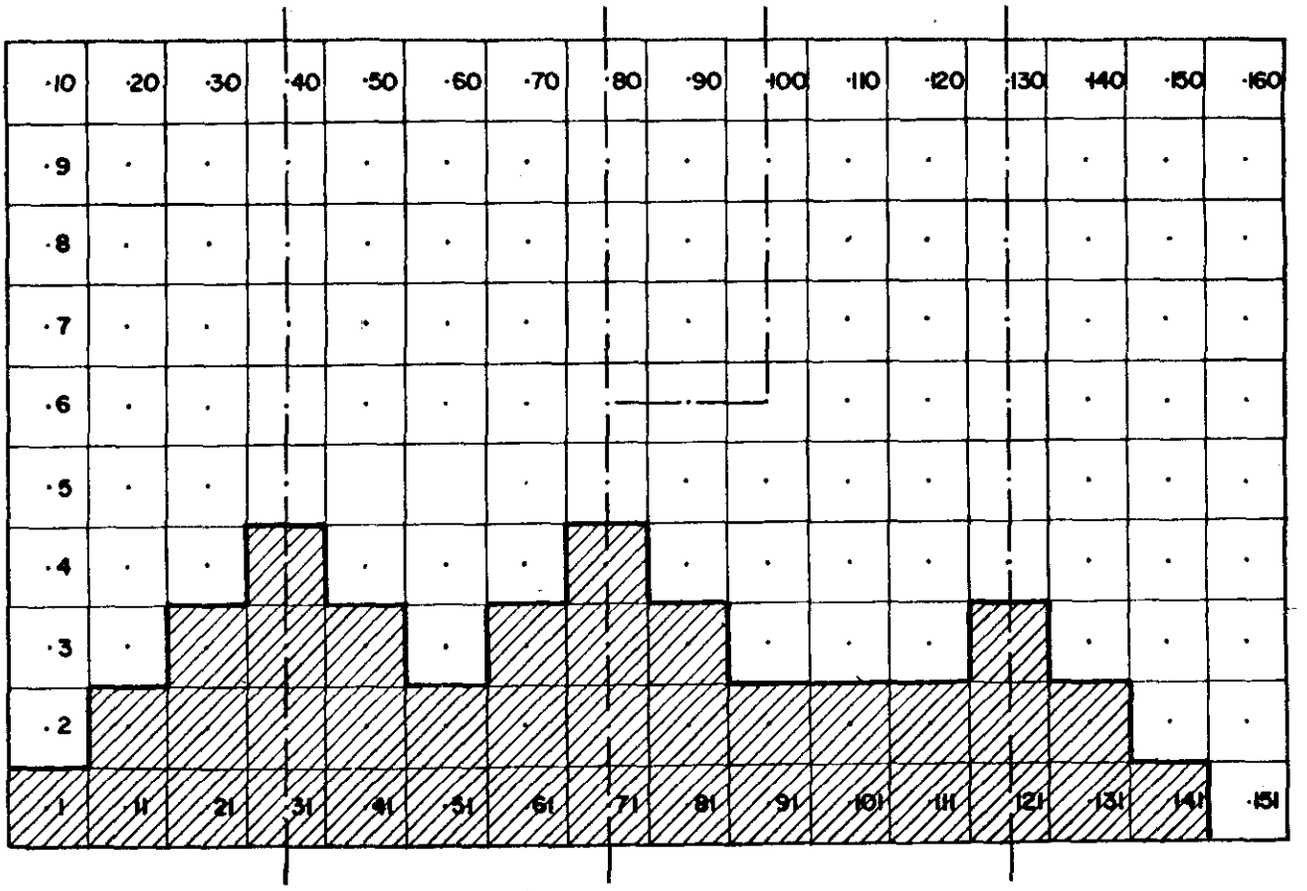

Fig. 56. DHM modelled floodplain at time = 7-hours

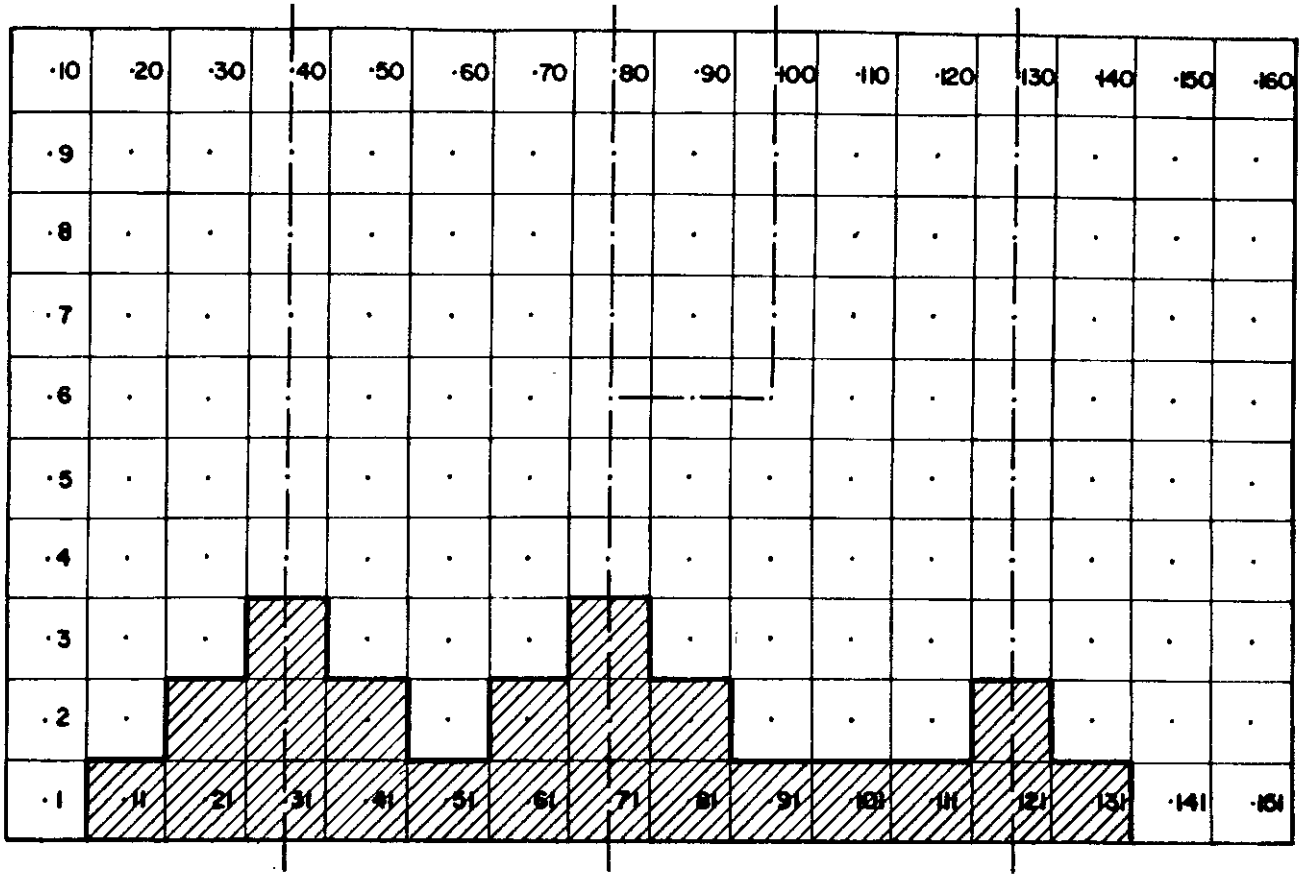

Fig. 57. DHM modelled floodplain at time = 10-hours

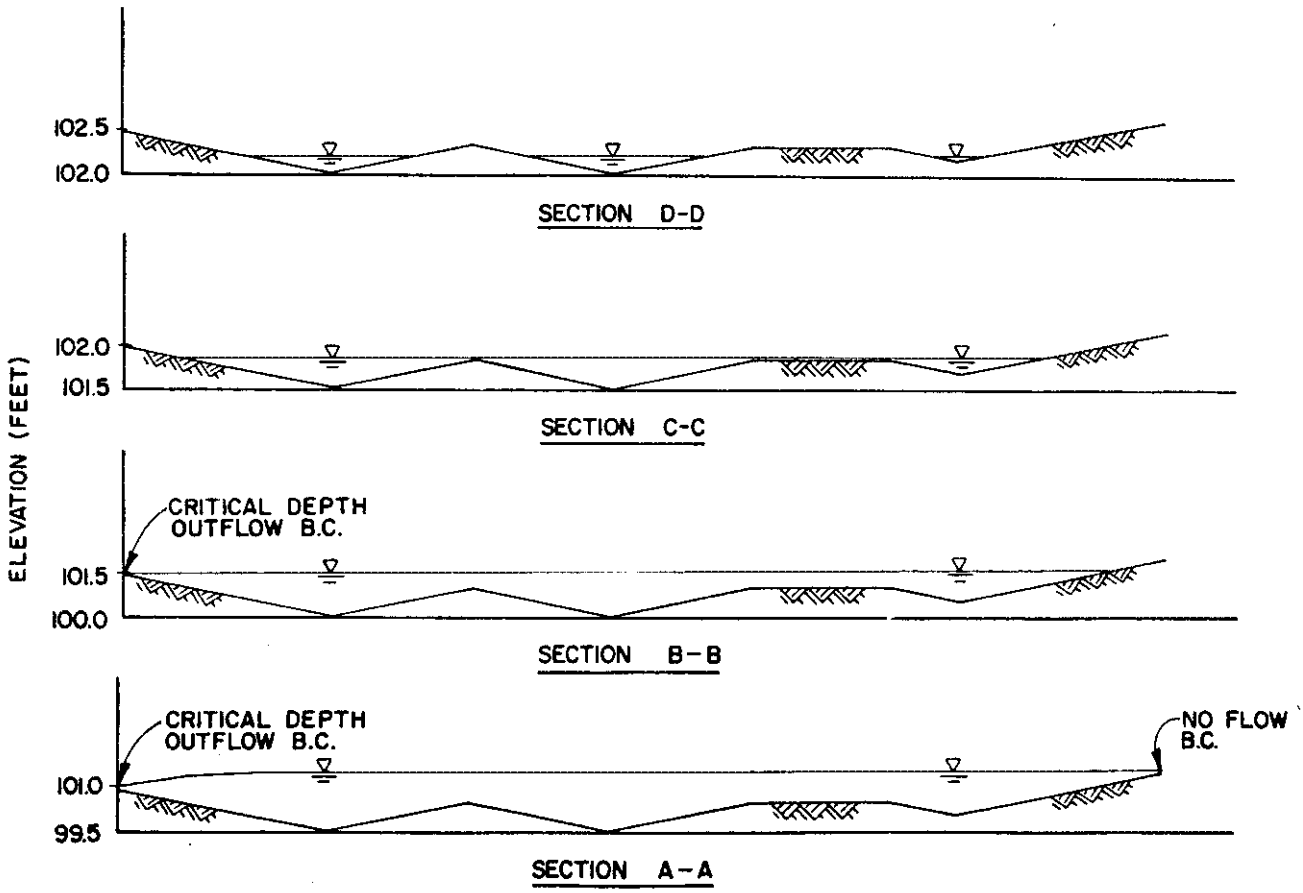

Fig. 58. Maximum water depth at different cross-sections

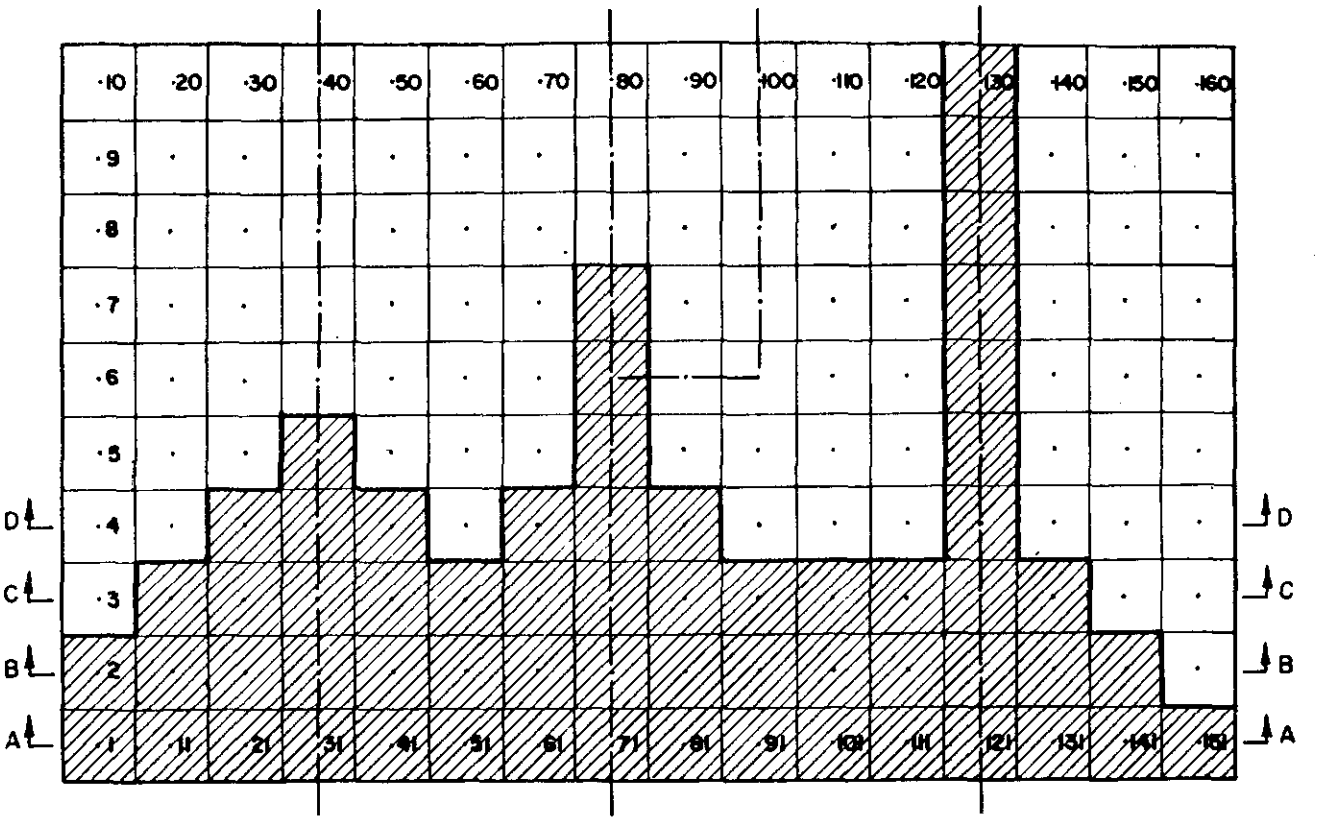

(a) Maximum Floodplain

Fig. 58.—cont.

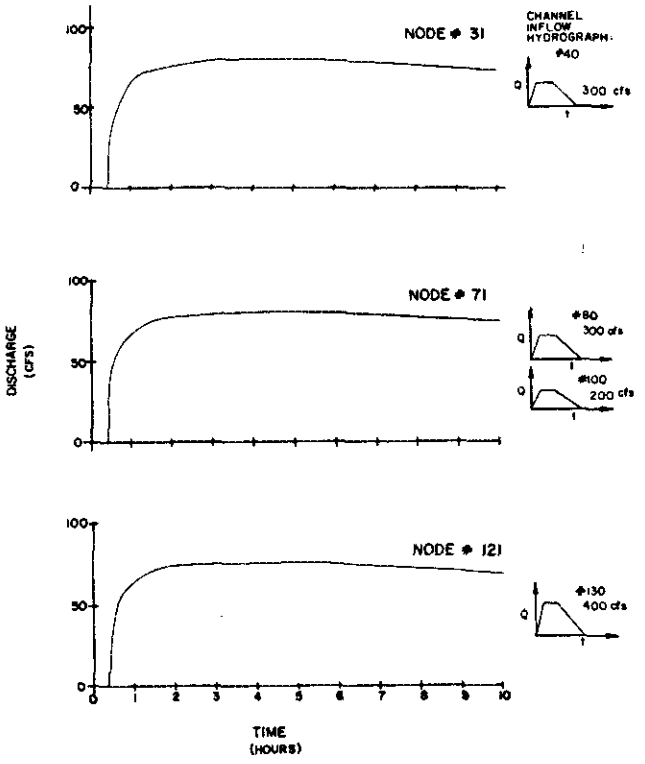

Fig. 59. Bridge flow hydrographs assumed outflow relation: ($Q = 10d$)

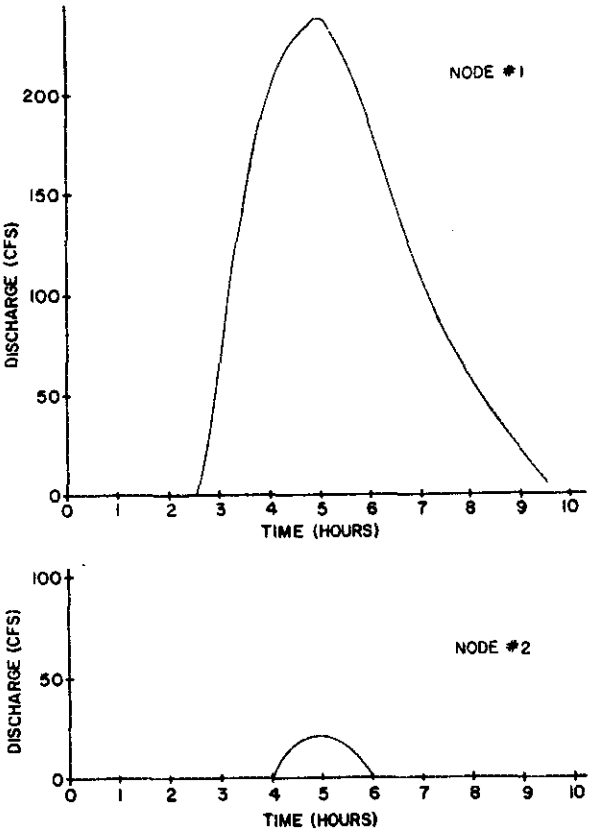

Fig. 60. Critical outflow hydrographs for flood plain

modelled in the open channels due to constrictions which, typically, are the source of flood system deficiencies.

In a recent report by Doyle *et al.* (1983), an examination of approximations of the one dimensional flow equation is presented. The authors write:

'The kinematic wave and diffusion wave approximations of the momentum equation provide simpler and faster computer solutions than the full dynamic equation and therefore are often used instead of the complete dynamic model. The choice of the approximations depends on which terms must be retained in the flow equation to accurately describe the stream system. Henderson (1966) gives the following values for terms of the momentum equation taken from a fast-rising flood for an actual river in steep alluvial country:

S_0,	$\frac{\partial y}{\partial x}$,	$\frac{V\partial V}{g\partial x}$,	$\frac{1}{g}\frac{\partial V}{\partial t}$
Feet per/mile 26,	1/2,	1/8 to 1/4,	1/20

These figures were computed for a flood in which the discharge increased from 10000 ft^3/s to 150000 ft^3/s and decreased again to 10000 ft^3/s within 24 hours. Even in this case, where the acceleration terms were comparatively large, they still are not as important as the bed slope term (S_0). In some situations, however, the discharge and bed slope can determine the magnitude of the other terms. On very small slopes (S_0 small) the pressure term might will be the same order of magnitude as S_0. If the discharge rises fast, then all terms may be important (especially on flat to mderate slopes). Omitting even small terms (in these situations) from the equation can introduce errors into the solution.

It has been shown repeatedly in flow-routing applications that the kinematic wave approximation always predicts a steeper wave with less dispersion and attenuation than may actually occur. This can be traced to the approximations made in the development of the kinematic wave equations wherein the momentum equation is reduced to a uniform flow equation of motion that simply states the friction slope is equal to the bed slope. If the pressure term is retained in the momentum equation (diffusion wave method), then this will help to stop the accumulation of error that occurs when the kinematic wave approximation procedure is applied.'

V.1 Results

The one-dimensional channel problem of Chapter 1 is used to compare the results between the DHM model and the kinematic routing. For the steep channel, both techniques show comparative results up to 10 miles for the maximum water depth (Fig. 61) and discharge rates at 5 and 10 miles (Figs 62 and 63). For the mild channel, the maximum water surface and discharge rates deviate more and more as the water flows downstream.

V.2 Conclusions

The DHM can be reduced to use the kinematic routing approximation of the complete flow equations. The simplified model, however, loses the capability to approximate backwater effects, ponding, channel overflow, flow over adverse gradients, and other flow effects which are important in flood channel system deficiency analysis.

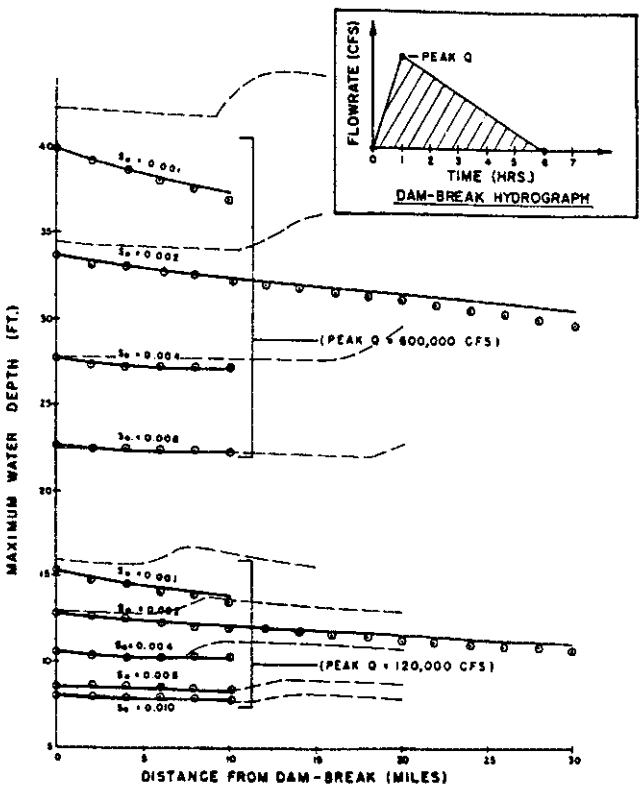

Fig. 61. Diffusion model (⊙), kinematic routing (dashed line) and K-634 model results (solid line) for 1000-foot width channel, Manning's n=0.040, and various channel slopes, S_0

For one-dimensional unsteady flow channel routing problems where backwater effects are negligible, the provided comparisons between the diffusion and kinematic routing approximations show significant differences which may be important to watershed models based on the kinematic routing technique. Because the diffusion routing technique is simple to implement, and due to the additional hydraulic approximation effects provided by diffusion routing, it is recommended that all kinematic wave based hydrologic models be modernized by use of the diffusion routing technique.

VI. CONCLUSIONS

A diffusion hydrodynamic model (DHM) is developed for use in civil engineering flood control studies. The DHM capabilities provides the practicing engineer with a flood control modelling capability not previously available, and only at a price of a home computer.

Although several applications are provided in the paper, further research is required as to the verification of predicted flooding depths, travel times, and other important hydraulic information.

VII. ACKNOWLEDGEMENTS

Acknowledgements are paid to United States Geological Survey, Sacramento, California, for their time and computational assistance with several sections of this report.

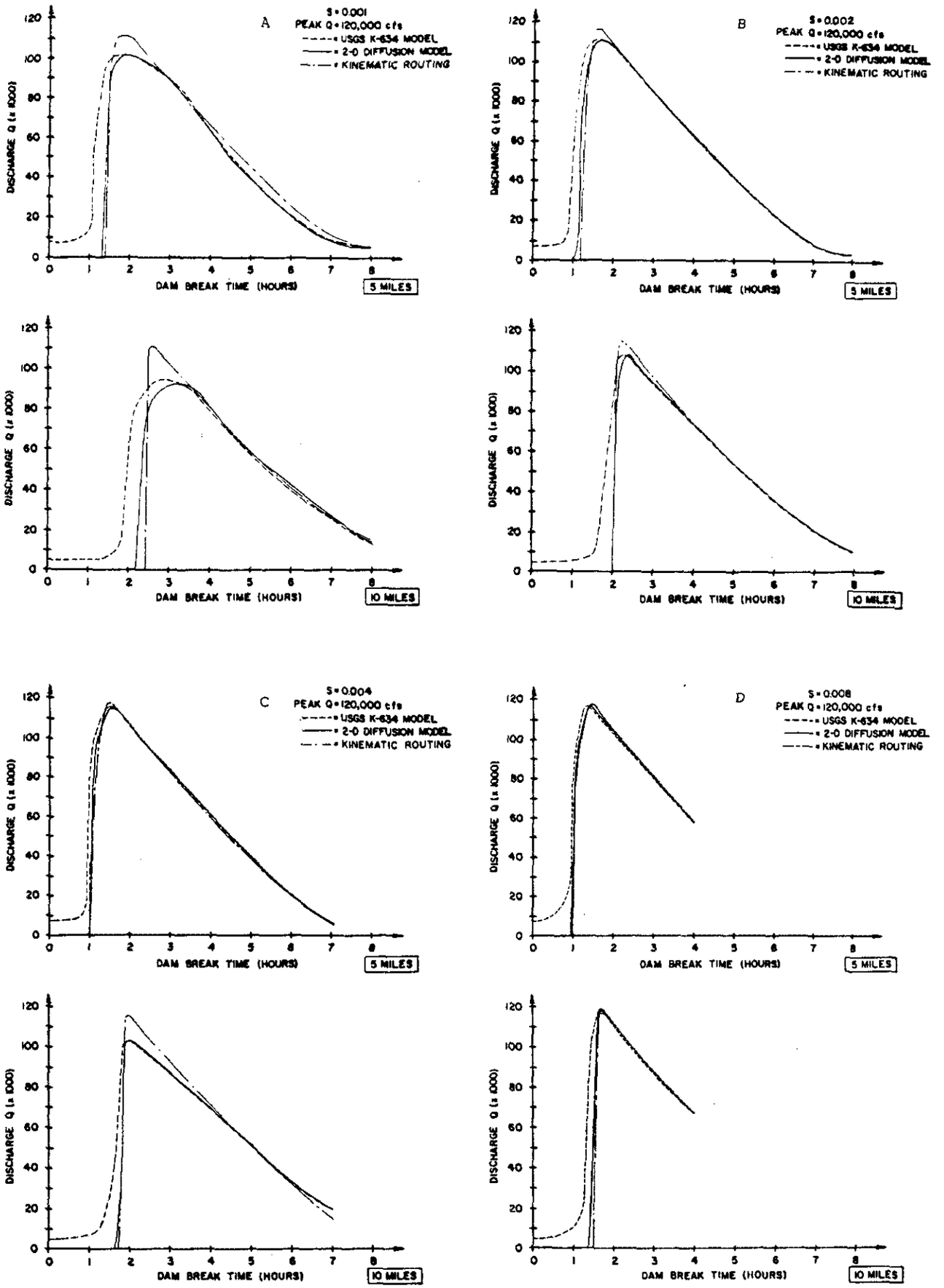

Fig. 62. Comparisons of outflow hydrographs at 5 and 10 miles downstream from the dam-break site

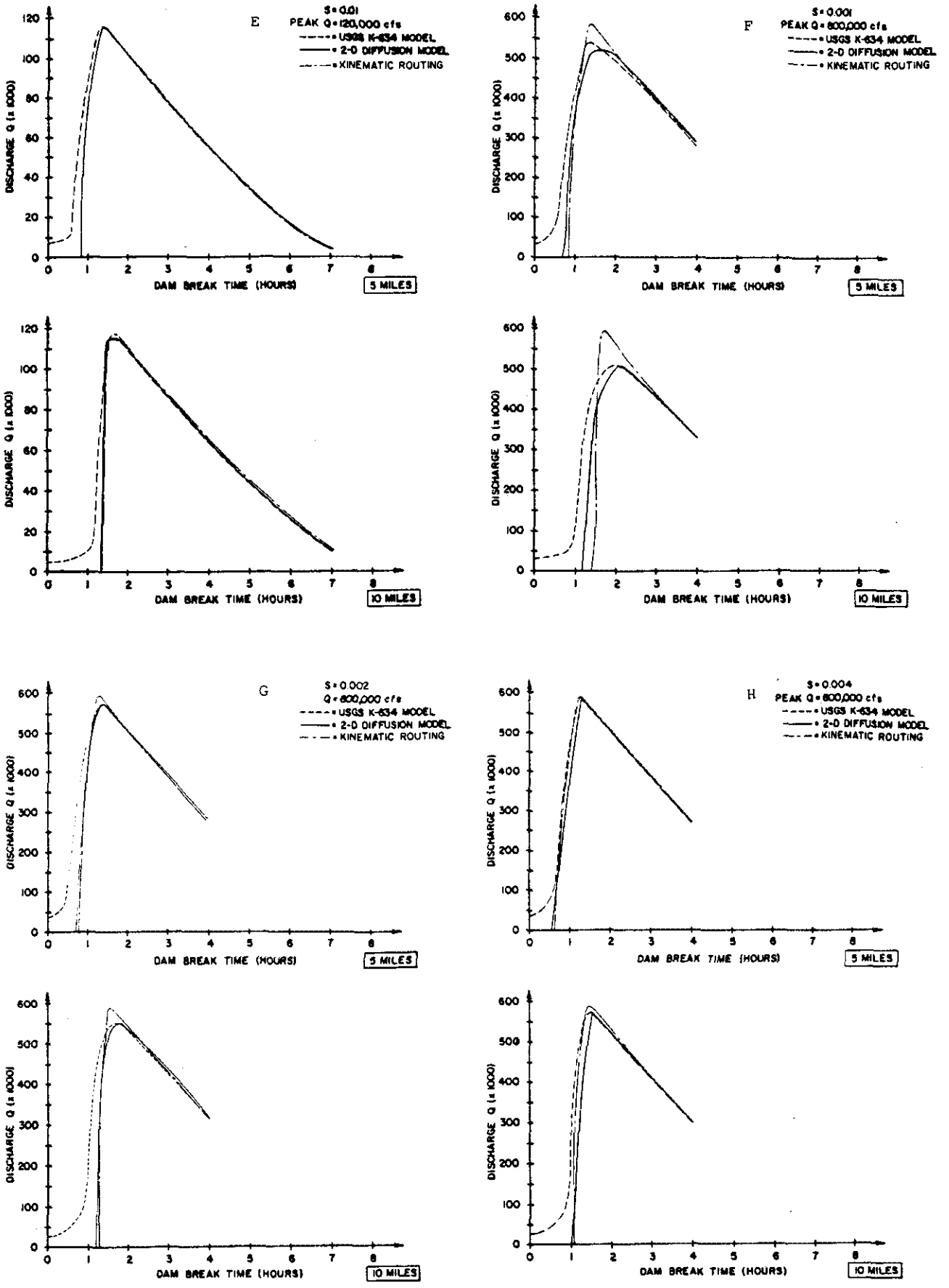
E
S = 0.01
PEAK Q = 120,000 cfs
USGS K-634 MODEL
2-D DIFFUSION MODEL
KINEMATIC ROUTING
DISCHARGE Q (x 1000)
DAM BREAK TIME (HOURS)
5 MILES
F
S = 0.001
PEAK Q = 600,000 cfs
USGS K-634 MODEL
2-D DIFFUSION MODEL
KINEMATIC ROUTING
DISCHARGE Q (x 1000)
DAM BREAK TIME (HOURS)
5 MILES
DISCHARGE Q (x 1000)
DAM BREAK TIME (HOURS)
10 MILES
DISCHARGE Q (x 1000)
DAM BREAK TIME (HOURS)
10 MILES
G
S = 0.002
Q = 600,000 cfs
USGS K-634 MODEL
2-D DIFFUSION MODEL
KINEMATIC ROUTING
DISCHARGE Q (x 1000)
DAM BREAK TIME (HOURS)
5 MILES
H
S = 0.004
PEAK Q = 600,000 cfs
USGS K-634 MODEL
2-D DIFFUSION MODEL
KINEMATIC ROUTING
DISCHARGE Q (x 1000)
DAM BREAK TIME (HOURS)
5 MILES
DISCHARGE Q (x 1000)
DAM BREAK TIME (HOURS)
10 MILES
DISCHARGE Q (x 1000)
DAM BREAK TIME (HOURS)
10 MILES

Fig. 62.—cont.

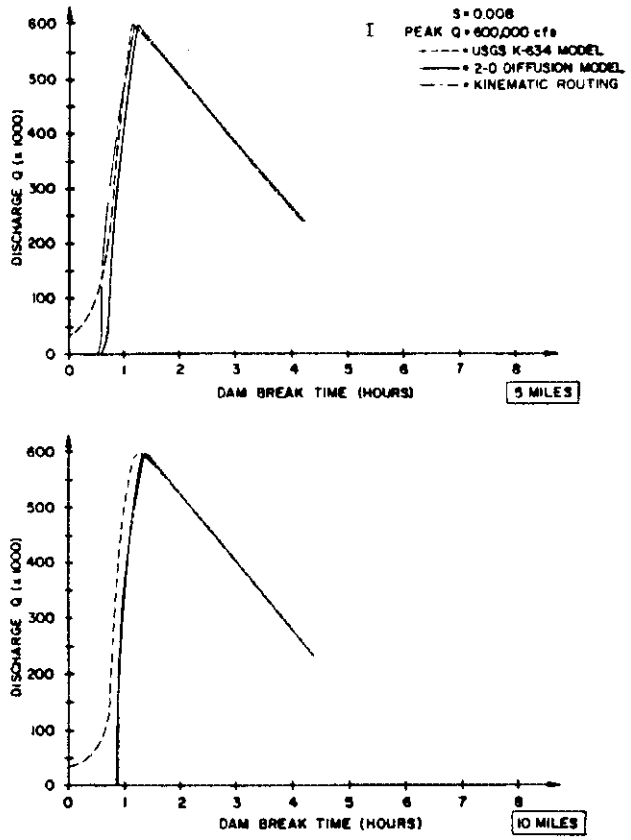

Fig. 62.—cont.

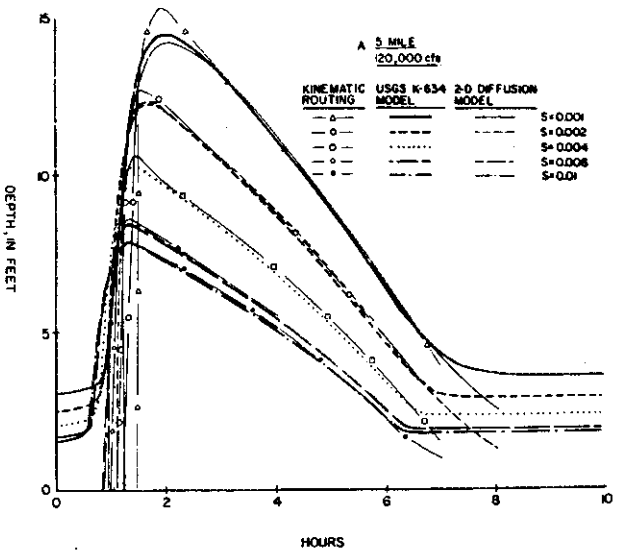

Fig. 63. Comparisons of depths of water at 5 and 10 miles downstream from the dam-break site

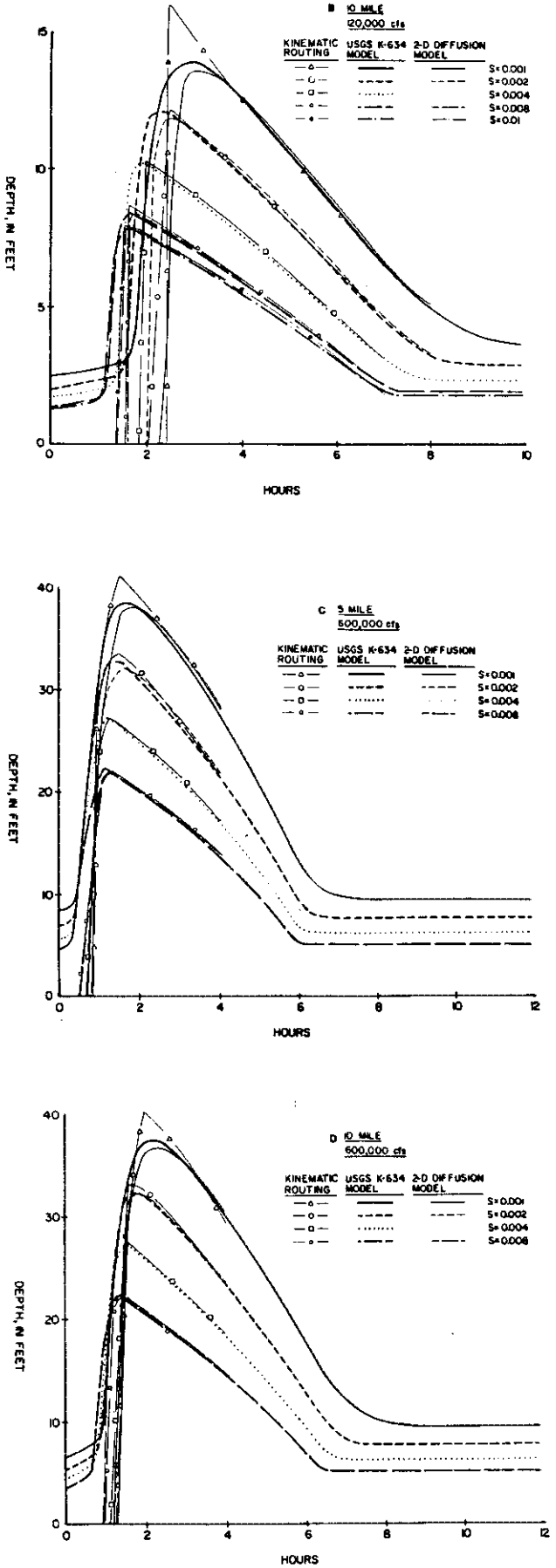

Fig. 63.—cont.

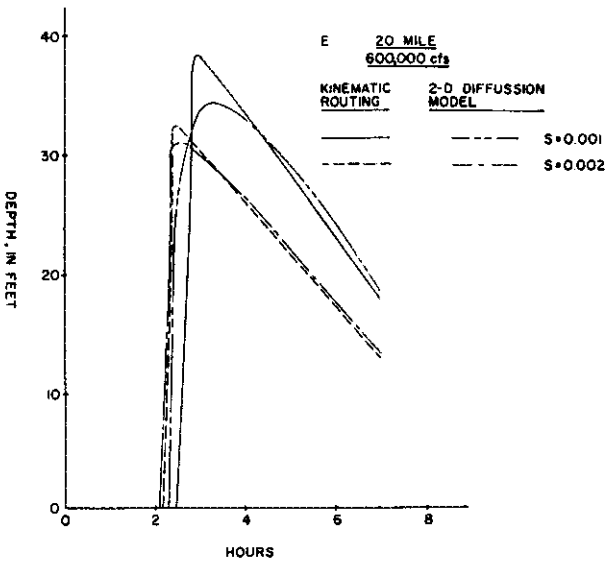

Fig. 63.—cont.

BIBLIOGRAPHY

Akan, A. O. and Yen, B. C. Diffusion-Wave Flood Routing in Channel Networks, *A.S.C.E., Journal of Hyd. Div.*, HY6, 1981

Basco, D. R. Introduction to Numerical Method – Part I and II, Verification of Mathematical and Physical Models in Hydraulic Engineering, A.S.C.E., Hyd., Special Conf., University of Maryland, College Park, Maryland, 1978

Chen, C. Laboratory Verification of a Dam-Break Flood Model, *A.S.C.E., Journal of Hyd. Div.*, HY4, 1980

Chen, C. and Armbruster, J. T. Dam-Break Wave Model: Formulation and Verification, *A.S.C.E., Journal of Hyd. Div.*, HY5, 1980

Doyle, W. H., Shearman, J. O., Stiltner, G. J. and Krug, W. R. A Digital Model for Streamflow Routing by Convolution Method, U.S.G.S. Wat. Res. Investigations *Report 83-4160*, 1983

Fread, D. L. The Development and Testing of a Dam-Break Flood Forecasting Model, Dam-Break routing Model Workshop, Hydrology Committee, U.S. Wat. Res. Council, Betheseda, Maryland, 1977

Henderson, F. M. Flood Waves in Prismatic Channels, *A.S.C.E., Journal of Hyd. Div.*, HY4, 1953

Henderson, F. M. Open Channel Flow, MacMillan Publishing Co., Inc., 1966

Hromadka II, T. V., Berenbrock, C. E., Freckleton, J. R. and Guymon, G. L. A Two-Dimensional Diffusion Dam-Break Model, *Advances in Water Resources*, 1985

Hromadka II, T. V. Including Inertia in A Diffusion Dam-Break Model, *Advances in Water Resources*, 1984, in review

Hunt, B. Asymptotic Solution of Dam-Break Problem, *A.S.C.E., Journal of Hyd. Div.*, HY1, 1982

Katopodes, Nokolaos and Strelkoff, Theodor. Computing Two-Dimensional Dam-Break Flood Waves, *A.S.C.E., Journal of Hyd. Div.*, HY9, 1978

Lai, C. Computer Simulation of Two-Dimensional Unsteady Flows in Estuaries and Embayments by the Method of Characteristics – Basic Theory and the Formulation of the Numerical Method, U.S. Geological Survey, Water Resources Investigations *Report 77-85*, 1977

Land, L. F. Mathematical Simulations of the Toccoa Falls, Georgia, Dam-Break Flood, *Wat. Resources Bulletin*, 1980a, **16**(6)

Land, L. F. Evaluation of Selected Dam-Break Flood-Wave Models by using Field Data, U.S.G.S. Wat. Res. Investigations *Report 80-44*, 1980b

McCuen, R. H. A Guide to Hydrologic Analysis Using S.C.S. Methods, Prentice-Hall, 1982

Miller, W. A. and Cunge, J. A. Simplified Equations of Unsteady Flow, Chapter 5 of Unsteady Flow in Open Channels, Water Resources Publications, Fort Collins, Colorado, 1975

Morris, E. M. and Woolhiser, D. A. Unsteady One-Dimensional Flow Over a Plane: Partial Equilibrium and Recession Hydrographs, *Water Resources Research*, AGU, 1980, **16**(2)

Ponce, V. M. Nature of Wave Attenuation in Open Channel Flow, *A.S.C.E., Journal of Hyd. Div.*, HY2, 1982

Ponce, V. M., Li, R. M. and Simons, D. B. Applicability of Kinematic and Diffusion Modles in *Verification of Mathematical and Physical Models in Hydraulic Engineering*, A.S.C.E., Hyd. Div., Special Conf., University of Maryland, College Park, Maryland, 1978

Ponce, V. M. and Tsivoglou, A. J. Modeling Gradual Dam Breaches, *A.S.C.E., Journal of Hyd. Div.*, HY7, 1981

Rajar, R. Mathematical Simulation of Dam-Break Flow, *A.S.C.E., Journal of Hyd. Div.*, HY7, 1978

Sakkas, J. G. and Strelkoff, Theodor. Dam-Break Flood in a Prismatic Dam Channel, *A.S.C.E., Journal of Hyd. Div.*, HY12, 1973

U.S. Army Corps of Engineers Two-Dimensional Flow Modeling Seminar, July 1981, Hydrologic Engineering Center, Davis, California

Xanthopoulos, Th. and Koutitas, Ch. Numerical Simulation of a Two-Dimensional Flood Wave Propagation Due to Dam Failure, *Journal of Hydraulic Research*, 1976, **14**(4)

APPENDIX

A.0 COMPUTER LISTINGS

```
      OPEN 5,"DHM21.DAT"
      OPEN 6,"DHM21.ANS"
      COMMON/BLK 1/FP(200,8),FC(200,6)
      COMMON/BLK 2/KIN(10),H(10,10,2),KOUT(10),HOUT(10,10,3)
      COMMON/BLK 3/NOSTA(10),STA(10,10,2),NODPX(50)
      COMMON/BLK 4/DMAX(200,2),TIMEX(200,2)
      COMMON/BLK 5/KINP(10),HP(10,10,2)
      DIMENSION NODDC(50),VEL(200,4),R(10,2),Q(4)
C
C     DEFINITIONS
C
C     FLOODPLAIN INFORMATION:
C
C     FP(I,J)=N,E,S,W,MANNINGS,ELEV,INITIAL DEPTH,TEMPORARY MEMORY
C     Q(I)=FLOWRATE PER UNIT WIDTH OF FLOW
C     R(I,1)=TIME COORDINATE FOR EFFECTIVE RAINFALL INTENSITY IN HOUR
C     R(I,2)=EFFECTIVE RAINFALL INTENSITY(IN/HR)
C     KINP(I)=INFLOW NODAL POINTS
C     HP(I,J,K)=INFLOW HYDROGRAPH FOR NODE I
C     DMAX(I,J)=MAXIMUN WATER DEPTH
C     TIMEX(I,J)=TIME CORRESPONDS TO MAXIMUN WATER DEPTH
C     NODDC(I)=CRITICAL DEPTH OUTFLOW NODES
C     VEL(I,J)=N-,E-,S-,AND W-EFFLUX VELOCITIES
C
C     DATA INPUT
C
C.....DECLARE COMPUTER UNITS
      NREAD=5
      NWRITE=6
      IWRITE=10
      TYPE '1'
C.....READ PROGRAM CONTROL DATA
      READ FREE(NREAD)DTMIN,DTMAX,DT1,DTD,SIMUL,ITER,TOUT,KODE,KMODEL
      READ FREE(NREAD)NNOD,NODC,SIDE,TOL,DTOL,DTOLP,TI,TO
C.....INPUT FLOODPALIN INFORMATION
      READ FREE(NREAD)((FP(I,J),J=1,7),I=1,NNOD)
C.....READ EFFECTIVE RAINFALL INTENSITY (LINEAR FUNCTION)
      READ FREE(NREAD)NERI
      IF(NERI.GE.1)READ FREE(NREAD)((R(I,J),J=1,2),I=1,NERI)
C.....READ INFLOW HYDROGRAPHS (LINEAR FUNCTION)
      READ FREE(NREAD)NPPI,NPPPI
      IF(NPPI.LT.1)GOTO 246
      DO 248 I=1,NPPI
248   READ FREE(NREAD)KINP(I),((HP(I,J,1),HP(I,J,2)),J=1,NPPPI)
C.....READ OUTFLOW CRITICAL DEPTH NODES
246   READ FREE(NREAD)NDC
      IF(NDC.GE.1)READ FREE(NREAD)(NODDC(I),I=1,NDC)
C.....READ SPECIFIED OUTFLOW NODES
      READ FREE(NREAD)NFLUX,TFOUT
      IF(NFLUX.GE.1)READ FREE(NREAD) (NODPX(I),I=1,NFLUX)
      TYPE '2'
      IF(NODC.LT.1)GOTO 220
C.....INPUT CHANNEL INFORMATION
      READ FREE(NREAD)(KK,(FC(KK,J),J=1,5),I=1,NODC)
      READ FREE(NREAD)NCHI,NPCHI,NCHO,NPCHO,NSTA,NPSTA
      IF(NCHI.LT.1)GOTO 241
C.....READ INFLOW HYDROGRAPHS (LINEAR FUNCTION)
      DO 240 I=1,NCHI
240   READ FREE(NREAD)KIN(I),((H(I,J,1),H(I,J,2)),J=1,NPCHI)
241   IF(NCHO.LT.1)GOTO 242
      DO 245 I=1,NCHO
C.....READ OUTFLOW BOUNDARY CONDITION NODES
C.....  QOUT = ALPHA*(DEPTH OF WATER)**BETA
      READ FREE(NREAD)(KOUT(I),(HOUT(I,J,1),HOUT(I,J,2),
     C HOUT(I,J,3),J=1,NPCHO))
245   CONTINUE
242   IF(NSTA.LT.1)GOTO 220
C.....READ STAGE CURVE (LINEAR FUNCTION)
      DO 230 I=1,NSTA
230   READ FREE(NREAD)(NOSTA(I),(STA(I,J,1),STA(I,J,2),J=1,NPSTA))
220   CONTINUE
      TYPE '3'
      ITTER=ITER
      IF(ITTER.EQ.0)ITTER=1
C.....WRITE BASIC INFORMATION TO OUTPUT FILE
      IF(KMODEL.EQ.1)WRITE(NWRITE,14)
14    FORMAT(/,10X,'*** KINEMATIC ROUTING ***',/)
      IF(KMODEL.NE.1)WRITE(NWRITE,141)
141   FORMAT(/,10X,'*** DIFFUSION ROUTING ***',/)
      WRITE(NWRITE,10)DTMIN,DTMAX,DTI,DTD,SIMUL,ITTER,TOUT
10    FORMAT(10X,'MIN. TIMESTEP(SEC.) = ',F5.2,/,
     C 10X,'MAX. TIMESTEP(SEC.) = ',F5.2,/,
     C 10X,'INCREASED TIMESTEP INTERVAL (SEC.) = ',F5.2,/,
     C 10X,'DECREASED TIMESTEP INTERVAL (SEC.) = ',F5.2,/,
     C 10X,'TOTAL SIMULATION(HOUR) = ',F5.2,/,
     C 10X,'UPDATE INTERVAL(TIMESTEPS) = ',I5,/,
     C 10X,'OUTPUT INTERVAL(HOUR) = ',F5.2)
      WRITE(NWRITE,11)NNOD,SIDE,NODC,TOL,DTOL,DTOLP
11    FORMAT(10X,'NUMBER OF NODAL POINTS FOR FLOOD PLAIN = ',I5,/,
     C 10X,'UNIFORM GRID SIDE(FEET) = ',F10.3,/,
     C 10X,'NUMBER OF NODAL POINTS FOR CHANNEL = ',I5,/
     C 10X,'RETARDING WATER DEPTH(FEET) = ',F5.4,/,
     C 10X,'TOLERANCE OF CHANGE IN WATER DEPTH(FEET) = ',F5.4,/,
     C 10X,'PERCENTAGE OF CHANGE IN WATER DEPTH = ',F5.1,' %')
      WRITE(NWRITE,6)
```

```
6       FORMAT(130('-'))
        WRITE(NWRITE,12)
12      FORMAT(//,10X,'NODAL POINT DATA ENTRY:',//,
     C  7X,'*** FLOOD PLAIN INFORMATION ***',/,
     C  10X,'NC = CENTRAL GRID NODE',/,
     C  10X,'NN,NE,NS,NW = NORTH, EAST, SOUTH, WEST NODAL POINTS',/,
     C  10X,'NBAR = NODAL POINT MANNINGS FRICTION FACTOR',/,
     C  12X,'(NEGATIVE SIGN INDICATES A CHANNEL PASSING THROUGH)',/,
     C  10X,'ELEV = NODAL POINT ELEVATION',/,
     C  10X,'DEPTH = INITIAL WATER DEPTH AT NODE',//)
        WRITE(NWRITE,13)
13      FORMAT(11X,' NC  NN  NE  NS  NW   NBAR   ELEV.  DEPTH')
        WRITE(NWRITE,15)(I,(FP(I,J),J=1,7),I=1,NNOD)
15      FORMAT(10X,5I4,1X,F6.4,2X,F6.1,1X,F5.1)
        WRITE(NWRITE,6)
50      IF(NERI.LT.1)GOTO 60
        WRITE(NWRITE,22)NERI
22      FORMAT(//,10X,'NUMBER OF EFFECTIVE RAINFALL INTENSITY ',
     C  'ENTRIES = ',I2,/,4X,'LINEAR FUNCTION IN EFFECTIVE RAINFALL',
     C  ' INTENSITY (IN/HR) ON WATERSHED:',/,10X,'HOUR    INTENSITY')
        WRITE(NWRITE,23)((R(I,J),J=1,2),I=1,NERI)
23      FORMAT(8X,F6.2,4X,F6.2)
        WRITE(NWRITE,6)
60      IF(NFPI.LT.1)GOTO 62
        DO 64 I=1,NFPI
        WRITE(NWRITE,117)KINP(I)
        DO 64 J=1,NPFPI
        WRITE(NWRITE,18)HP(I,J,1),HP(I,J,2)
64      CONTINUE
        WRITE(NWRITE,6)
62      IF(NDC.LT.1)GOTO 61
        WRITE(NWRITE,21)NDC
21      FORMAT(//,10X,'NUMBER OF CRITICAL-DEPTH OUTFLOW NODES = ',I4,//,
     C  10X,'CRITICAL-DEPTH OUTFLOW NODE NUMBERS:')
        WRITE(NWRITE,38)(NODDC(I),I=1,NDC)
38      FORMAT(10X,I3,1X,I3)
7       FORMAT(130('='))
        WRITE(NWRITE,6)
61      IF(NODC.LT.1)GOTO 260
        WRITE(NWRITE,17)
17      FORMAT(//,7X,'***CHANNEL INFORMATION***',/,
     C  10X,'NODE  NBAR  WIDTH   DEPTH   BOTTOM  INITIAL DEPTH')
        WRITE(NWRITE,16)(I,(FC(I,J),J=1,5),I=1,NNOD)
16      FORMAT(10X,I3,2X,F5.4,1X,F7.1,1X,F7.1,1X,F7.1,5X,F7.1)
        WRITE(NWRITE,6)
        IF(NCHI.LT.1)GOTO 116
        DO 51 I=1,NCHI
        WRITE(NWRITE,117)KIN(I)
        DO 51 J=1,NPCHI
        WRITE(NWRITE,18)H(I,J,1),H(I,J,2)
51      CONTINUE
117     FORMAT(/,10X,'INFLOW HYDROGRAPH AT NODE #',I3,/,
     C  12X,'HOUR     CFS')
18      FORMAT(10X,F5.1,4X,F7.0)
        WRITE(NWRITE,6)
116     IF(NCHO.LT.1)GOTO 119
        WRITE(NWRITE,19)
19      FORMAT(10X,'OUTFLOW IS APPROXIMATED AS THE FOLLOWING EQUATION:',
     C  /,12X,'QOUT = ALPHA*(DEPTH)**BETA')
        DO 250 I=1,NCHO
        WRITE(NWRITE,20)KOUT(I)
20      FORMAT(10X,'OUTFLOW NODE # ',I3,
     C  /,9X,'DEPTH LESS THAN',
     C  /,9X,'  OR EQUAL TO    ALPHA    BETA')
        DO 250 J=1,NPCHO
        WRITE(NWRITE,25)HOUT(I,J,1),HOUT(I,J,2),HOUT(I,J,3)
25      FORMAT(15X,F4.1,6X,F7.3,1X,F7.3)
250     CONTINUE
        WRITE(NWRITE,6)
119     IF(NSTA.LT.1)GOTO 260
        DO 52 I=1,NSTA
        WRITE(NWRITE,118)NOSTA(I)
        DO 52 J=1,NPSTA
        WRITE(NWRITE,39)STA(I,J,1),STA(I,J,2)
39      FORMAT(10X,F5.1,4X,F7.3)
52      CONTINUE
118     FORMAT(/,10X,'STAGE CURVE AT NODE #',I3,/,
     C  12X,'HOUR     FEET')
        WRITE(NWRITE,6)
260     CONTINUE
C
C
C       MAIN PROGRAM
C
C
C.......INITIALIZE CONSTANTS
        DSEC=DTMIN
        DT=DTMIN/3600.
        DTOLP=DTOLP*.01
        CHECKD=DTOL/DTOLP
        TTIME=0.
        QBC=0.
        QTEMP=0.
        KK=0
        TTOUT=TOUT
        TTFOUT=TFOUT
        KIT=0
        TIME=0.
        DO 40 J=1,NNOD
        DMAX(J,1)=0.
        TIMEX(J,1)=0.
        DMAX(J,2)=0.
        TIMEX(J,2)=0.
        FP(J,8)=0.
40      CONTINUE
C
C.......MAIN LOOP FOR MODEL
C
10000   KKOUT=0
        TMIN=99.
        TMAX=-99.
        TMEAN=0.
C
C.......FLOODPLAIN MODEL
C
2100    KFLUX=0
        IKODE=0
        TIME=TIME+DT
2110    FPMAX=0.
        FCMAX=0.
        IJK=0
        IF(NODC.NE.0 .AND. ITER.EQ.0)TTIME=DSEC
        IF(ITER.EQ.0 .AND. NODC.NE.0)GO TO 7777
C.......UPDATE TIME AND BOUNDARY CONDITION VALUES
        IF(NFPI.LT.1)GOTO 711
        DO 695 J=1,NFPI
        DO 710 I=2,NPFPI
        IF(TIME.GT.HP(J,I,1))GOTO 710
        QTEMP=HP(J,I-1,2)+(HP(J,I,2)-HP(J,I-1,2))*(TIME-HP(J,I-1,1))/
     C        (HP(J,I,1)-HP(J,I-1,1))
        GO TO 730
710     CONTINUE
700     QTEMP=HP(J,1,2)
730     QBC=QTEMP/SIDE
        IF(QBC.LT.0.)QBC=0.
        JJ=KINP(J)
        FP(JJ,8)=FP(JJ,8)+QBC
695     CONTINUE
C.......INCLUDE THE EFFECTIVE RAINFALL ON THE WATERSHED
711     IF(NERI.LT.1)GOTO 555
        DO 680 J=2,NERI
        IF(TIME.GT.R(J,1))GOTO 680
        RRATE=R(J-1,2)+(R(J,2)-R(J-1,2))*(TIME-R(J-1,1))/
     C        (R(J,1)-R(J-1,1))
        GO TO 660
680     CONTINUE
660     QRAIN=RRATE*SIDE*SIDE/(12.*3600.)
        DO 697 J=1,NNOD
        FP(J,8)=FP(J,8)+QRAIN/SIDE
697     CONTINUE
555     IF(NFLUX.EQ.0)GOTO 560
        IF(TIME.LT.TTFOUT)GOTO 560
        TTFOUT=TTFOUT+TFOUT
        IF(ITER.EQ.0 .AND. NODC.NE.0)GO TO 560
        WRITE(NWRITE,6)
        WRITE(NWRITE,1300)TIME
        IF(RRATE.NE.0.)WRITE(NWRITE,1301)RRATE
        IJK=1
        WRITE(NWRITE,213)
213     FORMAT(/,5X,'AVERAGE FLOW RATE FOR SPECIFIED FLOOD PLAIN ',
     C  'NODES :',/,10X,'NODE',5X,'QN',9X,'QE',9X,'QS',9X,'QW')
560     CONTINUE
C.......CALCULATE FLOW VELOCITIES AND FLOWRATES
        DO 1000 I=1,NNOD
        DO 690 II=1,4
        QQ=0.
        NQ=FP(I,II)
        IF(NQ.EQ.0.)GOTO 690
        CALL QFP(I,NQ,SIDE,QQ,ID,VV,TOL,KMODEL)
        IF(ID.EQ.1)GOTO 9999
690     Q(II)=QQ
C.......ADJUST FLOWRATES FOR DIRECTION
        Q(3)=-Q(3)
        Q(4)=-Q(4)
C.......ESTIMATE ACCUMULATION OF INFLOW
        QNET=Q(3)+Q(4)-Q(1)-Q(2)
        IF(NFLUX.EQ.0)GOTO 1010
        IF(IJK.NE.1)GOTO 1010
        QN=Q(1)*SIDE
        QE=Q(2)*SIDE
        QS=Q(3)*SIDE
        QW=Q(4)*SIDE
        DO 540 J=1,NFLUX
        IF(I.EQ.NODFX(J))WRITE(NWRITE,24)I,QN,QE,QS,QW
24      FORMAT(10X,I4,4(2X,E9.3))
540     CONTINUE
1010    FP(I,8)=QNET+FP(I,8)
1000    CONTINUE
C.......ACCOUNT FOR CRITICAL-DEPTH OUTFLOW NODES
        IF(NDC.LT.1)GOTO 1201
        DO 1100 J=1,NDC
        JJ=NODDC(J)
        QOUT=5.67*(FP(JJ,7)**0.5)*(FP(JJ,7)-TOL)
        IF(FP(JJ,7).LT.TOL)QOUT=0.
        FP(JJ,8)=FP(JJ,8)-QOUT
1100    CONTINUE
C.......UPDATE CHANGE OF WATER DEPTH
1201    DO 1200 J=1,NNOD
        FP(J,8)=FP(J,8)*DSEC/SIDE
        TEMP=ABS(FP(J,8))
        IF(TEMP.LT.DTOL)GOTO 1200
        IF(FP(J,7).LT.CHECKD)FPMAX=99.
        IF(FP(J,7).LT.CHECKD)GOTO 1231
        TOLP=TEMP/FP(J,7)
        IF(TOLP.GE.DTOLP)FPMAX=99.
        IF(TOLP.GE.DTOLP)GOTO 1231
1200    CONTINUE
C.......CALCULATE THE EFFLUX VELOCITIES
        DO 691 J=1,NNOD
        IF(KODE.NE.1)GOTO 692
        DO 691 II=1,4
        QQ=0.
        NQ=FP(J,II)
        IF(NQ.EQ.0.)GOTO 691
        CALL QFP(J,NQ,SIDE,QQ,ID,VV,TOL,KMODEL)
        VEL(J,II)=VV
691     CONTINUE
C.......CHECK INTERFACE MODEL UPDATE REQUEST
692     IF(IKODE.EQ.0)KIT=KIT+1
        IF(IKODE.EQ.0)TTIME=TTIME+DSEC
        IF(KIT.NE.ITER)GOTO 1231
        IF(NODC.LT.1)GOTO 1231
C
C.......UPDATE WATER DEPTH FOR CHANNEL
C
7777    CALL FLOODC(TIME,TTIME,NNOD,NCHI,NCHO,NPCHI,NPCHO,SIDE,NSTA,
     C  NPSTA,NODC,TOL,DTOL,DTOLP,NFLUX,KFLUX,ITER,FCMAX,NWRITE,CHECKD,
     C  KMODEL)
C.......UPDATE NEW TIMESTEP SIZE
1231    DD=AMAX1(FPMAX,FCMAX)
        IF(DD.GT.0.)DSECP=DSEC-DTD
        IF(DD.LE.0.)DSECP=DSEC+DTI
        IF(DSECP.LT.DTMIN)DSECP=DTMIN
        IF(DSECP.GT.DTMAX)DSECP=DTMAX
        DTT=DSECP/3600.
        IF(DD.LE.DTOL)GOTO 1255
        IF(DSEC.EQ.DTMIN)IKODE=1+IKODE
        IF(DSEC.NE.DTMIN)IKODE=1
        IF(IKODE.GE.3)GOTO 999
        TIME=TIME-DT+DTT
        TTIME=TTIME-DSEC+DSECP
        DO 1257 J=1,NNOD
        FP(J,8)=0.
1257    CONTINUE
        DT=DTT
        DSEC=DSECP
        GO TO 2110
C.......UPDATE DEPTH OF WATER
1255    DO 1259 J=1,NNOD
        FP(J,7)=FP(J,7)+FP(J,8)
        IF(FP(J,7).LT.0.)FP(J,7)=0.
        FP(J,8)=0.
        IF(NODC.LT.1)GOTO 1259
        FC(J,5)=FC(J,5)+FC(J,6)
        IF(FC(J,5).LT.0.)FC(J,5)=0.
        FC(J,6)=0.
1259    CONTINUE
        IF(DSEC.GT.TMAX)TMAX=DSEC
```

```
      IF(DSEC.LT.TMIN)TMIN=DSEC
C.....INTERFACE BETWEEN FLOOD PLAIN AND CHANNEL DEPTHS
      IF(KIT.NE.ITER)GOTO 1239
      IF(NODC.LT.1)GOTO 1239
      IF(ITER.NE.0)CALL CHANPL(NNOD,SIDE,TOL)
      TTIME=0.
      KIT=0
C.....CHECK OUTPUT REQUEST
1239  IF(TIME.LT.TTOUT)GOTO 1252
C.....USE FC(I,6) AND FP(I,8) TO STORE WATER SURFACE EELEVATIOS
      DO 1253 J=1,NNOD
      IF(NODC.LT.1)GOTO 1254
      FC(J,6)=FC(J,5)+FC(J,4)
      IF(ITER.EQ.0)GOTO 1253
1254  FP(J,8)=FP(J,7)+FP(J,6)
1253  CONTINUE
C.....UPDATE MAXIMUM WATER SURFACE VALUES
1252  DO 1230 J=1,NNOD
      TEMP=FP(J,7)
      TEST=DMAX(J,1)
      IF(TEMP.LT.TEST)GOTO 1230
      DMAX(J,1)=TEMP
      TIMEX(J,1)=TIME
1230  CONTINUE
      IF(NODC.LT.1)GOTO 1232
      DO 1237 J=1,NNOD
      TEMP=FC(J,5)
      TEST=DMAX(J,2)
      IF(TEMP.LT.TEST)GOTO 1237
      DMAX(J,2)=TEMP
      TIMEX(J,2)=TIME
1237  CONTINUE
1232  TMEAN=TMEAN+DSEC
      KKOUT=KKOUT+1
      DT=DTT
      DSEC=DSECP
      IF(TIME.GE.TI .AND. TIME.LE.TO)GOTO 9999
      IF(TIME.LT.TTOUT)GOTO 2100
C.....STORE FLOODPLAIN AND CHANNEL RESULTS IN OUTPUT FILE
9999  WRITE(NWRITE,6)
      WRITE(NWRITE,1300)TIME
      WRITE(IWRITE,1300)TIME
      IF(RRATE.NE.0.)WRITE(NWRITE,1301)RRATE
1300  FORMAT(//,5X,'MODEL TIME(HOURS) = ',F10.2)
1301  FORMAT(11X,'EFFECTIVE RAINFALL(IN/HR) = ',F6.2,/)
      IF(ITER.EQ.0 .AND. NODC.NE.0)GOTO 2001
      WRITE(NWRITE,26)
26    FORMAT(7X,'***FLOOD PLAIN RESULTS***')
      IF(NFPI.LT.1)GOTO 821
      DO 810 J=1,NFPI
      DO 820 I=2,NFPPI
      IF(TIME.GT.HP(J,I,1))GOTO 820
      QIN=HP(J,I-1,2)+(HP(J,I,2)-HP(J,I-1,2))*(TIME-HP(J,I-1,1))/
     C     (HP(J,I,1)-HP(J,I-1,1))
      GO TO 830
820   CONTINUE
830   WRITE(NWRITE,28)KINP(J),QIN
810   CONTINUE
821   KO=1
      IO=1
      JO=10
200   WRITE(NWRITE,1)(J,J=IO,JO)
      WRITE(NWRITE,2)(FP(J,7),J=IO,JO)
      WRITE(NWRITE,3)(FP(J,8),J=IO,JO)
      IF(KODE.EQ.1)WRITE(NWRITE,33)(VEL(J,1),J=IO,JO)
      IF(KODE.EQ.1)WRITE(NWRITE,74)(VEL(J,2),J=IO,JO)
      IF(KODE.EQ.1)WRITE(NWRITE,35)(VEL(J,3),J=IO,JO)
      IF(KODE.EQ.1)WRITE(NWRITE,36)(VEL(J,4),J=IO,JO)
33    FORMAT(5X,'VEL-N',10(3X,F8.3))
74    FORMAT(5X,'VEL-E',10(3X,F8.3))
35    FORMAT(5X,'VEL-S',10(3X,F8.3))
36    FORMAT(5X,'VEL-W',10(3X,F8.3))
1     FORMAT(/,5X,'NODE',7X,10(I3,8X))
2     FORMAT(5X,'DEPTH',10(3X,F8.3))
3     FORMAT(3X,'ELEVATION',F9.3,10(2X,F9.3))
      KO=KO+1
      IO=IO+10
      JO=10*KO
      IF(JO.LE.NNOD)GOTO 200
      IF(JO-NNOD.GE.10)GOTO 100
      JO=NNOD
      GO TO 200
100   DO 1360 J=1,NNOD
1360  FP(J,8)=0.
C.....OUTPUT OUTFLOW RATE AT CRITICAL-DEPTH NODES
      IF(NDC.LT.1)GOTO 2001
      WRITE(NWRITE,9)
9     FORMAT(/,5X,'OUTFLOW RATE AT CRITICAL-DEPTH NODES:',
     C  /,10X,'NODE   OUTFLOW RATE(CFS)')
      DO 1400 J=1,NDC
      JJ=NODDC(J)
      QOUT=5.67*(FP(JJ,7)**0.5)*SIDE*(FP(JJ,7)-TOL)
      IF(FP(JJ,7).LT.TOL)QOUT=0.
      WRITE(NWRITE,8)JJ,QOUT
8     FORMAT(10X,I4,5X,F10.2)
1400  CONTINUE
      WRITE(NWRITE,6)
2001  IF(NODC.LT.1)GOTO 2000
      WRITE(NWRITE,27)
27    FORMAT(//,7X,'***CHANNEL RESULTS***',/)
      IF(NCHI.LT.1)GOTO 321
      DO 310 J=1,NCHI
      DO 320 I=2,NPCHI
      IF(TIME.GT.H(J,I,1))GOTO 320
      QIN=H(J,I-1,2)+(H(J,I,2)-H(J,I-1,2))*(TIME-H(J,I-1,1))/
     C     (H(J,I,1)-H(J,I-1,1))
      GO TO 330
320   CONTINUE
330   WRITE(NWRITE,28)KIN(J),QIN
28    FORMAT(10X,'INFLOW  RATE AT NODE ',I3,' IS EQUAL TO ',F10.2)
310   CONTINUE
321   IF(NCHO.LT.1)GOTO 341
      DO 340 J=1,NCHO
      JJ=KOUT(J)
      DO 345 KJ=1,NPCHO
      IF(FC(JJ,5).GT.HOUT(J,KJ,1))GOTO 345
      QOUT=HOUT(J,KJ,2)*(FC(JJ,5)**HOUT(J,KJ,3))
      IF(FC(JJ,5).LT.TOL)QOUT=0.
      GO TO 346
345   CONTINUE
346   WRITE(NWRITE,29)JJ,QOUT
29    FORMAT(10X,'OUTFLOW RATE AT NODE ',I3,' IS EQUAL TO ',F10.2)
340   CONTINUE
341   CONTINUE
      KO=1
      IO=1
      JO=10
201   WRITE(NWRITE,1)(J,J=IO,JO)
      WRITE(NWRITE,2)(FC(J,5),J=IO,JO)
      WRITE(NWRITE,3)(FC(J,6),J=IO,JO)
      KO=KO+1
      IO=IO+10
      JO=10*KO
      IF(JO.LE.NNOD)GOTO 201
      IF(JO-NNOD.GE.10)GOTO 101
      JO=NNOD
      GO TO 201
101   DO 1361 J=1,NNOD
1361  FC(J,6)=0.
C
C.....END OF MAIN LOOP
C
2000  IF(ID.EQ.1)GOTO 999
      TMEAN=TMEAN/FLOAT(KKOUT)
      WRITE(NWRITE,53)TMIN,TMAX,TMEAN
53    FORMAT(//,5X,'MIN. TIMESTEP(SEC.) = ',F5.2,
     C   5X,'MAX. TIMESTEP(SEC.) = ',F5.2,
     C   5X,'MEAN TIMESTEP(SEC.) = ',F5.2,//)
      TTOUT=TTOUT+TOUT
      IF(TIME.LT.SIMUL)GOTO 10000
999   WRITE(NWRITE,7)
C.....OUTPUT THE MAXIMUM WATER SURFACE
      IF(ITER.EQ.0 .AND. NODC.NE.0)GOTO 6666
      WRITE(NWRITE,10001)
10001 FORMAT(///,10X,'MAXIMUM WATER SURFACE VALUES FOR FLOOD',
     C  ' PLAIN',/)
      KO=1
      IO=1
      JO=10
300   WRITE(NWRITE,1)(J,J=IO,JO)
      WRITE(NWRITE,2)(DMAX(J,1),J=IO,JO)
      WRITE(NWRITE,4)(TIMEX(J,1),J=IO,JO)
4     FORMAT(5X,'TIME ',10(3X,F8.3))
      KO=KO+1
      IO=IO+10
      JO=10*KO
      IF(JO.LE.NNOD)GOTO 300
      IF(JO-NNOD.GE.10)GOTO 400
      JO=NNOD
      GO TO 300
400   WRITE(NWRITE,7)
6666  IF(NODC.LT.1)GOTO 4400
      WRITE(NWRITE,10002)
10002 FORMAT(///,10X,'MAXIMUM WATER SURFACE VALUES FOR CHANNEL',/)
      KO=1
      IO=1
      JO=10
3300  WRITE(NWRITE,1)(J,J=IO,JO)
      WRITE(NWRITE,2)(DMAX(J,2),J=IO,JO)
      WRITE(NWRITE,4)(TIMEX(J,2),J=IO,JO)
      KO=KO+1
      IO=IO+10
      JO=10*KO
      IF(JO.LE.NNOD)GOTO 3300
      IF(JO-NNOD.GE.10)GOTO 4400
      JO=NNOD
      GO TO 3300
4400  WRITE(NWRITE,7)
C.....END OF PROGRAM
      IF(ID.EQ.1)WRITE(IWRITE,909)
909   FORMAT(2X,'*** DEPTH OF WATER IS EITHER GREATER THAN',
     1  ' 150 OR LESS THAN 0 ***',/,2X,'*** PROGRAM STOP ***')
      IF(IKODE.GE.3)WRITE(IWRITE,907)DSEC
907   FORMAT(2X,'*** MINIMUM TIMESTEP ',F4.1,' SEC. IS TOO LARGE!!',
     1  /,2X,' ***>  A SMALLER TIMESTEP SHOULD BE USED ***')
      STOP
      END

      SUBROUTINE FLOODC(TIME,TTIME,NNOD,NCHI,NCHO,NPCHI,NPCHO,SIDE,
     C  NSTA,NPSTA,NODC,TOL,DTOL,DTOLP,NFLUX,KFLUX,ITER,FCMAX,NWRITE,
     C  CHECKD,KMODEL)
C
C     THIS SUBROUTINE CALCULATES THE DEPTH OF WATER FOR
C     THE CHANNEL MODEL
C
      COMMON/BLK 1/FP(200,8),FC(200,6)
      COMMON/BLK 2/KIN(10),H(10,10,2),KOUT(10),HOUT(10,10,3)
      COMMON/BLK 3/NOSTA(10),STA(10,10,2),NODFX(50)
      COMMON/BLK 4/DMAX(200,2),TIMEX(200,2)
      DIMENSION Q(4)
C
C     DEFINITIONS
C
C     FC(I,J)=MANNINGS,WIDTH,DEPTH,ELEV,INITIAL DEPTH,TEMPORARY MEMORY
C     KIN(I)=ARRAY OF INFLOW NODE
C     H(I,J,1)=TIME COORDINATE FOR INFLOW RATE IN HOUR
C     H(I,J,2)=INFLOW RATE(CFS)
C     KOUT(I)=ARRAY OF OUTFLOW NODE
C     HOUT(I,J)=PARAMETERS FOR OUTFLOW NODE
C     Q(I)=VOLUME OF FLOW
C     NOSTA(I)=ARRAY OF STAGE STATION
C     STA(I,J,1)=TIME COORDINATE FOR STAGE CURVE
C     STA(I,J,2)=DEPTH OF WATER IN FEET
C
C     CHANNEL MODEL
C
C.....INITIALIZE CONSTANTS
      QBC=0.
      QTEMP=0.
      DO 40 J=1,NNOD
      FC(J,6)=0.
40    CONTINUE
      IF(KFLUX.EQ.1 .AND. ITER.EQ.0)WRITE(NWRITE,212)TIME
212   FORMAT(//,130('-'),/,5X,'MODEL TIME(HOUR) = ',F10.2,/)
      IF(KFLUX.EQ.1)WRITE(NWRITE,213)
C
C.....MAIN LOOP FOR CHANNEL MODEL
C
C.....UPDATE TIME AND BOUNDARY CONDITION VALUES
      IF(NCHI.LT.1)GOTO 711
      DO 695 J=1,NCHI
      DO 710 I=2,NPCHI
      IF(TIME.GT.H(J,I,1))GOTO 710
      QTEMP=H(J,I-1,2)+(H(J,I,2)-H(J,I-1,2))*(TIME-H(J,I-1,1))/
     C     (H(J,I,1)-H(J,I-1,1))
      GO TO 730
710   CONTINUE
730   QBC=QTEMP*TTIME
      IF(QBC.LT.0.)QBC=0.
C.....UPDATE INFLOW BOUNDARY CONDITION NODES
      JJ=KIN(J)
      FC(JJ,6)=QBC
695   CONTINUE
C.....CALCULATE FLOW VELOCITIES AND FLOWRATES
711   DO 1000 I=1,NNOD
      QNET=0.
      IF(FP(I,5).GT.0.)GOTO 1000
      DO 690 II=1,4
```

```
      QQ=0.
      NQ=FP(I,11)
      IF(FP(NQ,5).GT.0.)NQ=0
      IF(NQ.EQ.0.)GOTO 690
      CALL QFC(I,NQ,QQ,SIDE,TOL,KMODEL)
690   Q(II)=QQ
C.....ADJUST FLOWRATES FOR DIRECTION
      Q(3)=-Q(3)
      Q(4)=-Q(4)
C.....ESTIMATE ACCUMULATION OF INFLOW
      QNET=(Q(3)+Q(4)-Q(1)-Q(2))*TTIME
      IF(NFLUX.EQ.0)GOTO 1000
      IF(KFLUX.EQ.0)GOTO 1000
213   FORMAT(/,5X,'AVERAGE FLOW RATE FOR SPECIFIED CHANNEL NODES :',
     C  /,10X,'NODE',5X,'QN',9X,'QE',9X,'QS',9X,'QW')
      DO 540 J=1,NFLUX
      IF(I.NE.NODFX(J))GOTO 540
      WRITE(NWRITE,24)I,Q(1),Q(2),Q(3),Q(4)
24    FORMAT(10X,I4,4(2X,E9.3))
540   CONTINUE
1000  FC(I,6)=QNET+FC(I,6)
C.....ACCOUNT DISCHARGE AT OUTFLOW NODES
      IF(NCHO.LT.1)GOTO 741
      DO 1100 J=1,NCHO
      JJ=KOUT(J)
      DO 1110 K=1,NPCHO
      IF(FC(JJ,5).GT.HOUT(J,K,1))GOTO 1110
      QOUT=HOUT(J,K,2)*(FC(JJ,5)**HOUT(J,K,3))*TTIME
      IF(FC(JJ,5).LT.TOL)QOUT=0.
      GO TO 1111
1110  CONTINUE
1111  FC(JJ,6)=FC(JJ,6)-QOUT
1100  CONTINUE
C.....UPDATE THE WATER ELEVATIONS AT STAGE STATIONS
741   IF(NSTA.LT.1)GOTO 1201
      DO 740 I=1,NSTA
      NN=NOSTA(I)
      DO 750 J=2,NPSTA
      IF(TIME.GT.STA(I,J,1))GOTO 750
      DE=STA(I,J-1,2)+(STA(I,J,2)-STA(I,J-1,2))*(TIME-STA(I,J-1,1))
     C   /(STA(I,J,1)-STA(I,J-1,1))
      GO TO 760
750   CONTINUE
760   FCMAX=ABS(DE-FC(NN,5)-FC(NN,4))
      FC(NN,5)=DE-FC(NN,4)
      FC(NN,6)=0.
740   CONTINUE
C.....CHECK MAXIMUM CHANGE OF WATER DEPTH
1201  DO 1200 J=1,NNOD
      IF(NSTA.LT.1)GOTO 1253
      DO 1252 JJ=1,NSTA
      IF(J.EQ.NOSTA(JJ))GOTO 1200
1252  CONTINUE
1253  IF(FP(J,5).GT.0.)GOTO 1200
      A=0.
      KCO=0
      DO 1251 JJ=1,4
      NQ=FP(J,JJ)
      IF(FP(NQ,5).GT.0.)GOTO 1251
      A=A+(.25*FC(NQ,2)+.75*FC(J,2))*.5*SIDE
      KCO=KCO+1
1251  CONTINUE
      IF(KCO.EQ.1)A=2.*A
      FC(J,6)=FC(J,6)/A
1200  CONTINUE
      DO 1255 I=1,NNOD
      TEMP=ABS(FC(I,6))
      IF(TEMP.LT.DTOL)GOTO 1255
      IF(FC(I,5).LT.CHECKD)FCMAX=99.
      IF(FC(I,5).LT.CHECKD)RETURN
      TOLP=TEMP/FC(I,5)
      IF(TOLP.GE.DTOLP)FCMAX=99.
      IF(TOLP.GE.DTOLP)RETURN
1255  CONTINUE
      RETURN
      END

      SUBROUTINE CHANPL(NNOD,SIDE,TOL)
C
C     THIS SUBROUTINE UPDATES THE WATER SUFRACE ELEVATION
C     BETWEEN THE FLOODPLAIN AND CHANNEL MODELS
C
      COMMON/BLK 1/FP(200,8),FC(200,6)
C
      DO 100 I=1,NNOD
C.....CHECK INTERFACE BETWEEN CHANNEL AND FLOOD PLAIN
      IF(FP(I,5).GT.0.)GOTO 100
C.....A IS WATER LEVEL AT FLOOD PLAIN
C.....B IS WATER LEVEL AT CHANNEL
C.....FC(I,3) IS THE DEPTH OF CHANNEL
      A=FP(I,6)+FP(I,7)
      B=FC(I,4)+FC(I,5)
      IF(A.GT.B)GOTO 110
C.....FLOODING OF CHANNEL, B > A
      FP(I,7)=FP(I,7)+(B-A)*FC(I,2)/SIDE
      FC(I,5)=FP(I,7)+FC(I,3)
      GO TO 100
C.....FLOW INTO CHANNEL FROM GRID ELEMENT, A > B
110   IF(FC(I,3).LT.FC(I,5))GOTO 120
      VAL=(FC(I,3)-FC(I,5)+TOL)*FC(I,2)
      VW=(SIDE-FC(I,2))*(FP(I,7)-TOL)
C.....CASE 1 - NO FLOW INTO CHANNEL
      IF(VW.LT.0.)GOTO 100
      IF(VAL.GE.VW)GOTO 130
C.....CASE 2 - CHANNEL IS FULLED AFTER FILLING
      FP(I,7)=TOL+(VW-VAL)/SIDE
      FC(I,5)=FC(I,3)+FP(I,7)
      GO TO 100
C.....CASE 3 - FC(I,3) > FC(I,5)
130   FC(I,5)=FC(I,5)+VW/FC(I,2)
      FP(I,7)=TOL
      GOTO 100
C.....CASE 4 - FC(I,5) > FC(I,3)
120   FP(I,7)=B+(A-B)*(SIDE-FC(I,2))/SIDE-FP(I,6)
      FC(I,5)=FP(I,7)+FC(I,3)
100   CONTINUE
      RETURN
      END
C
      SUBROUTINE QFP(I,NQ,SIDE,QQ,ID,VEL,TOL,KMODEL)
C
C     THIS SUBROUTINE CALCULATES THE EFFLUX PER UNIT WIDTH
C     WHICH FLOWS ACROSS THE ADJACENT CONTORL VOLUMES
C
      COMMON/BLK 1/FP(200,8),FC(200,6)
      VEL=0.
      ID=0
      QQ=0.
      H=FP(I,7)+FP(I,6)
      IF(KMODEL.EQ.1)H=FP(I,6)
      IF(FP(I,7).EQ.0..AND.FP(NQ,7).EQ.0.)GOTO 2002
C.....DEPTHS ARE NONZERO
      HN=FP(NQ,7)+FP(NQ,6)
      IF(KMODEL.EQ.1)HN=FP(NQ,6)
      GRAD=(HN-H)/SIDE
      HBAR=.5*(FP(I,7)+FP(NQ,7))
      IF(GRAD)150,2002,170
C.....H > HN
150   IF(FP(I,7).LT.TOL)GOTO 2002
      YBAR=FP(I,7)-TOL
      GOTO 180
C.....HN > H
170   IF(FP(NQ,7).LT.TOL)GOTO 2002
      YBAR=FP(NQ,7)-TOL
180   IF(YBAR.LT.TOL)GOTO 2002
      XNBAR=.5*(ABS(FP(I,5))+ABS(FP(NQ,5)))
      AGRAD=ABS(GRAD)
      IF(AGRAD.GT..00001)GOTO 185
      QQ=0.
      GOTO 2002
185   XK=1.486/XNBAR*YBAR*HBAR**.667/SQRT(AGRAD)
      IF(HBAR.LT.0.)ID=1
      IF(HBAR.GT.150.)ID=1
      QQ=-XK*GRAD
      VEL=QQ/YBAR
2002  CONTINUE
      RETURN
      END

      SUBROUTINE QFC(I,NQ,QQ,SIDE,TOL,KMODEL)
C
C     THIS SUBROUTINE CALCULATES VOLUME OF WATER THAT
C     FLOWS ACROSS THE ADJACENT CONTROL VOLUMES
C
      COMMON/BLK 1/FP(200,8),FC(200,6)
      QQ=0.
      DCH=.5*(FC(I,3)+FC(NQ,3))
      WID=.5*(FC(I,2)+FC(NQ,2))
      H=FC(I,4)+FC(I,5)
      IF(KMODEL.EQ.1)H=FC(I,4)
      IF(FC(I,5).EQ.0..AND.FC(NQ,5).EQ.0.)GOTO 2002
C.....DEPTHS ARE NONZERO
      HN=FC(NQ,4)+FC(NQ,5)
      IF(KMODEL.EQ.1)HN=FC(NQ,4)
      GRAD=(HN-H)/SIDE
      IF(GRAD)150,2002,170
C.....H > HN
150   IF(FC(I,5).LT.TOL)GOTO 2002
      YBAR=FC(I,5)
      GOTO 180
C.....HN > H
170   IF(FC(NQ,5).LT.TOL)GOTO 2002
      YBAR=FC(NQ,5)
180   HBAR=.5*(FC(I,5)+FC(NQ,5))
      WETT=2.*HBAR+WID
      WETC=2.*DCH+WID
      WET=AMIN1(WETC,WETT)
      A=WID*HBAR
      R=A/WET
      IF(HBAR.LT.TOL)GOTO 2002
      XNBAR=.5*(FC(I,1)+FC(NQ,1))
      AGRAD=ABS(GRAD)
      IF(AGRAD.GT..00001)GOTO 185
      QQ=0.
      GOTO 2002
185   XK=1.486/XNBAR*R**0.667/SQRT(AGRAD)
      VEL=-XK*GRAD
      QQ=VEL*WID*YBAR
2002  CONTINUE
      RETURN
      END
```

A.1 EXAMPLE INPUT FILE

```
1. 30. 1. 10. 10. 1 .5 0 2
160 36 500 .0001 .1 10. 0 0
  2  11   0   0  .040   101.000   0.
  3  12   1   0  .040   101.500   0.
  4  13   2   0  .040   102.000   0.
  5  14   3   0  .040   102.500   0.
  6  15   4   0  .040   103.000   0.
  7  16   5   0  .040   103.500   0.
  8  17   6   0  .040   104.000   0.
  9  18   7   0  .040   104.500   0.
 10  19   8   0  .040   105.000   0.
  0  20   9   0  .040   105.500   0.
 12  21   0   1  .040   100.500   0.
 13  22  11   2  .040   101.000   0.
 14  23  12   3  .040   101.500   0.
 15  24  13   4  .040   102.000   0.
 16  25  14   5  .040   102.500   0.
 17  26  15   6  .040   103.000   0.
 18  27  16   7  .040   103.500   0.
 19  28  17   8  .040   104.000   0.
 20  29  18   9  .040   104.500   0.
  0  30  19  10  .040   105.000   0.
 22  31   0  11  .040   100.000   0.
 23  32  21  12  .040   100.500   0.
 24  33  22  13  .040   101.000   0.
 25  34  23  14  .040   101.500   0.
 26  35  24  15  .040   102.000   0.
 27  36  25  16  .040   102.500   0.
 28  37  26  17  .040   103.000   0.
 29  38  27  18  .040   103.500   0.
 30  39  28  19  .040   104.000   0.
  0  40  29  20  .040   104.500   0.
 32  41   0  21 -.040    99.500   0.
 33  42  31  22 -.040   100.000   0.
 34  43  32  23 -.040   100.500   0.
 35  44  33  24 -.040   101.000   0.
 36  45  34  25 -.040   101.500   0.
 37  46  35  26 -.040   102.000   0.
 38  47  36  27 -.040   102.500   0.
 39  48  37  28 -.040   103.000   0.
 40  49  38  29 -.040   103.500   0.
  0  50  39  30 -.040   104.000   0.
 42  51   0  31  .040   100.000   0.
 43  52  41  32  .040   100.500   0.
 44  53  42  33  .040   101.000   0.
 45  54  43  34  .040   101.500   0.
 46  55  44  35  .040   102.000   0.
 47  56  45  36  .040   102.500   0.
 48  57  46  37  .040   103.000   0.
```

```
 49  58  47  38  .040   103.500   0.
 50  59  48  39  .040   104.000   0.
  0  60  49  40  .040   104.500   0.
 52  61   0  41  .040   100.500   0.
 53  62  51  42  .040   101.000   0.
 54  63  52  43  .040   101.500   0.
 55  64  53  44  .040   102.000   0.
 56  65  54  45  .040   102.500   0.
 57  66  55  46  .040   103.000   0.
 58  67  56  47  .040   103.500   0.
 59  68  57  48  .040   104.000   0.
 60  69  58  49  .040   104.500   0.
  0  70  59  50  .040   105.000   0.
 62  71   0  51  .040   100.000   0.
 63  72  61  52  .040   100.500   0.
 64  73  62  53  .040   101.000   0.
 65  74  63  54  .040   101.500   0.
 66  75  64  55  .040   102.000   0.
 67  76  65  56  .040   102.500   0.
 68  77  66  57  .040   103.000   0.
 69  78  67  58  .040   103.500   0.
 70  79  68  59  .040   104.000   0.
  0  80  69  60  .040   104.500   0.
 72  81   0  61 -.040    99.500   0.
 73  82  71  62 -.040   100.000   0.
 74  83  72  63 -.040   100.500   0.
 75  84  73  64 -.040   101.000   0.
 76  85  74  65 -.040   101.500   0.
 77  86  75  66 -.040   102.000   0.
 78  87  76  67 -.040   102.500   0.
 79  88  77  68 -.040   103.000   0.
 80  89  78  69 -.040   103.500   0.
  0  90  79  70 -.040   104.000   0.
 82  91   0  71  .040   100.000   0.
 83  92  81  72  .040   100.500   0.
 84  93  82  73  .040   101.000   0.
 85  94  83  74  .040   101.500   0.
 86  95  84  75  .040   102.000   0.
 87  96  85  76 -.040   102.500   0.
 88  97  86  77  .040   103.000   0.
 89  98  87  78  .040   103.500   0.
 90  99  88  79  .040   104.000   0.
  0 100  89  80  .040   104.500   0.
 92 101   0  81  .040   100.500   0.
 93 102  91  82  .040   101.000   0.
 94 103  92  83  .040   101.500   0.
 95 104  93  84  .040   102.000   0.
 96 105  94  85  .040   102.500   0.
 97 106  95  86 -.040   103.000   0.
 98 107  96  87 -.040   103.500   0.
 99 108  97  88 -.040   104.000   0.
100 109  98  89 -.040   104.500   0.
  0 110  99  90 -.040   105.000   0.
102 111   0  91  .040   101.000   0.
103 112 101  92  .040   101.500   0.
104 113 102  93  .040   102.000   0.
105 114 103  94  .040   102.500   0.
106 115 104  95  .040   103.000   0.
107 116 105  96  .040   103.500   0.
108 117 106  97  .040   104.000   0.
109 118 107  98  .040   104.500   0.
110 119 108  99  .040   105.000   0.
  0 120 109 100  .040   105.500   0.
112 121   0 101  .040   100.500   0.
113 122 111 102  .040   101.000   0.
114 123 112 103  .040   101.500   0.
115 124 113 104  .040   102.000   0.
116 125 114 105  .040   102.500   0.
117 126 115 106  .040   103.000   0.
118 127 116 107  .040   103.500   0.
119 128 117 108  .040   104.000   0.
120 129 118 109  .040   104.500   0.
  0 130 119 110  .040   105.000   0.
122 131   0 111 -.040   100.000   0.
123 132 121 112 -.040   100.500   0.
124 133 122 113 -.040   101.000   0.
125 134 123 114 -.040   101.500   0.
126 135 124 115 -.040   102.000   0.
127 136 125 116 -.040   102.500   0.
128 137 126 117 -.040   103.000   0.
129 138 127 118 -.040   103.500   0.
130 139 128 119 -.040   104.000   0.
  0 140 129 120 -.040   104.500   0.
132 141   0 121  .040   100.500   0.
133 142 131 122  .040   101.000   0.
134 143 132 123  .040   101.500   0.
135 144 133 124  .040   102.000   0.
136 145 134 125  .040   102.500   0.
137 146 135 126  .040   103.000   0.
138 147 136 127  .040   103.500   0.
139 148 137 128  .040   104.000   0.
140 149 138 129  .040   104.500   0.
  0 150 139 130  .040   105.000   0.
142 151   0 131  .040   101.000   0.
143 152 141 132  .040   101.500   0.
144 153 142 133  .040   102.000   0.
145 154 143 134  .040   102.500   0.
146 155 144 135  .040   103.000   0.
147 156 145 136  .040   103.500   0.
148 157 146 137  .040   104.000   0.
149 158 147 138  .040   104.500   0.
150 159 148 139  .040   105.000   0.
  0 160 149 140  .040   105.500   0.
152   0   0 141  .040   101.500   0.
153   0 151 142  .040   102.000   0.
154   0 152 143  .040   102.500   0.
155   0 153 144  .040   103.000   0.
156   0 154 145  .040   103.500   0.
157   0 155 146  .040   104.000   0.
158   0 156 147  .040   104.500   0.
159   0 157 148  .040   105.000   0.
160   0 158 149  .040   105.500   0.
  0   0 159 150  .040   106.000   0.
0
0 0
9
1 2 3 4 5 6 7 8 9
0 0
31 .015 10. 6. 93.5 0.
32 .015 10. 6. 94.0 0.
33 .015 10. 6. 94.5 0.
34 .015 10. 6. 95.0 0.
35 .015 10. 6. 95.5 0.
36 .015 10. 6. 96.0 0.
37 .015 10. 6. 96.5 0.
38 .015 10. 6. 97.0 0.
39 .015 10. 6. 97.5 0.
40 .015 10. 6. 98.0 0.
71 .015 10. 6. 93.5 0.
72 .015 10. 6. 94.0 0.
73 .015 10. 6. 94.5 0.
74 .015 10. 6. 95.0 0.
75 .015 10. 6. 95.5 0.
76 .015 10. 6. 96.0 0.
77 .015 10. 6. 96.5 0.
78 .015 10. 6. 97.0 0.
79 .015 10. 6. 97.5 0.
80 .015 10. 6. 98.0 0.
86 .015 10. 5.5 97.0 0.
96 .015 10. 5. 98.0 0.
97 .015 10. 5. 98.5 0.
98 .015 10. 5. 99.0 0.
99 .015 10. 5. 99.5 0.
100 .015 10. 5. 100.0 0.
121 .015 10. 6. 94.0 0.
122 .015 10. 6. 94.5 0.
123 .015 10. 6. 95.0 0.
124 .015 10. 6. 95.5 0.
125 .015 10. 6. 96.0 0.
126 .015 10. 6. 96.5 0.
127 .015 10. 6. 97.0 0.
128 .015 10. 6. 97.5 0.
129 .015 10. 6. 98.0 0.
130 .015 10. 6. 98.5 0.
4 5 3 1 0 0
40 0 0 1 300 3 300 5 0 12 0
80 0 0 1 300 3 300 5 0 12 0
100 0 0 1 200 3 200 5 0 12 0
130 0 0 1 400 3 400 5 0 12 0
31 30 30 1
71 30 30 1
121 30 30 1
```